4.

Benthic Habitat Distribution and Subsurface Geology Selected Sites from the Rhode Island Ocean Special Area Management Study Area

by

Monique LaFrance, Emily Shumchenia, John King, Robert Pockalny, Bryan Oakley, Sheldon Pratt, Jon Boothroyd

University of Rhode Island, October 5, 2010

Executive Summary

The goal of this study was to use acoustic surveys (swath bathymetry, side-scan and sub-bottom sonar) and ground-truth surveys to delineate the benthic habitat distribution and subsurface geology for selected sites within the RI Ocean Special Area Management Plan (SAMP) study area. Benthic habitat distribution and subsurface geology were examined for two sites, a 53.5 sq mi area located in state waters to the south of Block Island (BI) and a 68 sq mi area within federal waters (FED) in eastern Rhode Island Sound. A total of more than 150 square miles were surveyed and further characterized by ground-truth studies. Two approaches, top-down and bottom-up, were employed to characterize benthic habitats. Both approaches yielded statistically strong and significant abiotic-biotic relationships. The traditional, top-down method yielded full-coverage habitat maps that describe broad-scale patterns in both benthic geological and biological resources based on geologically-defined map units. The bottom-up method identified a subset of six abiotic variables and offered fine-scale habitat class details. However, in order to complete a bottom-up integration of the abiotic and biotic data, as has been completed for smaller-scale projects, a greater density in ground-truth samples would be necessary. The recommended approach, therefore, is to use the top-down method to describe the benthic biological assemblages found within each geologic depositional environment type. The subsurface geology studies revealed that locations to the south of Block Island were large enough and have sufficient thicknesses of unconsolidated sediments to allow installation of foundation structures by pile driving thereby facilitating the construction of a small wind farm. In addition, the area of the buried valley structures in the central FED area and the general western FED area had a sufficient thickness of unconsolidated sediments to facilitate the installation of a larger wind farm. However further work is probably necessary to the west and to the south of the FED area to find sufficient space for a 100+ turbine wind farm.

Table of Contents

List of Figures

more dominant than Polychaetes. A total of 7 phyla were recovered within BI and FED. All 7 phyla are seen within BI and 6 are present within FED (Cnidaria is absent).

Figure I-12. Bubble plot of diversity within (a.) BI and (b.) FED. The size of the bubble is proportional to the diversity (measured at the genus level) at each station. Note the scales are the same for both BI and FED to allow comparison between study areas.

Figure I-13. Bubble plot of abundance within (a.) BI and (b.) FED. The size of the bubble is proportional to the abundance at each station. Note the scales are the same for both BI and FED to allow comparison between study areas.

Figure I-14. Benthic geologic environment of (a.) BI and (b.) FED study areas. The environments were derived from side-scan imagery, sub-bottom profile imagery, sediment samples, and underwater video. The polygons are labeled by depositional environment form (capital letters) followed by facies (lower case letters). Shades of the same color are used to place emphasis on the form type, because this is the unit shown to be most highly correlated to the macrofaunal assemblage (see figure I-15). The unit abbreviations are as follows: Form: DB = Depositional Basin; GAF = Glacial Alluvial Fan; GDP = Glacial Delta Plain; GLF = Glacial Lake floor; GLN = Glacial Lacustrine Fan; HM = Hummocky Moraine; ISM = Inner Shelf Moraine; MS = Moraine Shelf; PBM = PJ-BB Moraine; Facies: bgc = boulder gravel concentrations; cgp = cobble gravel pavement; csd = coarse sand with small dunes; cs = coarse sand; csd = coarse sand with small dunes; fs = fine sand; pgcs = pebble gravel coarse sand; si = silt; sic = coarse silt; sisa = silty sand; ss = sheet sand; ssg = sand sheet with gravel; sw = sand waves.

Figure I-15. Top-down habitat classification map of the (a.) BI and (b.) FED study areas. Each map unit, as defined by the form type of the depositional environment, is classified according the most abundant genus. Form type was chosen as the map unit for the BI and FED study areas because an ANOSIM revealed the macrofaunal assemblages within form type are significantly different (global $R = 0.593$, $p = 0.001$). The boundaries of the form-facies unit of depositional environment are outlined in black. The dominant genus found at each sample site is also indicated on the top-down classification maps. This data layer was added to the maps so that the unity and variability among samples with within each map unit could be seen.

Figure I-16. LINKTREE output for BI and FED. A total of 22 classes were identified within BI and FED (class numbers labeled in red). Each class is defined by a series of quantitative thresholds of the five abiotic variables identified in the BIOENV procedure. Note that BI and FED share five classes, while 13 classes contain only BI samples and four classes contain only FED samples. The threshold for each split (labeled as black letters) is listed in Table I-12.

Figure I-17. Spatial extent of classified benthic habitats within (a.) BI and (b.) FED using bottom-up method. The habitat map is comprised of 78, 100 m resolution pixels. Full-coverage benthic habitat maps cannot be produced at this time because interpolation is not possible due to the lack of auto-correlation between grain size point samples.

Figure I-18. Bottom-up habitat classification map for (a.) BI and (b.) FED. A total of 22 benthic habitat classes were identified from the analyses. The habitats were classified by the most dominant genus. Between two and three genera were used to classify the habitats if those genera had equal or nearly equal abundances. The final in a series of thresholds defining each habitat class is also provided. Refer to Figure I-16 for the list of all thresholds. BI and FED share five classes and there are 13 habitats present only within BI and 9 only within FED. Note habitat class size is NOT to scale. Classes are mapped at 100 m pixel resolution (see Figure I-17).

Figure II-1. Map showing locations of previous sub-bottom surveys within the SAMP area.

Figure II-2. Sub-bottom seismic tracklines (white lines) superimposed on bathymetry (http://www.ngdc.noaa.gov/mgg/coastal/crm.html) for the Block Island (top) and the Federal (bottom) survey areas. The yellow lines identify the location of seismic sections shown Figures 3 and 4.

Figure II-3. Processed seismic cross-sections of selected lines from Block Island survey area (see Fig 2, top) with sub-bottom interpretations. The yellow regions correspond to the sediment-water interface at the top and the deepest visible reflection at the bottom. The questions marks indicate sections of the seismic record where our identified deepest reflector extends below the resolvable depth limit. Multiple reflections of the sediment-water interface (white dashed lines) and internal reflectors (blue dashed lines) within the identified sediment package are indicated. The locations of crossing lines are indicated with arrows and appropriate line number. The vertical axis of the section is plotted as two-way travel time (milliseconds) and thickness of the sediment section (MBSF, meters below seafloor), assuming a seismic velocity of 1500 m/s.

Figure II-4. Processed seismic cross-sections of selected lines from Federal survey area (see Fig 2, bottom) with sub-bottom interpretations. Axes labels and highlighted attributes are the same as in Figure 3.

Figure II-5. (top) Sediment isopach of the Federal survey area comparing our sediment thickness estimates (colored contours) with a previous study (gray shading) by O'Hara, [1980]. (bottom) Sediment thickness contours from the O'Hara study are overlain on side-scan reflectivity.

Figure II-6. Map showing ease of construction for wind turbines in the BI study area.

List of Tables

floor; GLN = Glacial Lacustrine Fan; HM = Hummocky Moraine; ISM = Inner Shelf Moraine; MS = Moraine Shelf; PBM = PJ-BB Moraine; Facies: sisa = silty sand; bgc = boulder gravel concentrations; cgp = cobble gravel pavement; cs = coarse sand; csd = coarse sand with small dunes; fs = fine sand; pgcs = pebble gravel coarse sand; si = silt; sic = coarse silt; ss = sheet sand; ssg = sand sheet with gravel; sw = sand waves.

Table I-11. Biotic description of Depositional Environment form type. For each form type, the stations within the form and the most abundant genus are listed. The overall within-group similarity and the genus most responsible for the within-group similarity, both identified by the SIMPER procedure, are also provided. The forms marked with ** are classes for which the same genus is the most abundant and is the most responsible for the within-group similarity.

Table I-12. LINKTREE thresholds. Reported here is the final threshold of each split. The branch to the left side of the LINKTREE is listed first and the branch to the right side of the LINKTREE is listed second in brackets. For example, for split A, the stations on the left side of the split have a threshold of < 24.7 % coarse sand and the stations on the right side of the split have a threshold of > 26.9 % coarse sand. Note that many of the thresholds are defined by narrow ranges of the abiotic variables.

Table I-13. Biotic description of LINKTREE classes. For each class, the stations comprising the class and the most abundant genus are listed. The overall within-class similarity and the genus most responsible for the within-class similarity, both identified by the SIMPER procedure, are also provided. The classes marked with ** are classes for which the same genus is the most abundant and is the most responsible for the within-class similarity.

List of Appendices

Appendix I. Correlation between sediment and acoustic variables.

Appendix II. Detailed results of underwater video transects. Note that percent cover of sediment types and bottom types at each station are not given.

1. General Introduction for Benthic Habitat Distribution and Subsurface Geology

This report represents the current status of, and subsequent ground-truth studies done for the Rhode Island Ocean Special Area Management Plan (RI SAMP) between August, 2008 and the present. The RI SAMP study area is shown in Figure I-1. Some of the work is ongoing and additional data will be added to this report in the near future. The report is structured in two subsections: (1) benthic habitat distribution and (2) subsurface geology, both of which are focused on a 53.5 sq mi survey area around the south end of Block Island and a 68 sq mi survey area within federal waters located in eastern Rhode Island Sound (Figure I-2).

2. General Background

The project team leadership consists of geologists, geophysicists, and biologists. The names, affiliations, and areas of expertise are summarized in Table 1, below.

Table 1: Project Science Team

NAME	AFFILIATION	EXPERTISE
John W. King	Professor, URI Graduate School of Oceanography, URI	Geology, Geophysics, Habitat Mapping
Jon Boothroyd	Professor, URI Department of Geosciences; Rhode Island State Geologist	Geology, Geophysics, Habitat Mapping
Rob Pockalny	Marine Research Scientist, Graduate School of Oceanography, URI	Geophysics, Geology, Mapping
Sheldon Pratt	Research Associate, Graduate School of Oceanography, URI	Benthic Biology, Habitat Mapping
Sam Debow	Manager, Operations, Graduate School of Oceanography, URI, Special Research	Ship operations, Bathymetry and Side-scan Sonar Mapping

The SAMP study area is too large (approximately 1,500 square miles) to be surveyed in detail in this study. Therefore, the results of prior studies were compiled to determine the extent of existing coverage and to identify data gaps. Existing coverage was not extensive. In addition, areas that would be potential sites for development of offshore wind farms based on multiple criteria, including minimal user conflict, were identified by a Tier 1 screening approach (Spaulding et al., 2010). Two areas were examined in detail, one within Block Island Sound (BIS) and the other in Rhode Island Sound (RIS) (refer to Figure I-2). The BIS study area (referred to as BI hereafter) is located within state waters around the south end of Block Island. The Rhode Island Sound study area (referred to as FED hereafter) is located in federal waters to the west of Martha's Vineyard.

3. General Methods for Acoustic Data Acquisition and Processing

Side-scan, swath bathymetric, and sub-bottom data for the 53.5 square mile BI study area were obtained in September 2008 on the R/V Endeavor on a ten day cruise and over a period of ten days aboard the R/V Eastern Surveyor during July and August of 2009. For the 68 square mile FED study area, these acoustic datasets were collected in part during a four day cruise in August 2009 on the EPA OSV Bold, and in September 2009 on the R/V Endeavor during a nine day cruise. Sub-bottom data were also collected in BI and FED over several day cruises throughout the summer of 2009 aboard the R/V McMaster.

A pole-mounted custom composite system allowed simultaneous acquisition of bathymetry, side-scan, and sub-bottom data. The system integrates a Teledyne Benthos C3D-LPM interferometric sonar, used to acquire swath bathymetric and side-scan sonar data, and a Teledyne Benthos CHIRP III/3.5 kHz sub-bottom sonar system. A simultaneous trigger within the sub-bottom system prevents acoustic interference with the C3D system. The sub-bottom system can be switched from a high-resolution CHIRP mode (operating at 2-7 kHz, sweeping linearly from low to high) to a lower resolution 3.5 kHz mode when deeper sub-bottom penetration is needed. Bottom penetration using the CHIRP III system was limited in areas of hard bottom. In these areas a more powerful sub-bottom system, a Datasonics Bubble Pulser (400-Hz), was used to obtain deeper penetration.

During the surveys, raw side-scan and bathymetry data were continuously recorded in digital XTF format using Triton Isis acquisition software (BI 2008) or in digital OIC format using Ocean Imaging Consultants (OIC) GeoDas acquisition software (BI 2009; FED). The side-scan raw amplitude pixel data were digitally recorded on an 8-bit scale, resulting in the backscatter being displayed as a grey scale image with values ranging from 0-255. The sub-bottom data were acquired with SonarWiz software (Chesapeake Technology, Inc.) in the form of digital SEG-Y files. The incoming raw data were monitored in real-time with topside processors.

The acoustic data for BI aboard the R/V Eastern Surveyor and R/V McMaster, were collected with a Trimble Pathfinder ProXT differential GPS to assure positional accuracy (sub-meter horizontal accuracy) of the data, a TSS Meridian Gyroscope to correct for vessel heading (+/- 0.60° secant latitude dynamic accuracy, 0.10° secant latitude static error), and a TSS DMS-05 motion reference unit (MRU) for real-time correction of the vessel's motion (pitch, heave, and roll) (+/- 0.05° dynamic accuracy). For FED data obtained on the EPA OSV Bold, a Hemisphere GPS VS100 series corrected for position (DGPS, horizontal accuracy < 0.6 m 95% confidence) and heading (< 0.30° rms) of the vessel, while the TSS DMS-05 MRU offered real-time correction of the vessel's motion. An Applanix POS-MV V4 system was used for positional accuracy (DGPS, horizontal accuracy: 0.5 – 2 m), vessel true heading (accuracy 0.025°), and vessel motion correction (accuracy: roll and pitch: 0.005°; heave: 3.5 cm) for FED data collected aboard the R/V Endeavor.

Survey speed was between 4 and 6 knots. All survey lines were planned and logged in real-time using Hypack (version 6.2a) navigation software. The acoustic surveys were composed of parallel track lines spaced such that 100% or greater coverage of the seafloor was achieved. The coverage range of the bathymetry data is approximately 8 – 10X the water depth, whereas the side-scan range is approximately 20X the water depth. Therefore, the bathymetery data was the limiting factor when planning survey lines. In order to obtain 100% coverage, a line spacing scheme was implemented such that each swath overlapped at least 25% with its neighboring swath on each side and resulted in every portion of the seafloor being imaged at least once.

The raw XTF and OIC files were processed into side-scan backscatter (2 m pixel resolution) mosaics using OIC Cleansweep (version 3.4.25551, 64-bit) software. Side-scan backscatter intensity is the intensity at which sound returns to the sonar after hitting the seafloor and is indicative of the density, slope, roughness of the seafloor (Goff et al., 2000). Stronger backscatter is depicted by lighter pixels and represents highly reflective (usually harder or rougher) surfaces, whereas weaker backscatter (darker pixels) represents acoustically absorbent (usually softer or smoother) bottoms (Wille, 2005). For the side-scan, bottom tracking, angle-varying gains (AVG) and look-up tables (LUT) were applied to the data as necessary to correct for water column returns, arrival angle, and to increase the signal-to-noise ratio of the backscatter returns. These corrections helped create a uniform image that most effectively displayed the features of the seafloor. The backscatter intensity mosaic is displayed on a false color scale as an inverse grey-scale image, ranging from zero (black) to 255 (white). The final side-scan backscatter mosaics were exported as geo-referenced .tiff files.

Bathymetry maps indicate the depths and topography of the seafloor within a survey area. The raw bathymetry files were processed into mosaics (10 m resolution) using Cleansweep. Each swath was corrected for tide, vessel motion, and sonar mount angle. In addition, an angle filter (< 8º and > 82º) was applied to remove potential outlier soundings. Because adjacent swaths partially overlapped, the data could be filtered to 6-8X the water depth, ensuring the highest quality soundings were used to build the mosaics. The final bathymetry mosaics were exported as ArcGrid files.

SECTION 1: BENTHIC HABITAT DISTRIBUTION

1.1 Introduction

Maps of the benthic environment are important marine spatial planning tools for understanding the ecosystem services provided to humans (food, nutrient cycling, storm buffering, aesthetic) and for measuring the impacts of our past and future activities (resource extraction, recreation, dredging, construction) (McArthur, 2010). The Interagency Ocean Policy Taskforce (IOPTF) has identified "habitat maps" as foundational data for the management and planning of U.S. nearshore and offshore waters (IOPTF, 2009). Our operative definition of "habitat" is that of the National Oceanic and Atmospheric Administration (NOAA): "bottom environments with distinct physical, geochemical, and biological characteristics that may vary widely depending upon their location and depth; often characterized by dominant structural features and biological communities." (NOAA CSC, 2010). Further, the International Council for the Exploration of the Sea (ICES) stresses that benthic habitats consist of both abiotic (substrate, bathymetry and water energy) and biotic (flora and fauna) components (ICES, 2006). The activity of "habitat mapping" has been defined as "plotting the distribution and extent of habitats to create a complete coverage map of the seabed with distinct boundaries separating adjacent habitats" representing the "best estimate of habitat distribution at a point in time, making best use of the knowledge…available at that time." (Foster-Smith et al., 2007).

A simplified list of steps to habitat mapping has been proposed by Van Lancker and Foster-Smith (2007): (1) Process coverage (side-scan, bathymetry) data; (2) Process ground-truth data; (3) Integrate the coverage and ground-truth data; (4) Design and layout the habitat map.

The most important step of the four outlined above is the integration step, which has been accomplished using different strategies and methods depending on the types of data available and the overall goals of the mapping project. Marine benthic habitat mapping has traditionally consisted of a "top-down" protocol where acoustic tools are used to delineate landscape-level features that are usually geological in origin, followed by the ground-truthing of these features and biological characteristics (Brown et al., 2002, Solan et al., 2003, Eastwood et al., 2006). This approach involves minimal ground-truthing, allowing for the development of a benthic habitat map that is less cost- and time-intensive. The adoption of the top-down method implies that acoustic classes or geologic features contain distinct biological assemblages. As a result, the sampling scheme and subsequent data integration process, where habitats are defined, is often geology-centric (e.g., Greene et al., 1999), even when the reported purpose of the mapping is driven by management of biological resources (Kenny et al., 2003, Diaz, et al., 2004). The alternative to this "top-down" methodology is the "bottom-up" approach. The purpose of the "bottom up" protocol is to establish relationships between biological communities and environmental variables in order to delineate habitat map units. Habitat units are built based on biological similarity and are then given environmental context by establishing statistical (e.g., multivariate) relationships with associated abiotic variables (underlying geology and/or overlying oceanography). These relationships could then be used to interpolate between individual samples of fauna to create predictive biological assemblages maps (Hewitt et al., 2004, McBreen et al., 2008). Because the bottom up approach preserves organism-environment relationships, it has better potential to generate units that are ecologically meaningful (Hewitt et al., 2004, Rooper and Zimmerman, 2007, Verfaillie et al., 2009). The trade-off to producing a benthic habitat map using the bottom up method is the increase in cost and time required to both the collect and process the data.

Integrating biotic and abiotic data presents significant challenges. One of the first challenges to arise is the choice of variables to include or exclude from the analyses. This choice is usually addressed by including all available variables, then statistically eliminating those that do not show relationships with the biology, for example. A second major challenge is the coverage extent and spatial resolution of the different datasets. Full coverage acoustic data can be collected rapidly over large scales and at high resolutions (2 m pixel resolution, for example). The resulting products are often used to interpret broad-scale seafloor features (several to hundreds of meters in size). In comparison, point-coverage ground-truth data are widely spaced, with samples typically encompassing a much smaller seafloor area (< 1 m^2). The resulting data are examined at a fine scale (individual sediment grains and organisms are resolved). Describing patterns at scales of ecological importance amidst the varying scales of data acquisition is an issue that the mapping community continues to work to address (ICES, 2007). A third challenge is that both coverage and ground-truth data represent single sampling events in time, and therefore cannot always provide information about the temporal dynamics of habitats. Clues to temporal dynamics and disturbance can be found in benthic community analysis (e.g., indicator species) and geologic facies mapping (e.g., mobile sand waves) so that some generalizations may be avoided. The three challenges discussed here are at least partly addressed by NOAA's draft habitat scheme, the Coastal and Marine Ecological Classification Standard (CMECS) (Madden et al., 2010). CMECS was created to document and describe ecologically meaningful units using a common terminology for science, management and conservation. The CMECS structure organizes habitat data hierarchically from geologic setting to biotope (Table I-1), and provides ample opportunity to describe temporal dynamics and/or relevance. CMECS is currently seeking approval and endorsement as the national marine habitat classification standard by the Federal Geographic Data Committee.

Predicting biological communities poses a challenge, as well. Biological communities in physically rigorous environments are adapted to high environmental variability whereas communities in more stable environments are more influenced by biological interactions such as competition and symbioses (Pratt, 1973). This observation would suggest that biological community composition is more readily predictable in physically rigorous environments than in stable quiescent environments. Both types of environments exist within the RI Ocean SAMP study area.

Strategy

Rhode Island Sound (RIS) and Block Island Sound (BIS) are transitional waters that separate the estuaries of Narragansett Bay and Long Island Sound from the outer continental shelf (refer to Figure I-1). Providing the link between near-shore and offshore processes as well as state and federal waters, these transitional waters are both important from an ecological and management perspective. RIS and BIS are also valuable human-use areas, including for alternative energy sites, commercial and recreational fishing, boating, shipping routes and ferry routes, and tourism. In order to appropriately zone for such uses, a solid understanding of the benthic ecosystem is essential. Characterizing benthic environments is important because the organisms living there reflect long-term environmental conditions (Elliot, 1994), serve as a trophic link between primary producers and commercially and ecologically important species (e.g., fish) (Snelgrove, 1998), and affect local sedimentary processes (Gray, 1974, Rhoads, 1974).

Since it was not feasible to map benthic habitats covering the entire RI Ocean SAMP study area at a resolution (spatial or taxonomic) acceptable for marine spatial planning and management, our goal for the two study years was to achieve this resolution by describin and mapping relationships between the biology and abiotic (environmental) variables in two large target areas that are also prime potential sites for offshore wind development. We expect that many of the organism-sediment and community-environment relationships that we define will be generally applicable across the SAMP area. This information will be a valuable contribution in making scientifically valid, ecosystem-based management decisions for Rhode Island's coastal waters.

We will use both the top-down and bottom-up methods to examine biotic and abiotic and features of the benthic environment at fine scales. The top-down approach will define benthic community patterns based on geological map units (i.e. depositional environments). This approach has been used in several studies to various degrees of success (e.g. Greene et al., 1999; Brown et al., 2002; Solan et al., 2003; Eastwood et al., 2006). The bottom-up method will integrate the biotic and abiotic data and use a step-wise multivariate approach to determine which abiotic variables best explain the pattern in benthic communities across the target study areas. We will then use a classification tree to identify habitats by grouping stations according to benthic community pattern and significant thresholds of the relevant abiotic variables. The bottom-up method has been used in estuarine habitat classification (Valesini et al., 2010) and estuarine habitat mapping (Shumchenia and King, 2010), but never in offshore environments where data density tends to be much lower.

1.2 Background

Prior work

Two previous studies (McMaster, 1960, CONMAP, 2005) within the SAMP area have produced coarse resolution maps of surficial sediment type (Figure I-3 (upper panels). Two others (Figure I-3, lower panels) (Boothroyd and Oakley, this volume; McMullen et al., 2007-

2009) have produced maps that begin to integrate depositional environment (Figure I-3, lower left panel), and transport process information (Figure I-3, lower right panel) with grain size information. All of these studies produced variations of geological "habitat" maps. The maps shown in Figure I-3 (upper panel) are produced by grain size analysis of bottom grab samples. The map in Figure I-3 (lower left panel) is produced by interpretation of bathymetry data and limited sub-bottom sonar and side-scan data in terms of the major geoforms (e.g., moraine, lake floor) within the study area. The map in Figure I-3 (lower right panel) is based on interpretation of high-resolution swath bathymetry and side-scan sonar data in terms of geological processes but with limited ground-truth studies. The map shown in Figure I-3 (lower right panel) is the only previous benthic habitat study within the SAMP area that is based on mapping data of comparable quality to that obtained by the RI Ocean SAMP project.

The current spatial distribution and availability of mapping data of comparable quality to the mapping data obtained by the RI Ocean SAMP project is shown in Figure I-4. Note that none of the data currently available is located in areas that are considered high priority sites for wind development.

A major goal of the RI Ocean SAMP project is to produce benthic habitat maps from high-quality, complete coverage acoustic studies that are extensively ground-truthed. The SAMP project acquires both geological and biological ground-truth data. Acquisition of both types of data allows us to produce a multidimensional geological habitat map that includes geoform, grain size, and depositional environment information and a biological habitat map. The distribution of recent, high-quality ground-truth data of both geological and biological data obtained by previous studies is shown in Figure I-5. Again, very little previous data is available from potential high-priority sites for offshore wind development.

1.3 Methods - Construction of RI Ocean SAMP benthic habitat distribution maps

Acoustic data analyses

Although both side-scan backscatter and multibeam bathymetry datasets were collected at very high resolution (2 m and 10 m pixels, respectively), creating habitat maps at this level of detail would be prohibitive (computation time, file sizes) in the analyses and generation of broad-scale habitats. Therefore, 100 m pixel size was chosen, a scale at which major geophysical changes and boundaries across both study areas were still visible in the side-scan backscatter and bathymetry mosaics. The mean, minimum, maximum and standard deviation of both the side-scan and bathymetry were calculated at 100 m resolution. These parameters were calculated using ArcMap 9.3 with the Block Statistics feature in the Spatial Analyst Toolbox with the original 2 m side-scan and 10 m bathymetry as the input datasets. Block Statistics is a non-overlapping function that performs statistics on a group of pixels (i.e. 10 m bathy pixels and 2 m side-scan pixels) that are aggregated to form a coarser resolution dataset (i.e. 100 m bathy and side-scan pixels) (for further details of this procedure, visit http://webhelp.esri.com/arcgisdesktop/9.2/index.cfm?TopicName=An_overview_of_the_Neighborhood_tools). In addition, the slope and aspect were determined at 100 m resolution from the 2 m resolution bathymetry dataset using the Neighborhood Statistics function in the Spatial Analyst extension.

In addition to the acoustic data collected for this study, a dataset of 1.9 million National Ocean Service (NOS) soundings (meeting IHO S-44 and NOAA standards; vertical resolution is 0.5 – 1.0 m) was also compiled. These soundings were used to create a dataset that is a broad-scale measure of surface roughness throughout the Ocean SAMP study area. Using the Neighborhood Statistics function, this surface roughness dataset was derived by calculating the standard deviation of the slope (100m resolution) within a search radius of 10 pixles (i.e. 1000 m) using a moving widow algorithm (Damon, 2010). Therefore, the resulting data layer has a 100 m pixel resolution and each pixel has a value that reflects the surrounding 1000 m.

Bottom samples

Surface samples were collected aboard the R/V McMaster using a Smith-McIntyre grab sampler (0.05 m^2 area). Sampling stations were positioned within distinct geophysical bottom types (Figure I-6). The bottom types were identified through visual interpretation of the side-scan backscatter and bathymetry imagery (Hewitt et al., 2004; Brown et al., 2002, Greene et al., 1999). Stations were spread across the BI and FED study areas such that most major geophysical units contained at least one bottom sample. At each station, the latitude and longitude was recorded from a Trimble differential GPS (DGPS, +/- 3 m accuracy) as the grab sampler was deployed.

A total of 88 grabs samples were collected throughout BI and FED. There were 56 grabs collected within the 53.5 sq mi BI study area, averaging out to approximately 1 grab sample per square mile. For FED, bottom samples were concentrated within the western two-thirds (45.5 sq mi) of the entire study area (68 sq mi). In total, 32 grabs were collected, resulting in approximately one grab per 1.5 square miles. Grab samples were acquired over four occasions between October 2008 and August 2009 within BI and over two days within FED, one in December 2009 and one in June 2010.

Of the 88 sample stations, 78 were included in further analyses. Ten sites were removed because little or no material was recovered by the Smith-McIntyre grab sampler after three attempts (BI 4-6, 18, 30, 608, 1308, 1408, and Fed 22 and 40). Typically, unsuccessful grabs are an indication the seafloor is comprised of coarse sediments that are not easily recovered. Underwater video was taken at five (BI 4-6, 18, 30) of the ten unsuccessful grab stations. For four stations (BI 5, 6, 18, 30), the video confirms the samples were located in areas of coarse sediments (gravels, cobbles, boulders). It is unclear why no grab was collected at the remaining station (BI 4); video indicates the area ~275m from the station is composed of fine-grained sand.

Sediment samples

A sub-sample (~ 25 ml) was taken from the surface of each Smith-McIntyre grab sample and analyzed using a Mastersizer 2000E particle size analyzer. The Mastersizer generated the weight percent of each Wentworth particle size fraction (e.g., very fine sand, fine sand, medium sand, etc.), along with the standard deviation of the particle size distribution for the entire sample.

Macrofaunal samples

The remaining material from each Smith-McIntyre grab was sieved on 1 mm mesh and macrofauna were retained. All individuals were counted and identified to at least the genus level. In addition, a functional group designation (e.g. surface burrower, tube-builder, mobile) for each genus was made. The macrofauna abundances from the BI and FED study areas were pooled and only the genera contributing to 97% of the total abundance between the two areas were included in further analyses. This eliminated genera with very low abundances (< 0.09% of the total abundance, equivalent to < 19 individuals) and resulted in the removal of 663 individuals from the study (out of 21,862). The statistical software package, PRIMER 6 (PRIMER-E Ltd.), was used to 4th root transform all abundances to reduce the influence of highly abundant genera and the Bray-Curtis similarity index was used to create a matrix of station-similarity.

For statistical analyses, genus-level abundance data was used, with the exception of three genera: *Ampelisca*, *Lumbrineries*, and *Nucula*. The tube-building amphipod genus, *Ampelisca*, remained separated into the species *A. vadorum* and *A. agassizi* because it was noted that *A. vadorum* is a dominant species within BI, but rare within FED, while the opposite is true for *A. agassizi*. The two species belonging to the genus *Lumbrineries*, small surface-burrowing polychaetes, were examined on the species level *(L. hebes* and *L. fragilis*) due to abundance differences between the two species over BI and FED, with *L. hebes* being much more abundance than *L. fragilis*. *Nucula annulata and Nucula delphinodonta, deposit feeding molluscs,* were kept separate because *N. annulata* exhibited a much higher abundance within FED. Examining these three genera at the species-level allows for investigation into if the individual species have distinct relationships with their respective environments.

Underwater video

Underwater video transects were taken at 42 of the 56 sample locations within BI (stations 1-38 and 40-43) using an underwater video system consisting of an Applied Microvideo underwater video camera and two LED lights mounted to a sled made of PVC. The video data were collected over three consecutive days in June 2009 on the R/V McMaster using a video camera mounted to the sled and towed behind the vessel. Each transect was acquired at drifting speed and was five minutes in duration (resulting ground coverage averages ~130m, with ranges from ~30m to ~230m). Hypack navigation software and a Trimble DGPS (+/- 3 m accuracy) were used for navigation and to continuously record the vessel's track lines (latitude, longitude, time) during video acquisition. The timing of the video and navigation recording was synchronized to allow for the video time to be correlated to the GPS fixes.

Quantitative parameters were derived from visual analysis of the underwater video within BI for 37 of the 42 samples (see "Bottom samples" section above for details of excluded stations). Specifically, the general sediment composition and types of seafloor (bottom) present along each transect were recorded. These data were expressed as percentages of the total of each transect (e.g. bottom type is 50% boulder field, 25% flat sand, 25% tube mat). The number of bottom types that existed within each transect was also noted. In terms of biological information, the video for each station was qualitatively examined for the presence and approximate abundance of organisms (i.e. algae, fish, and invertebrates).

Top-Down Habitat Mapping Approach

Benthic geologic environments

Within BI and FED, the extent of the Quaternary depositional environments were interpreted from high resolution side-scan sonar and bathymetric images, sub-bottom seismic reflection profiles, as well as surface sediment grab samples and underwater video imagery collected for this study. Published geologic maps and online databases of surface sediment samples were also revisited to aid in interpretation (Needell et al., 1983; Needell and Lewis, 1984; Needell et al., 1983; NOAA/NGDC, 1976; O'Hara and Oldale, 1980). These datasets are listed in Table I-2. Quaternary depositional environments interpreted with map units > 10 of square kilometers correspond to the Geoform level in CMECS, and include moraines, glacial lake floor basins, deltas, alluvial fans and shelf valleys.

Refined Quarternary depositional environments are equivalent to the subform level in CMECS and represent the modern (Late Holocene) processes acting on the study area, and are known as benthic geologic habitats. Benthic geologic habitats are spatially recognizable areas of the seafloor with geologic characteristics different from adjacent units, and are mapped with units < 10 square kilometers (most polygons were < 1 square kilometers). These map units include information on the surface sediment characteristics, bed roughness, and includes depositional environments such as sand wave fields, low-energy depositional basins, and depositional cobble gravel pavement. The benthic geologic habitats are named based on a combination of Quaternary depositional environment, surface sediment grain size and a descriptor of the bed configuration or any other pertinent information. As an example, areas on the Quaternary moraine with coarse sand with small dunes would be mapped as ISM csd for an Inner Shelf Moraine, coarse sand with small dunes.

Multivariate analyses

An analysis of similarity (ANOSIM) was performed in PRIMER 6 on the biotic Bray-Curtis similarity matrix (derived from the 4th root transformed genus-level macrofaunal abundances) using benthic geologic environment as a factor. ANOSIM tests the null hypothesis that there are no differences between groups of samples when examined in the context of an *a-priori* factor (benthic geologic environment) (Clarke and Gorley, 2006). An R value of 0 indicates there are no differences between groups (i.e., null hypothesis is accepted), while an R value greater than 0 (null hypothesis rejected) reflects the degree of the differences. The test is permuted 999 times to generate a significance level, p ($p < 0.05$ is considered significant in this study).

PRIMER 6 was then used to perform a similarity percentages (SIMPER) routine. SIMPER is a tool that compares pairs of sample by looking at the degree (percentage) to which each individual genus contributes to the within-group similarity of the sample groups (in this case samples are grouped by depositional environment type) and reporting the average within-class similarity of each group (Clarke and Gorley, 2006). SIMPER also reports the average percent dissimilarity of the sample groups between all pairs of samples and how each genus contributes to this dissimilarity.

Mapping

The map units of the top-down habitat map are defined by the benthic geologic environment polygons using form type. For each map unit, the biotope was classified by the most abundant genus within samples retrieved there. This was calculated by taking the average abundance of each genus across all the stations belonging to each form.

Bottom-up habitat mapping approach

Univariate analysis

The Pearson correlation coefficient, r, was used to investigate the relationship between macrofaunal diversity (total # genera per site) and abundance (total # individuals per site) and two indicators of environmental heterogeneity – surface roughness and standard deviation of the sediment grain size. It was hypothesized that both environmental parameters would be positively correlated ($r \gg 0$) with both macrofauna diversity and abundance.

Multivariate analyses

A suite of abiotic variables were generated from the multiple data layers (side-scan backscatter, bathymetry, sediment samples, underwater video) at each of the 78 bottom sampling stations (Table I-3). In PRIMER 6, a draftsman plot was created to assess the correlation between the abiotic variables. Variables that were highly correlated, and, therefore, redundant ($r > 0.85$) were eliminated from the analysis. The remaining variables were then normalized to correct for differences in units, and a resemblance matrix created based on the Euclidean distance metric.

The biotic Bray-Curtis similarity matrix (genus-level, 4th root transformed) and the abiotic Euclidean distance resemblance matrix were subject to the BIOENV procedure in PRIMER 6. The BIOENV approach identifies a subset of abiotic variables that best "explain" the patterns in the macrofaunal composition (Clarke and Gorley, 2006). The approach analyzes the extent to which the abiotic parameters "match" the biological data by searching for high rank correlations between the biotic Bray-Curtis similarity matrix and the abiotic Euclidean distance matrix. The BIOENV output is the highest Spearman rank correlation coefficient, rho, between combinations of abiotic variables and the biotic similarity matrix. The BIOENV routine was permuted 999 times to allow for the significance ($p < 0.05$) of the results to be assessed.

The BIOENV procedure was performed twice. The first BIOENV (BIOENV + video) included the abiotic underwater video variables in addition to the remaining abiotic parameters (refer to Table I-3). This first BIOENV was carried out on only the 37 BI stations for which video was collected, as all variables must be present at all stations in order to run BIOENV. The second run of BIOENV (BIOENV + BI & FED) was conducted without the underwater video variables so that all 78 stations between BI and FED could be included. The maximum number of variables permitted in the output was capped at five for the BIOENV + video (due to computation constraints) and ten for the BIOENV + BI & FED.

The variables identified as important by BIOENV + BI & FED were entered into the LINKTREE procedure in PRIMER 6 to classify the macrofauna samples according to patterns in these important abiotic variables. LINKTREE groups the macrofauna samples by successive binary division using the abiotic variables as drivers and maximizing the ANOSIM R value at each division (Clarke and Gorley, 2006). The ANOSIM R was constrained to be greater than 0.30 and the minimum group size was set at two. Each resulting class is defined by a suite of biological samples and quantitative thresholds of the abiotic variable(s).

A similarity profile test (SIMPROF) within the LINKTREE procedure was used to determine if a group of samples should be split into further LINKTREE classes and to evaluate the significance of each LINKTREE class. The test was permuted 999 times and at a significance level of 5%. The SIMPROF procedure tests the null hypothesis that a group of non-*a priori* divided samples (i.e. those within each LINKTREE class) are not different from one another (Clarke and Gorely, 2006). Therefore, if the SIMPROF test is significant for samples within a LINKTREE class, the samples do not differ from one another and are not split; the opposite is true if the SIMPROF test is not significant for a group of samples. An ANOSIM was performed on the LINKTREE classes to test the null hypothesis that there are no significant ($p < 0.05$) differences in the macrofaunal assemblages among LINKTREE classes.

The SIMPER procedure in PRIMER 6 was used to determine both the overall and individual contributions of each genus to the within-group similarity and between-group dissimilarity of the resulting LINKTREE classes. In addition, the most abundant genus per class was determined by averaging the abundance for every genus across all samples within each class.

Mapping

The lack of spatial auto-correlation (i.e. samples closer in space will be more similar than those further away) among the grain size point samples prevented the use of traditional interpolation methods (e.g. Ordinary Kriging, Inverse Distance Weighting) to create full-coverage data layers. Interpolation via linear relationships between the full-coverage acoustic variables and the point-coverage sediment variables was also not possible in this study because the correlations, r^2, were not strong (see Appendix I for r^2 values). Instead, a conservative approach was taken to create the bottom-up benthic habitat maps in order to preserve the accuracy of the maps. The maps were created in ArcInfo by classifying pixels for which abiotic data were available (78, 100 m pixels). The habitat classes follow the LINKTREE classification and are described in terms of their biotic and abiotic characteristics, with each class being labeled by the dominant genus and the final in a series of LINKTREE thresholds.

1.4 Results

Acoustics

The side-scan backscatter mosaics reveal both BI and FED have heterogeneous benthic environments (Figure I-7). Interpreted bottom types include sheet sands, sand waves, and boulder fields, along with flat sandy and muddy environments. The bathymetry, slope, and surface roughness of the two areas (Figures I-8, I-9, I-10, respectively) also reflect heterogeneity in varying degrees of smooth and rough bottom.

The mean side-scan backscatter intensity (100 m resolution) within BI and FED ranged from 40.99 to 239.13 and the standard deviation varied from 7.35 to 98.61 (Table I-4).

Bathymetry (100 m resolution) ranged from 13.8 m to 44.0 m. The slope was between 0.01˚ and 1.54˚ and the standard deviation of the slope (measure of surface roughness) was between 0.05˚ and 1.39˚. The aspect had a range of 9.36˚ to 354.21˚. BI appears to have a more variable benthic environment, as evidenced by wider ranges in the acoustic variables (backscatter, slope) and their standard deviations (refer to Table I-4).

Bottom Samples

Sediment samples

Of the 78 stations between the BI and FED study areas, medium grained sand is the dominant sediment (29.7%), followed by coarse sand (24.3%) and fine sand (20.8%), which together account for 74.8% of the sediment sampled (Table I-5). Medium sand ranged between 0.4% and 76.3% for individual sediment samples, whereas coarse sand and fine sand ranged between 0% to 69.6% and 0 to 62.7% of individual sediment sample composition, respectively. Overall, BI is a coarse sediment area, with medium, coarse, and very coarse grained sands accounting for 83.2% of the sediment samples. The FED sediment samples, however, are mostly finer sediments, as 75.2% of the samples are made up of very fine, fine, and medium grained sands. Similar to the acoustic data, BI seems to exhibit more heterogeneous sediment size characteristics, having a larger range with regard to the standard deviation of grain size (90.6 µm to 459.8 µm range for BI versus a range of 61.4 µm to 316.2 µm for FED).

Macrofaunal samples

More than 21,000 individuals belonging to seven phyla and 87 genera were sampled across the 78 stations within the BI and FED study areas (Table I-6). For both areas, the majority of the recovered macrofauna (97.1%) belonged to three phyla: Arthropoda (Crustacea) (53.4%), Annelida (Polychaeta) (24.2%), and Mollusca (19.5%) (Figure I-11). In terms of spatial distribution, the most abundant genus was *Lumbrineries hebes,* a small surface burrowing polychaete (recovered at 69.2% of the stations sampled) (Table I-7). The second and third spatially most abundant genera were the small surface burrowing amphipod crustacean, *Unciola* (56.4% of stations), and the bivalve clam, *Astarte* (52.6% of stations). With regard to counts of individuals, the most abundant genera were *Ampelisca vadorum* (comprised 18.6 % of the total individuals) and *Byblis* (12.6%), both tube-building amphipod crustaceans, followed by *Nucula annulata* (8.3%), a deposit feeding mollusc (refer to Table I-7).

Overall, FED showed a higher average diversity per station (23 genera versus 16), whereas BI had a higher average abundance per station (281 individuals versus 257) (Table I-8). The average diversity (total number of genera per sample) between both study areas was 19, ranging from 4 to 34 genera (Table I-8). The highest diversity was found within FED at stations F21, F32, and F39, each having 34 genera present (Figures I-12). FED stations F35 (33 genera) and F34 and F36 (each with 31 genera) also exhibited high diversity. The average abundance (total number of individuals within each sample) within BI and FED was 272 and ranged between 6 and 1,541 individuals. The highest abundance occurred within BI at station BI2 (1,541 individuals), followed by BI stations BI1, BI37, and BI16 (each with > 1,000 individuals) (Figure I-13). The stations with the lowest diversity are BI 24 (4 genera), BI25 (5 genera), and BI3 (6 genera). The lowest abundance was found at BI stations BI24 (6 individuals recovered), BI3 (10 individuals) and BI25 (12 individuals).

Underwater video

The underwater video dataset currently does not include transects collected within FED or at BI stations 108 through 1408. Therefore, the findings presented below are preliminary and may change as additional data is incorporated into the analyses.

Video transects were collected as close to the point grab sample location as possible. Of the 44 video transects, 25% were collected within 30 m of the grab sample location, 61% within 100 m, 84% within 150 m, and 100% within 300 m.

The underwater video transects showed that nearly half of the stations (18 of 37) within BI had bottom environments comprised of flat surfaces characterized by little relief (see Table I-9 for summary or Appendix II for more detailed video findings). Sediment composition for these areas varied widely ranging from fine sand to cobble. The second most dominant bottom type was fine or coarse grained sand ripples (seen at 17 stations) that exhibited a regular or irregular pattern. Boulder fields were found at 10 stations and four stations were comprised of soft sediments dominated by dense tube-mats. The number of bottom types along each station transect ranged from one to 11, with one bottom being the most common (24 of the 37 stations).

The first BIOENV procedure, BIOENV + video, identified a subset of five variables as most influential to the macrofaunal assemblage composition (Rho = 0.635, p = 0.001). The five variables comprising the best correlation were percent coarse sand from the grain size analysis, percent fine sand as identified from the video analysis, maximum backscatter intensity, water depth (m), and surface roughness. The single variable having the highest correlation with the biology was percent coarse sand from the grain size analysis (Rho = 0.374).

Top-Down Habitat Mapping Approach

Benthic geologic environments

Block Island

Four Quaternary (glacial) depositional environments were interpreted from the high-resolution bathymetry data, including; Moraines, delta plain, alluvial fan and lake floor basins (Figure I-14a., Table I-10). The depositional environments were arbitrarily separated into geographic regions: North of the moraine shoal southwest of Block Island is considered Block Island Sound, and north of the moraine shoal southeast of Block Island is Rhode Island Sound; south of the moraine shoals is the Inner Continental Shelf. The moraines were separated into to two categories; Moraine Shoal for the two segments of moraine continuous with Block Island, dominated by outcrops of boulder gravel, and sandy Inner Shelf Moraines south of the moraine shoals. The moraine shoal that forms Southwest Ledge is as shallow as six meters below sea-level and waves break on it during storms. The formation of the Inner Shelf Moraine and the concentration of boulder gravel on the inner shelf south of the moraine remain enigmatic. The Inner Shelf Moraine may represent the maximum advance of the Laurentide Ice Sheet at Block Island, or ice tectonics as the ice margin fluctuated and deformed the stratified (Alluvial fan) deposited in front of the ice margin.

Map unit MS bgc (Moraine Shoal boulder gravel concentrations) is spatially the most extensive depositional environment, covering 30 square kilometers (11.6 square miles; 21.7% of study area) within BI. Portions of the inner shelf moraine, and extending onto the inner shelf south of the moraine is a large sand wave field, with orientations suggesting sediment transport in both an east to west and southeast to northwest directions, or towards Block Island Sound. Crest to crest spacing of the sand waves average 100 m, but range from 10 to 300 m, and are likely active only during storm events.

Extending south from the moraine shoals, two broad areas interpreted to represent alluvial fans that were deposited by braided rivers graded to either a glacial lake on the inner shelf south of the study area, or to the Late Wisconsinan low-stand marine shoreline. This area is dominated by sandy and gravelly depositional environments, and map unit GAF csd (Glacial

Alluvial Fan coarse sand with small dunes encompasses 29 square kilometers (11.3 square miles, 21.3% of BI study area) and GAF pgcs (Glacial Alluvial Fan pebble gravel coarse sand, 13 square kilometers (5.1 square miles, 9.5%). The small dunes in map unit GAF csd represent wave orbital bedforms, and are ubiquitous in depositional environments with coarse sand throughout the study area. Crest to crest spacing averages 1 m, and ranges from 0.75 to 2 m (Clifton, 1976). Based on the water depth and grain size within this unit, the velocity needed to form these bedforms can be estimated at 0.75 – 1.5 m s^{-1}. At a depth of 25 m, these velocities are reached with a minimum wave height of 4 – 5 m, with a period of 10 seconds (Komar, 1976; Sherwood, 2007).

North of the moraine at Southwest Ledge, a relatively flat area at -30 m below present sea-level is interpreted as a glacial delta that formed when the ice front was at the small segment of Moraine in the northwest corner of the study area. This probably represents a small glacial lake that existed between the ice front and moraine that was filled by the prograding delta. The surface sediment characteristics of this unit are dominated by pebble gravel and coarse sand depositional environments.

Two deeper areas (30 – 40 m below present sea-level) on the western and northern end of the study areas were mapped as depositional basins, and are dominated by fine-grained (silt to silty sand sized) sediment. The northern basin was interpreted as a lake floor basin, and underwater video and sub-bottom seismic reflection data suggests that the lake floor may crop out in portions of this map unit. The depositional basin on the western edge of the study area extends into Block Channel and occupies a closed depression (> 40 m water depth). Lake floor was not identified in video or seismic data from this map unit, so it was not further classified as a lake floor depositional basin.

Federal Site

Four main Quaternary (glacial) depositional environments were interpreted from the high-resolution bathymetry and sub-bottom seismic reflection data, including; Moraines, delta plain, lacustrine fan and lake floor basins (Figure I-14b; Table I-10). The moraines were separated into to two categories; the section of the moraine that is correlated to the Point Judith-Buzzards Bay moraine, and Hummocky Moraine. Hummocky moraine represents moraine segments not correlated with regional ice margins, although the three separate hummocky moraines along the southern edge of the FED study area may represent an ice margin between the terminal, Beacon Hill - Vineyard moraine of the Laurentide Ice Sheet known locally in this region as 'Coxes Ledge' and the Point Judith-Buzzards Bay moraine that occupies 11.4 sq km (4.4 sq mi) of the FED site. The hummocky moraine in the northeastern section of the FED site was originally interpreted as coastal plain strata (Figure 4, Needell et al., 1983), however reexamination of the stratigraphic relationships in the original seismic reflection profiles (Seismic line 27, Needell et al., 1983; McMullen et al., 2009) suggests this is a Quaternary deposit. The surface expression of these moraine deposits in the region are dominated by outcrops of cobble gravel pavement (PBM cgp, HM cgp) and boulder gravel pavement (PBM bgc, HM bgc). Smaller areas have sand waves (Map units PBM sw, HM sw, crest to crest spacing >200 m) and coarse sand with small dunes (Map units PBM csd, HM csd, crest to crest spacing was not resolved with the side-scan data for the FED site, but is interpreted to be 1-2 m)). Based on the water depth and grain size within this unit, the velocity needed to form these bed forms can be estimated at 0.75 – 1.5 m s^{-1}. At a depth of 30 m, these velocities are reached with a minimum wave height of 5 m, with a period of 10 seconds (Komar, 1976; Sherwood, 2007).

Within the deeper areas of the FED site (water depths mostly deeper than 35 m below present sea-level), are interpreted to represent a former glacial lake floor basin. Sub-bottom seismic reflection profiles throughout this area indicate. The two main benthic geologic habitats identified here are glacial lake floor coarse silt and glacial lake floor fine sand, encompassing 60.6 sq km and 41.7 sq km (23.4 and 16.1 sq mi) respectively. Surface sediment samples from these units range from silt to fine sand. Sub-bottom seismic reflection profiles throughout the lake floor basins have limited penetration; perhaps due to small amounts of methane gas in the relatively organic rich surface sediments. Where visible, lake floor deposits are up to 40 m thick. In the central portion of the lake floor basin, several areas with slightly higher (1-2 m) topography than adjacent areas with coarse sand and gravel, (Units GLF cs, GLF sw GLF ss), may represent small lacustrine fans, or sand and gravel transported onto the lake floor during Holocene transgression. Sub-bottom data collected from this unit was inconclusive, as was published side-scan data (Neddell et al., 1983).

In the southeast corner of FED, an area, between the areas interpreted to be hummocky moraine, is a region that is shallower than the adjacent lake floor basin, but deeper than the adjacent moraines. This is interpreted to represent a glacial lacustrine fan, deposited at the margin of the ice sheet, on the floor the glacial lake ponded behind the terminal moraine.

Surface sediment samples were not collected from this map unit, however the side-scan sonar facies indicates this is probably similar to the adjacent coarse silt low-energy basin units. On the eastern edge of FED, adjacent to the outcrop of hummocky moraine, a relatively flat area at 30 to 35 m below present sea-level is interpreted as a glacial delta that formed when the ice front retreated from the position marked by the hummocky moraine. This feature probably represents a portion of the glacial lake filled by the prograding delta. The surface sediment characteristics of this unit are based almost exclusively on the side-scan sonar data, and is interpreted to be dominated by sandy depositional environments are sandy, with some areas interpreted to be comprised of coarse sand with gravel and scattered outcrops of boulder gravel.

Multivariate analyses

The ANOSIM procedure was conducted on three depositional environment categories: unit, form, and form-unit combined. The results of the ANOSIM using form type as a factor showed the strongest relationship with the biology (global R = 0.593, p = 0.001). This result indicates that there are significantly different macrofaunal assemblages among form types. The ANOSIM procedure using form as a factor was also performed on BI and FED samples individually, both yielding lower global R values than when the study areas are combined (BI: R=0.281, p=0.002; FED: R=0.291, p=0.009). Within BI and FED, eight of the nine form types were sampled for macrofauna (refer to Table I-10). The form that was not sampled comprised only 2.6% of the study areas (3.2 sq mi). All five forms within BI were sampled and three of the five forms contained grab samples within FED (the two forms not sampled make up less than 8% of the FED study area (5.5 sq mi)).

The SIMPER results showed that the depositional environment form within-group similarity ranged from 29.11% to 53.21% (Table I-11). The samples in the Glacial Lake floor form exhibited the most similarity (53.21%), followed by Depositional Basin (46.36%) and PJ-BB Moraine (43.57%). The contribution for each of the seven genera most responsible for the within-form group similarity ranged between 10.05% and 29.30%. A different genus was the most responsible for the within-group similarity of each form group, with the exception of the genus *Astarte* (leads two groups).

Mapping

For the BI and FED study areas, the top-down approach resulted in broad-scale habitat maps consisting of five map units, as defined by depositional environment form type, with biotopes labeled by dominant genus within each map unit (Figure I-15). Within BI, Depositional Basin and Glacial Delta Plain are both defined as *A. vadorum* biotopes. Glacial Alluvial Fan and Moraine Shoal are classified by *Byblis* and *Jassa*, respectively. The remaining form in BI, Inner Shelf Moraine, is defined by two genera, *Lumbrineries hebes* and *Polycirrus*, whose abundances are nearly identical. For FED, Hummocky Moraine and PJ-BB Moraine are both defined by *Byblis* biotopes, Glacial Delta Plain is classified as an *A. vadorum* biotope, and Glacial Lake floor is defined by two species, *N. annulata* and *A. agassizi*, which have very high abundances relative to the other genera in the sample group. The biotope for Glacial Lacustrine Fan is undefined because the bottom sampling effort focused on the eastern 2/3 of the FED study area and this form type (3.2 sq mi area) is located in the south-west corner.

The dominant genus in each sample is also indicated on the top-down classification maps. This data layer was added to the maps so that the unity and variability among samples with within each map unit could be seen. For example, the majority of samples within the Glacial Delta Plain and Depositional Basin forms is are dominated by the genus, *Ampelisca vadorum*, for which the biotope is named (refer to Figure I-15). However, within the Glacial Alluvial Fan, Hummocky Moraine, and PJ-BB Moraine forms, defined as *Byblis* biotopes, only one-third of the samples are dominated by *Byblis*.

Bottom-Up Habitat Mapping Approach

Univariate analyses

The Pearson correlation coefficient rejected the hypothesis that there is a positive relationship between macrofaunal diversity and abundance with regards to surface roughness ($r = -0.30$ and $r = 0.12$, respectively) or the standard deviation of the sediment ($r = -0.17$ and $r = -0.04$, respectively).

Multivariate analyses

The second BIOENV procedure, BIOENV + BI & FED, identified a subset of six abiotic variables as being the most correlated the macrofaunal composition (Rho = 0.697, $p = 0.001$).

The variables responsible were percent medium sand, percent coarse sand, standard deviation of the grain size (µm), maximum backscatter intensity, mean depth (m), and surface roughness. Mean depth was the single variable having the highest correlation (Rho = 0.522) with the macrofaunal assemblage.

The LINKTREE created using the subset of abiotic variables identified in the BIOENV + BI & FED procedure resulted in 22 classes, each of which are defined by a series of abiotic thresholds of the six input variables (Figure I-16; Table I-12). Of the 22 classes, 13 classes were comprised of only BI samples, four of only FED samples, and five contained samples from both BI and FED. The BI area contained 18 LINKTREE classes, whereas nine were found within FED. The number of samples in each class ranged from 2 to 14. Each of the class breaks were significant (> 5%) and all R values were between 0.36 and 0.81. Percent medium sand was responsible for six of the thresholds, surface roughness for five thresholds, and mean depth, percent coarse sand, standard deviation of the sediment, and maximum backscatter intensity were responsible for four, three, two, and one threshold, respectively. A number of these thresholds are defined over a narrow range (refer to Table I-12). For example, split "J" divides to the left at surface roughness less than 0.120 and to the right at greater than 0.124, and split "M" is defined by mean water depth less than 19.0 m to the left and greater than 19.7 m to the right. The ANOSIM indicated there are strong differences (R = 0.833, p = 0.001) between the macrofaunal assemblage among LINKTREE classes.

Within each LINKTREE class, the most abundant genus was determined (Table I-13). For class 8, 9, 16, and 17, the two most abundant genera were noted because both genera had equal very high abundances compared to other genera present. Class 12 identified three genera because they share equal abundance. Tube-building amphipods dominated the classes, being the most abundant genus or sharing most abundant for 12 classes. Specifically, the genus, *Byblis*, was dominant or shared dominance for six classes, the species, *Ampelisca vadorum*, for five classes, and the genus, *Jassa*, for one class. Polychaete genera were the most abundant or shared abundance for eight classes and molluscs for five classes.

The SIMPER results showed that the overall LINKTREE class similarity ranged from 5.8% to 64.76% (refer to Table I-13). The genus most responsible for the within-class similarity of each LINKTREE class contributed between 8.82% and 100.00% to the similarity. For 16 of the 22 classes, the single genus contributing most to the within-class similarity was recorded and for six classes, between two and four genera are given because they contribute equally or nearly equally. In total, SIMPER identified 19 genera for the 22 LINKTREE classes as being most responsible for the similarity within a group (either solely or in conjunction with other genera). Most of these genera were either crustaceans (accounting for eight genera, four of which were tube-building amphipods) or polychaetes (seven genera). The genera responsible for multiple classes were *Lumbrineries hebes,* which was responsible for the greatest similarity for five classes (either solely or in part), followed by *Byblis, Nucula annulata, and Polygordius* each for three classes, and *Nemertean* for two. The same genus was the most abundant and the most responsible for the within-group similarity for eight of the 22 classes, six of which were the tube-building amphipods and two were the mollusc, *Nucula annulata*.

Mapping

The benthic habitat maps included 78 pixels of 100 m resolution (Figure I-17). The maps contained 22 benthic habitat classes, as identified in the LINKTREE procedure. These classes, or biotopes, were classified according to the dominant genus in terms of abundance and the final threshold defining the class (Figure I-18). Five biotopes are classified by the two – three most abundant genera because both genera showed equal or very high abundances relative to the other genera within the group samples. The biotope defined by *Polycirrus* occurred most often, encompassing 14 pixels, all within BI, followed closely by the biotope classified as *A. agassizi – N. annulata*, having 13 pixels all within FED. The *Byblis – N. annulata* biotope defined five pixels within FED. The remaining classes each encompassed 2-3 pixels. Of the 22 benthic habitat classes, over half (13) were contained solely within BI, four were found within FED only, and BI and FED share five classes (each defined by the tube-building amphipods, either *Byblis* or *A. Vadorum*). Therefore, in total, 18 classes are seen within BI and 9 within FED.

In total, 17 different genera define the 22 biotopes. Polychaetes account for seven of the 17 genera, followed by tube-building amphipods (four genera), then molluscs (three), crustaceans (two), and oligochaetes (one). Though polychaetes are the dominant genera, crustaceans define (at least in part) 15 of the 22 biotopes, 13 of which are tube-building amphipods (because *Byblis* classifies six biotopes and *A. vadorum* five). Each of the seven polychaete genera define one class and the molluscs are responsible for five classes (*N. annulata* appears three times), and the two crustaceans share the classification of one biotope.

1.5 Discussion

Maps of the distribution of benthic habitats are valuable tools for numerous ecological and management reasons, including understanding ecosystem patterns and processes, determining environmental baselines, impact assessment, and conservation efforts. The purpose of this study was to construct benthic habitat maps for two areas, BI and FED, within the RI Ocean SAMP study area using methods not before applied to offshore environments. To generate the habitat maps, both top-down and bottom-up methodologies were employed. The top-down approach follows the idea that geologic environments or features, such as sediment type, contain distinct biological assemblages. The bottom-up approach, on the other hand, integrates multiple types of data over various scales and establishes relationships between macrofaunal communities and environmental parameters.

Comparison of the Top-Down and Bottom-Up Benthic Habitat Mappings Techniques

This study revealed the benefits and disadvantages of the top-down and bottom-up habitat classification methods. Both approaches were successful in that they exhibited strong and statistically significant relationships with the macrofauna assemblage. The top-down classification provided full-coverage habitat maps using geologically-defined map units. The bottom-up classification identified a subset of abiotic parameters (five for BIOENV + video, six + BI & FED, respectively) most influencing the macrofauna patterns.

A potential drawback of the top-down method is that the habitat classes are defined on a broad scale; five depositional environment forms defined eight map units in each BI and FED. Furthermore, within some biotopes the majority of the bottom samples are dominated by the genus the biotope is named for, whereas within other biotopes, only a few bottom samples are dominated by the biotope-defined genus. That the relationship was statistically strongest between form type and the biology is likely because there are a high number of samples within these map units relative to other, smaller scale units. For instance, the majority of the form-facies map units are un-sampled. The major weakness of the bottom-up method is that full-coverage maps could not be created; the lack of spatial auto-correlation between point sample datasets (i.e. grain size) prohibited interpolation.

The top-down and bottom-up approaches differ largely in the number of habitat classes yielded by each and how they are distributed. These differences are likely due to the scale at which each classification approach was mapped, since the top-down map units expand over square miles and the bottom-up map strictly classifies 100 m map units. Also, in the top-down method, forms are merged into one biotope if they are dominated by the same genus (i.e. DB and GDP are represented as the same *Ampelisca vadorum* biotope), whereas, within the bottom-up approach, each LINKTREE-defined class remains its own biotope (i.e. there are five *Ampelisca vadorum* biotopes, each defined by a different series of abiotic thresholds).

Both classification methods showed tube-building amphipods are responsible for defining over half of the habitat classes, indicating amphipods dominate the abundance within the BI and FED study areas. Tube-building amphipods form very dense, abundance-rich tube mats and a grab sample within one of these mats may contain over 1,000 individuals (as was found in stations BI 1 and 2). Because biotopes are defined by the dominant genus among the within-form/class samples, the amphipod genera may be masking patterns and other influential genera within the study areas. Evidence of this overshadowing by amphipods can be seen in the top-down classification maps where biotopes are classified by a tube-building amphipod, but in many of the individual bottom samples that same amphipod is not the most abundant. Furthermore, examination of the macrofauna data shows that tube-building amphipods account for five of the top ten most abundant genera within BI and FED (refer to Table I-7), but appear only twice in the top ten spatially (% of samples found within) most abundant genera.

Comparison of BI and FED Study Areas

The results of the benthic habitat classifications suggest the macrofaunal assemblages vary between the two study areas and primarily have their own associations with the environment. That the two study areas differ is supported by the majority of the benthic habitat classes being observed solely within either BI or FED. We hypothesize that physical processes creating different benthic environments within BI and FED are responsible for the lack of similarity in the macrofaunal assemblages within each study area. For example, the depositional environment maps reveal that each study area has undergone different geologic processes, as BI and FED have only one depositional environment form in common. The location of the BI and FED study areas may also influence the biological patterns. BI is located close to land (Block Island) and exhibits increasing water depth with increasing distance from the coast. Because of its location, BI is a dynamic environment, as exemplified by the presence of mobile sand waves and sheet sands visible in the side-scan backscatter mosaic and depositional environment map. The benthic communities within BI may be more affected by storms and other mixing events (adversely in the sense of habitat damage and favorably in terms of nutrient cycling and mixing) and may exhibit more light availability. The FED study area is located in the heart of Rhode Island Sound and has deeper water depths that change based on the presence/absence of glacial moraines. FED appears to be a more stable environment and the benthic communities are likely influenced by factors such as stratification (possibly resulting in nutrient deficiencies) and light limitation.

If the goal of the mapping effort was to characterize the finest-scale abiotic-biotic relationships in both areas, then the observed degree of separation between BI and FED classes supports the case for conducting separate analyses and generating separate maps for each study area. From a management perspective, overly-site-specific analyses and maps may not be as useful as a geographically-broad analysis that allows habitat comparisons between areas. Our approach addresses the latter point, and the results indicate that BI and FED may differ fundamentally in terms of how species utilize the benthic environment.

Heterogeneity

There is a high degree of benthic habitat heterogeneity, particularly within BI and the glacial moraines of FED. The large number of bottom types that exist over a range of spatial scales within these study areas demonstrates this heterogeneity, which is visible in the side-scan and bathymetry mosaics and in the depositional environments maps. Further evidence of benthic habitat heterogeneity within BI and FED lies in there being little to no spatial autocorrelation (e.g. samples closer in space are more similar than those further away) between percent fine, medium or coarse sand samples within BI or FED. Sediment samples were collected at a density of one (BI) or 1.5 (FED) samples per square mile, suggesting habitat changes occur over spatial resolutions (i.e. scales) less than one square mile. Evidence of this habitat heterogeneity over small scales exists and is not an artifact of sampling density is seen in the examination of the side-scan, bathymetry, and slope maps. Additional evidence is found in the LINKTREE results; the thresholds used to define benthic habitat classes occur over narrow ranges of the abiotic variables (refer to Table I-12).

Scale

The scale at which the environmental parameters and acoustic patterns are examined is important in assessing abiotic-biotic relationships. This importance can be seen in the results of the BIOENV procedures (+ video and + BI & FED), which indicate the macrofauna patterns within BI and FED are linked to sediment characteristics at both fine and broad spatial scales.

The fine scale link is with the grain size from the analysis of the sediment sample (i.e. percent medium and coarse sand). Similar sediment-macrofauna relationships have been observed in a number of previous studies (Gray, 1974, Rhoads, 1974, Chang et al.,1992, Snelgrove and Butman,1994, Zajac et al., 2000, Ellingsen, 2002, Verfaillie et al., 2009). A broad-scale link between sediment and macrofauna is seen with the bottom type cover (i.e. percent fine sand bottom) of the underwater video. Other studies (Brown and Collier, 2008, Rooper and Zimmerman, 2007, Kendall et al., 2005), have also found underwater video metrics (such as sediment composition) to be valuable in constructing and classifying habitat maps. Recognizing this, our aim is to incorporate underwater video analyses in both BI and FED habitat maps when the full datasets are available.

The BIOENV results also reveal relationships between macrofauna patterns with small and broad scale environmental heterogeneity, via the standard deviation of the sediment grain size and surface roughness, respectively. That the macrofauna have such a close relationship to these two datasets is interesting because they are very different measures of environmental heterogeneity; standard deviation of the sediment is a point sample that measures variation in the size of grains of sediment within a sample, while surface roughness is a 100 m pixel resolution dataset calculated as the standard deviation of the slope within a 1000 m radius. The surface roughness link is particularly intriguing since the biology is sampled over $0.05m^2$ area and surface roughness integrates data from as far as 1000 m away. Perhaps the two measures of environmental heterogeneity influence the macrofauna in different ways. For example, previous studies (e.g. Gray, 1974; Ellingsen, 2002) have reported positive relationships between habitat variety and species diversity, following the rationale that a greater degree of sediment heterogeneity offers more potential niches, and therefore, allows for higher diversity (Rosenzweig, 1995).

Mean water depth is another influential broad-scale factor linked to the macrofauna. This parameter, in fact, exhibited the highest correlation with the biology in the BIOENV procedure. The details behind this depth-biology relationship are difficult to sort out because water depth could represent one or more of numerous physical environmental gradients, including temperature, pressure, and the availability of light and nutrients. The amount of turbulence and mixing at and near the seafloor due to wave and wind energy might be indirectly indicated by water depth, as well. Further studies that examine any depth-dependent variables will help resolve this relationship.

BIOENV also indicated a broad-scale link between macrofauna and the maximum backscatter intensity of the side-scan sonar mosaic. The reason for this relationship, though, is not clear. Studies have shown positive correlations between backscatter intensity and grain size (Goff et al., 2000, Hewitt et al., 2004, Collier and Brown, 2005). Therefore, the maximum backscatter intensity may represent a macrofauna-sediment size link.

Scale of data analysis was also found to be important in assessing the relationship between measures of environmental heterogeneity (in this study, surface roughness and standard deviation of the sediment grain size) and macrofaunal patterns, diversity and abundance. The univariate analysis showed little correlation between either surface roughness or standard deviation of grain size with either diversity, or abundance, whereas the multivariate BIOENV procedures (BIOENV + video and BIOENV + BI & FED) showed strong correlations with both surface roughness and standard deviation of grain size with macrofaunal assemblage composition. We hypothesize the reason for this mismatch is related to the statistical method and the scale at which the macrofaunal and abiotic data within BI and FED were examined, rather than the resolution of the surface roughness and standard deviation of grain size datasets (because both were rejected by the Pearson correlation and identified in the BIOENV analysis). Multivariate analyses tend to be more sensitive than univariate methods to small changes in faunal composition (Gray et al., 1990, Warwick and Clarke, 1991, 1993). The BIOENV routine considers the composition of the macrofaunal assemblage for each station, whereas the Pearson correlation coefficient utilizes a summary statistic for the diversity and abundance at each station. Because of this difference, the BIOENV procedure may discern finer scale relationships between the biology and the abiotic variables. For example, one or more genera may be influencing the results of the BIOENV if a strong link exists with one or more abiotic parameters. Such links were found by Olsgard and Somerfield (2000) who reported polychaetes exhibited the strongest relationship to the environmental parameters. Similarly, in another study (Ellingsen, 2002), molluscs, followed by polychaetes, had stronger connections to the environmental variables than crustaceans and echinoderms.

Macrofaunal Diversity and Abundance

Macrofauna diversity and abundance were linked in this study. The majority of stations with a high diversity also had a high abundance (e.g. BI 2, 16, 37 and F13, 32, 36) and diversity was particularly high in samples containing tube-building organisms. This association between diversity and tube-builders suggests tube-mat structures provide valuable habitats. Ellingsen (2002) suggested polychaete tube-mat structures may increase sediment heterogeneity (i.e. habitat complexity), and, as a result, positively influence benthic ecosystems. It is also possible that tube-builders positively interact with other genera (predator, prey, competition), which results in increased diversity. Pratt (1973) reported that suspension feeders (such as tube-building amphipods) physically dominate hard surfaces, but, despite this, a diverse range of fauna (deposit feeders, predators, browsers) reach high densities in mature epifaunal assemblages. Pratt (1973) also noted that within Rhode Island Sound there was a correlation between the presence of the amphipod, *Ampelisca agassizi*, and the abundances of several infaunal species including detritus feeding amphipods, isopods, cumaceans, and a polychaete, *Prionospio malmgreni*.

Environmental conditions may explain the reason for the stations with the lowest macrofauna diversity also having the lowest abundance (e.g. BI 3, 24, 25, 42). Comparison of stations BI 24 and BI 42 (both classified as *Protohaustorius* biotopes) and BI 25 (classified as *Byblis* biotope) with the grain size analysis, underwater video, and benthic geologic environment indicate that these sampling stations occur within the inner shelf moraine on large-scale medium and coarse grained sand waves or sheets. Station BI 3 (*Polycirrus* biotope) is located on the moraine shoal within an area of boulders and very coarse grained material. The existence of sand waves, sheets, and ripples suggest sediment mobility. Therefore, these dynamic environments may present conditions too stressful for many genera, as organisms living in these areas must be adapted for movement in sand and be able to recover from periodic burial (Pratt 1973).

Station BI 23 is unique among all BI and FED samples because it has low diversity (9 genera), but high abundance (680 individuals), with the tube-building amphipod, *Byblis*, accounting for 97% of this abundance. This station exhibits biologic characteristics contradictory to other macrofaunal assemblages containing tube-building amphipods found in this study and by Pratt (1973), which have high diversity. The reason this environment can support *Byblis*, but few other genera (including other tube-builders) is not resolved. Data from the underwater video, benthic geologic environment and grain size analysis show that BI 23 is located within the glacial alluvial fan in a sandy, rippled environment, which may partly explain the low diversity. Station BI 23 may also have low diversity and high abundance if the area has undergone a recent disturbance event and is in the process of recovery. A study of disturbance from dredge spoil on a stable sand area found that amphipod species, including *Byblis*, were among the early colonizers of the spoil material (Pratt 1973).

Temporal Variability

Temporal variability can present a challenge to benthic habitat mapping, both in data collection and in creating final products. In terms of data collection, it is possible seasonal differences in macrofaunal community composition are reflected in our results. However, Steimle (1982) reported there were no clearly defined seasonal changes between biological communities examined in February and in September within BIS. Steimle also presented evidence to suggest BIS is a relatively stable environment. Furthermore, Vincx et al. (2007) used a pooled biological data spanning 10 years and all seasons to produce a habitat suitability model to map macrobenthic communities for an area in the North Sea, for which the average *a posteriori* accuracy of 77% was reported.

With regard to temporal variability and creating final products, benthic habitat maps often do not reflect the temporal dynamics of mobile features since they are created using abiotic and biotic datasets representing single sampling/survey events in time. However, qualitative descriptors of temporal patterns/variability may be inferred from abiotic and biotic data. For instance, stations BI 22-25 are unstable physical environments (mobile sheet sands, sand waves, sand ripples) and characteristics (abiotic and biotic) of the benthic habitats in these areas may change. With regard to biotic data, temporal variability may be indicated by the presence of opportunistic species that reflect recent habitat disturbance, or the presence of large, long-lived individuals that indicate a more stable environment and potentially lower temporal variability in macrofauna composition (Pearson 1978). For example, station BI 23 has low diversity, but a high abundance of the genus, *Byblis*, which can be viewed as an opportunistic genus, since it was found to be an early colonizer at a dredge spoil material site (Pratt 1973).

Future work

The narrow ranges of the LINKTREE thresholds and the uncertainty of whether water depth is influencing macrofaunal patterns or another parameter manifesting itself as water depth is instead the dominant influence, indicate that our statistical methods were very sensitive to environmental and biological characteristics Both of these findings argue for including additional data types (e.g. sediment organic content, average annual surface chlorophyll concentration, rugosity, nutrient and light availability, temperature, current flow, and trophic interactions) in the future that may help refine abiotic-biotic relationships and habitat patterns.

The high degree of environmental heterogeneity within BI and FED impedes our ability to confidently interpolate the grain size point samples into full-coverage data layers using traditional methods (such as Ordinary Kriging and Inverse Distance Weighting). Our concern for retaining accuracy is echoed by Brown and Collier (2008), who remarked that interpolation methods can often lead to erroneous assumptions in the resulting map, particularly if the degree of seafloor heterogeneity reflected by surficial geology and biota is high. Consequently, taking a conservative approach and constructing benthic habitat maps for BI and FED that retain the original extent of the available abiotic data was the most accurate approach. Future studies will examine the linear relationship between the grain size data (point-coverage) and acoustic data (full-coverage) to assess the possibility of interpolating the grain size data via linear regression.

1.6 Conclusion

In the BI and FED areas within the RI Ocean SAMP study area, benthic habitat classification maps were created using two classification approaches, top-down and bottom-up. Both approaches exhibited statistically strong and significant abiotic-biotic relationships. The traditional, top-down method yielded full-coverage habitat maps that describe broad-scale patterns in both benthic geological and biological resources based on geologically-defined map units. The bottom-up method, not before applied to offshore environments, used data integration methods to establish meaningful relationships between the biological communities and environmental parameters. This approach identified six abiotic variables that influence the macrofauna composition and defined benthic habitat classes on a finer-scale. However, spatial heterogeneity in these abiotic variables prevented broad-scale extrapolation of habitat map units using the bottom-up method. Given a higher spatial density of bottom samples, this problem could be rectified.

This study supports including all available environmental parameters to investigate abiotic-biotic relationships. The macrofauna showed strong correlations with variables over a range of scales. Broad-scale relationships were found with the macrofauna and depositional environment form type (used in the top-down analysis), mean water depth, surface roughness, and maximum backscatter intensity (identified in the bottom-up analysis). Fine-scale links existed between the macrofauna and grain size measurements; specifically percent medium and coarse sand and standard deviation of the sediment. Furthermore, that the abiotic-biotic relationships were statistically strong despite geologic and biologic differences within BI and FED suggests that the macrofaunal assemblages primarily have their own associations with environmental parameters.

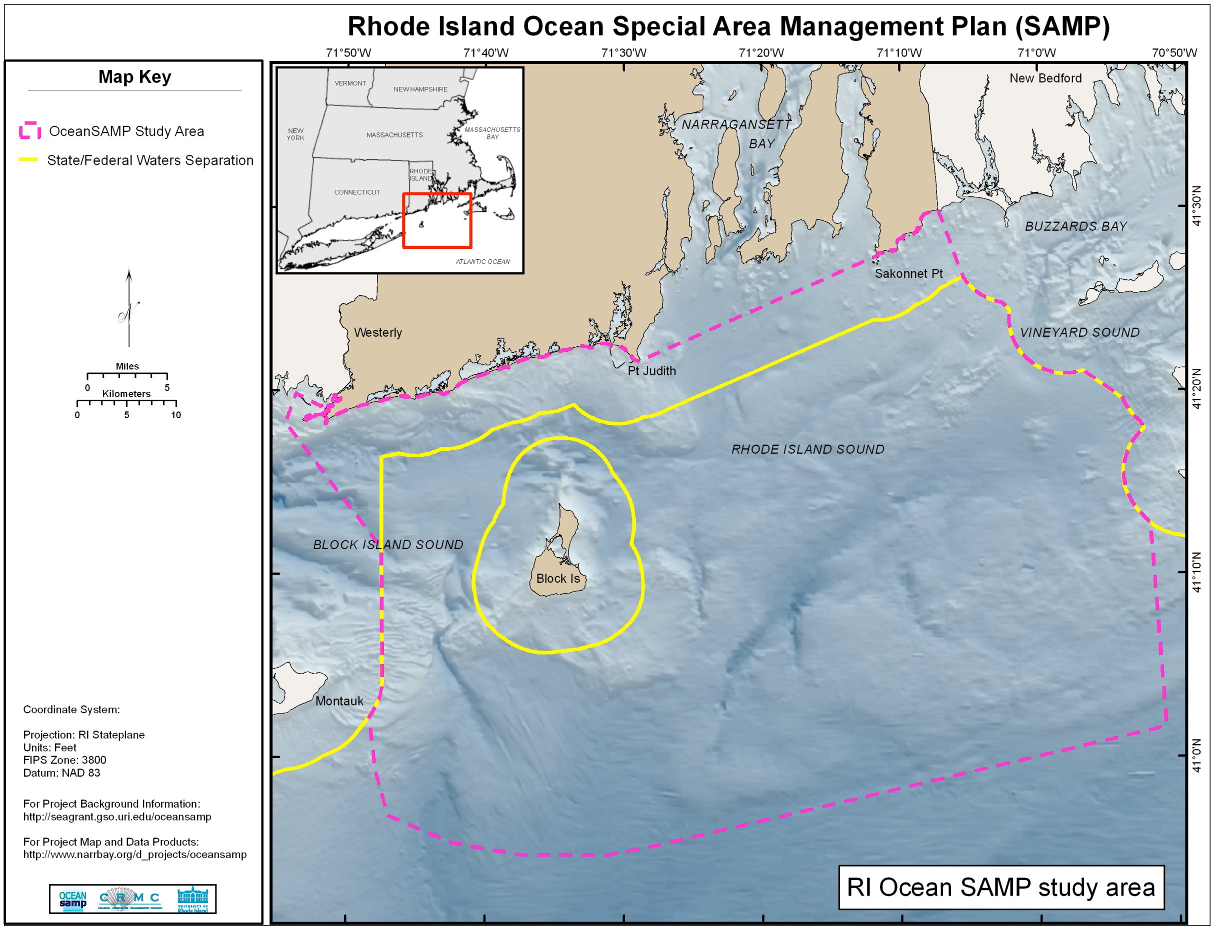

Figure I-1. RI Ocean SAMP study area.

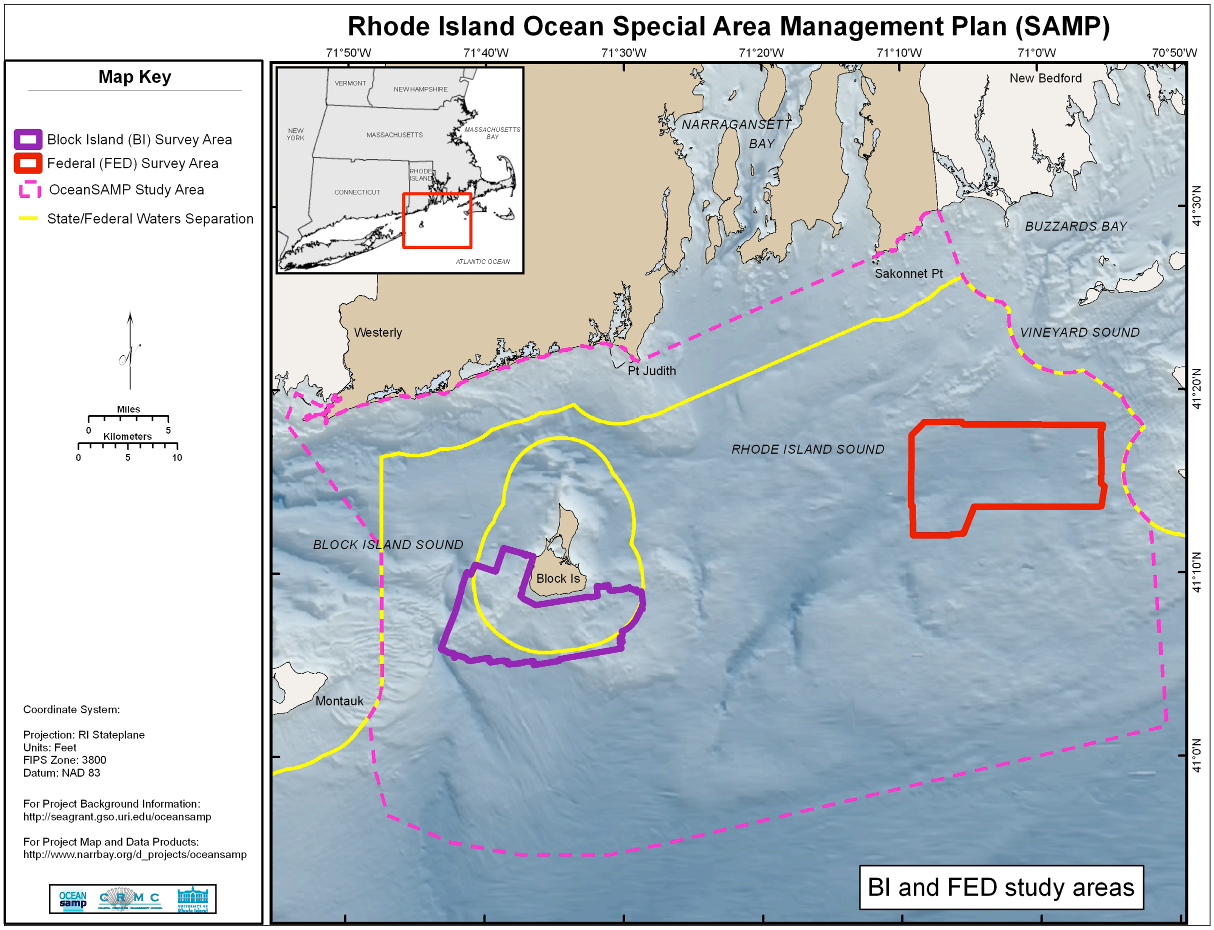

Figure I-2. Locations of BI and FED study areas within RI Ocean SAMP study area.

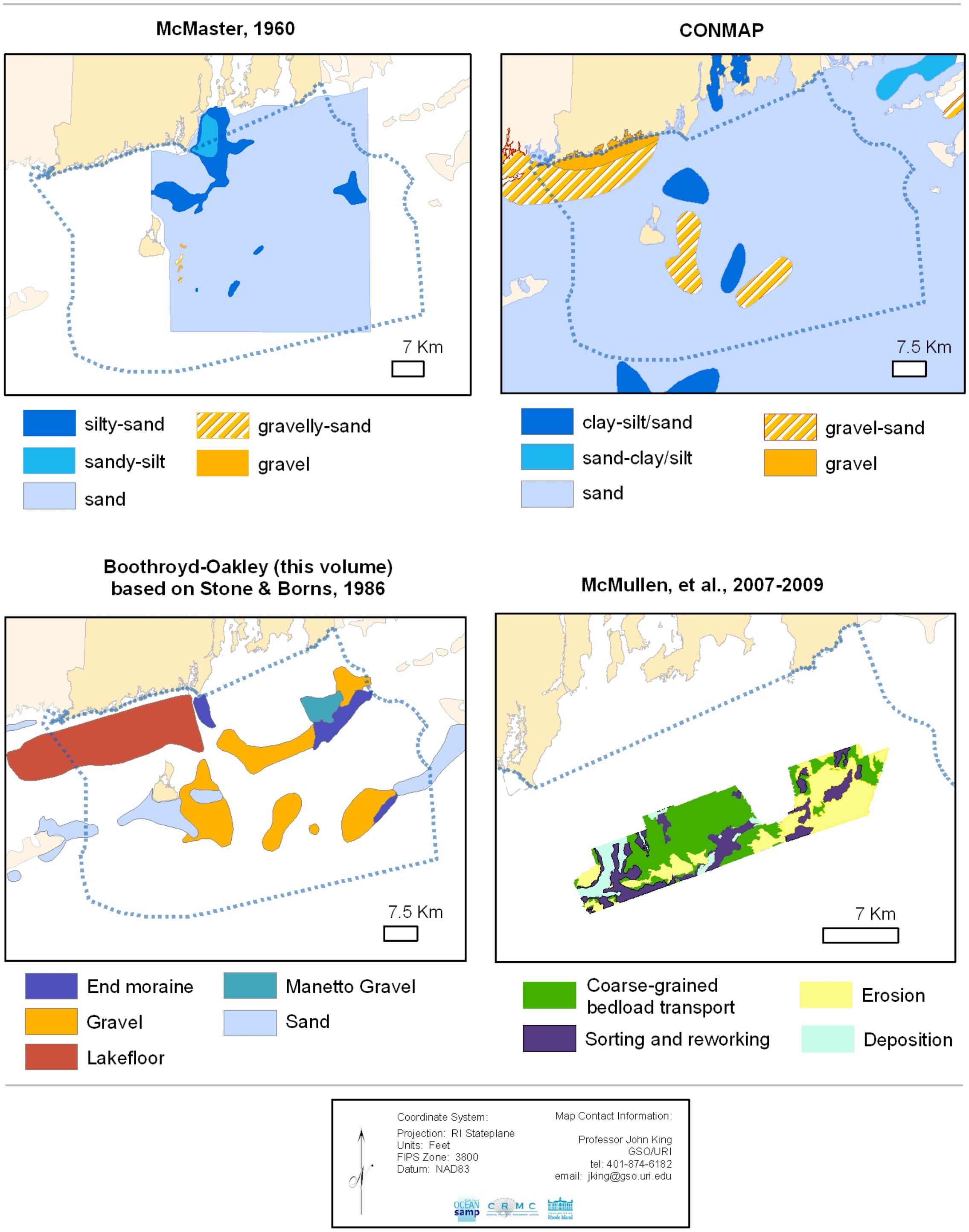

Figure I-3. Results of previous studies of surficial sediments in RI Ocean SAMP study area.

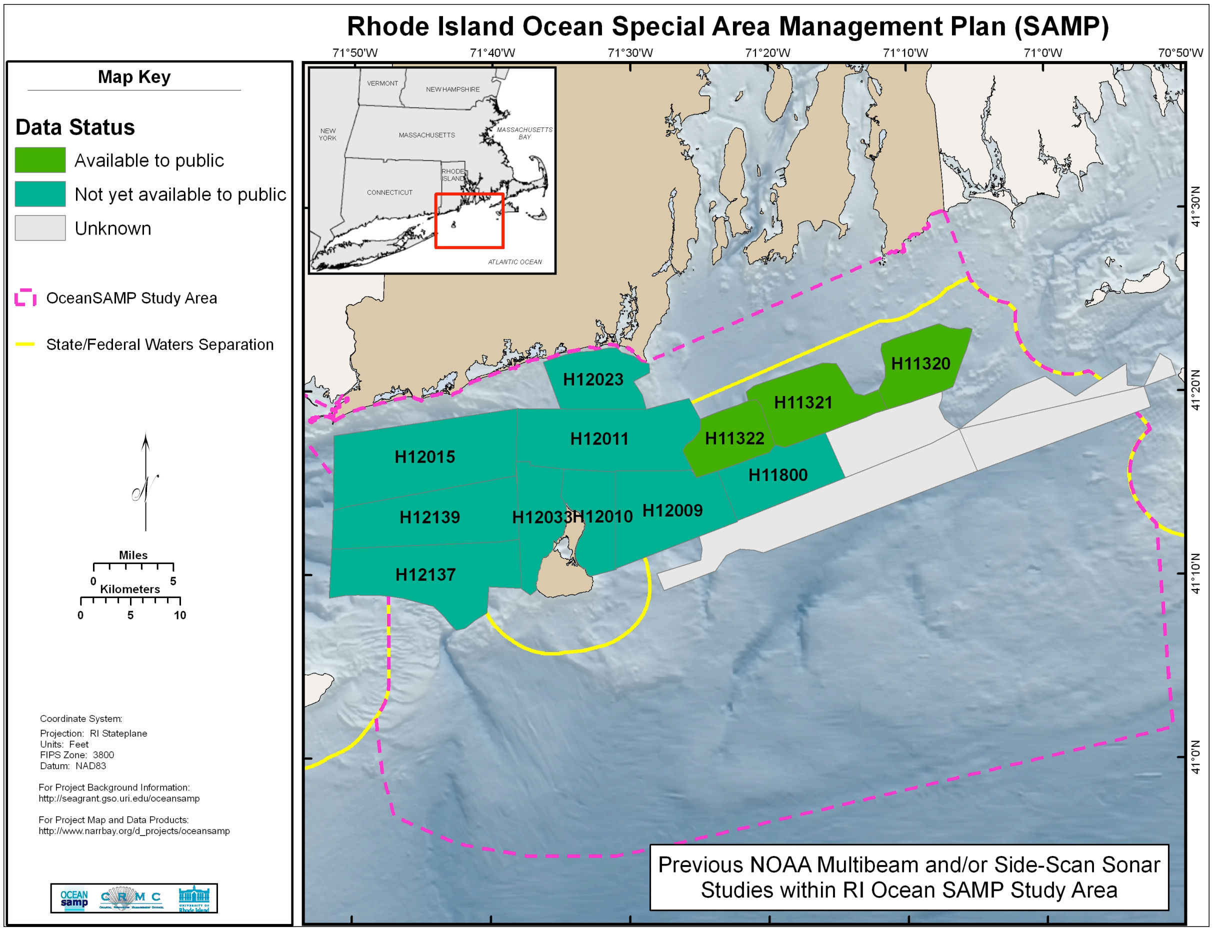

Figure I-4. High-resolution swath bathymetry and side-scan sonar surveys within the RI Ocean SAMP study area by NOAA.

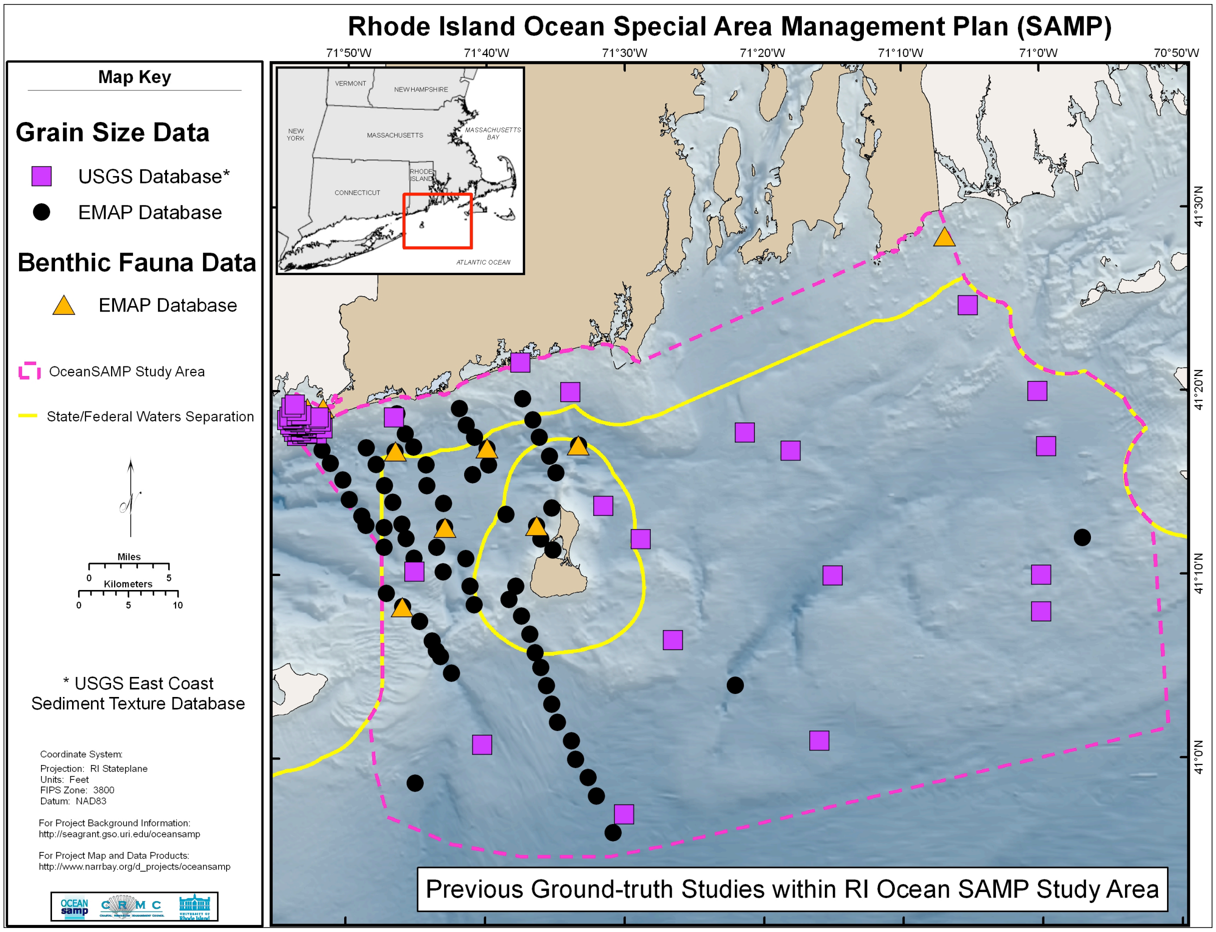

Figure I-5. Previous ground-truth studies within RI Ocean SAMP study area. EMAP 2002, U.S. Geological Survey 2005, usSEABED, 2005.

a.

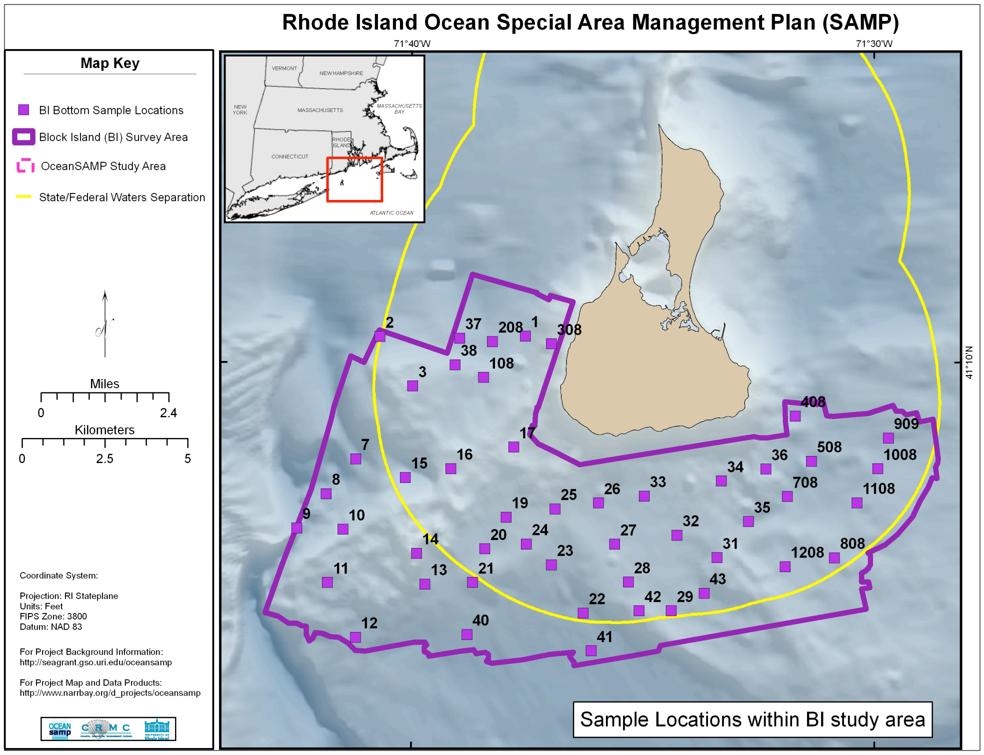

b.

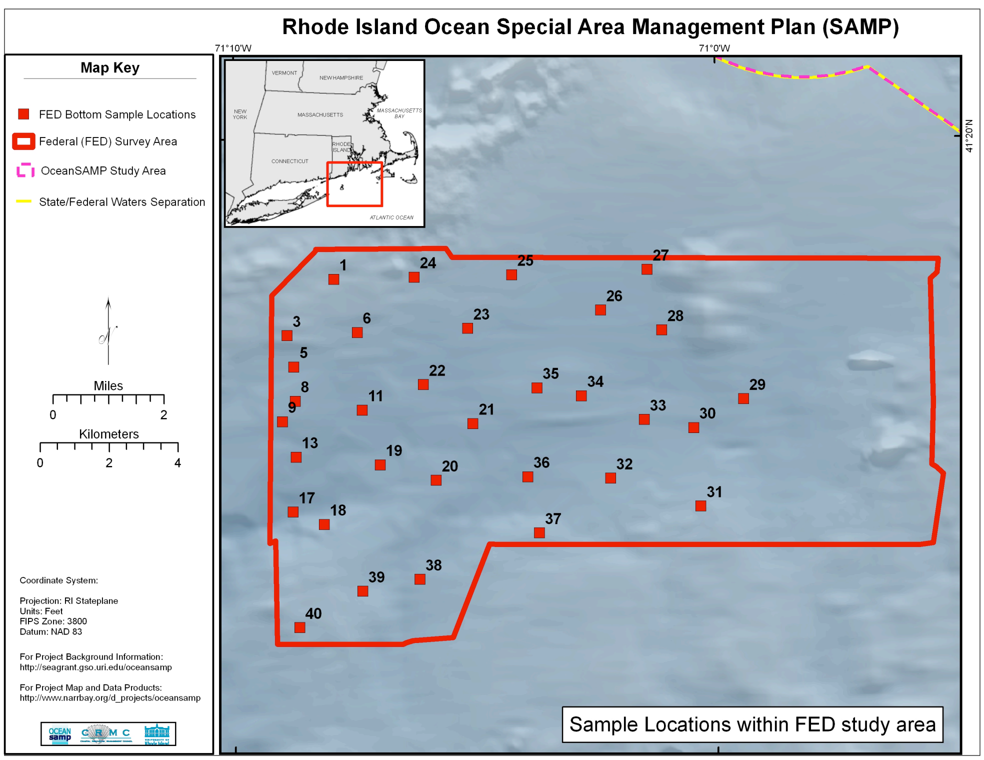

Figure I-6. Locations of the bottom samples taken within (a.) BI and (b.) FED. BI samples 4, 5, 6, 18, 30, 608, 1308, 1408, along with FED 22 and 40 were eliminated from the study because little to no material was recovered in the bottom sample. Underwater video was collected for BI stations 1-45 only.

a.

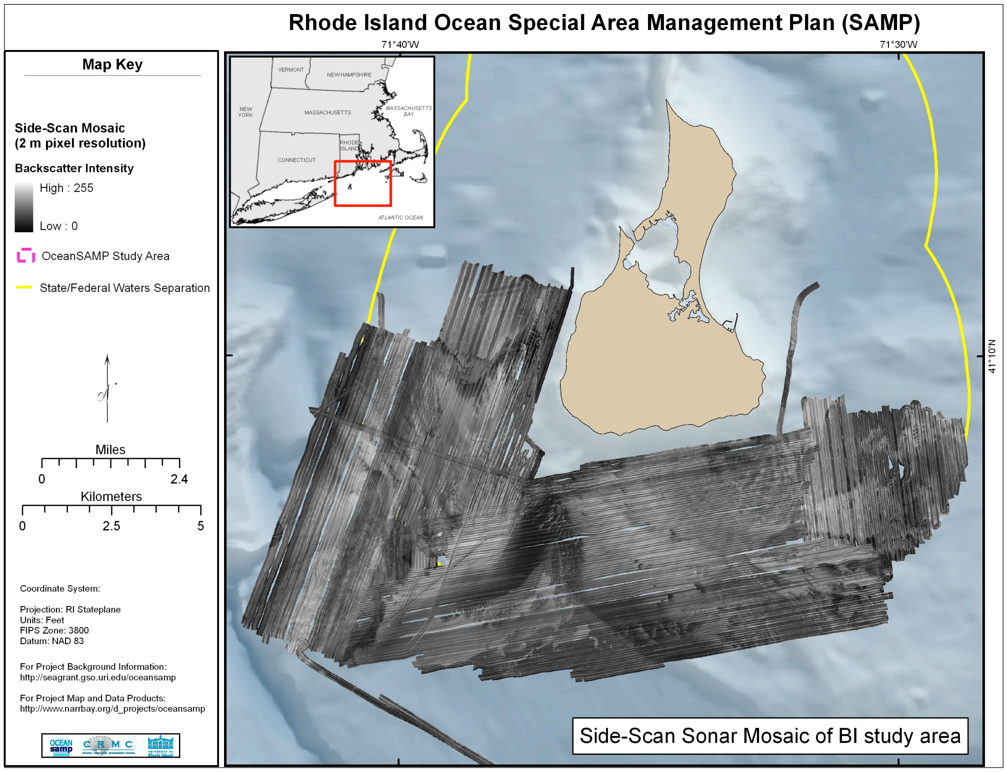

b.

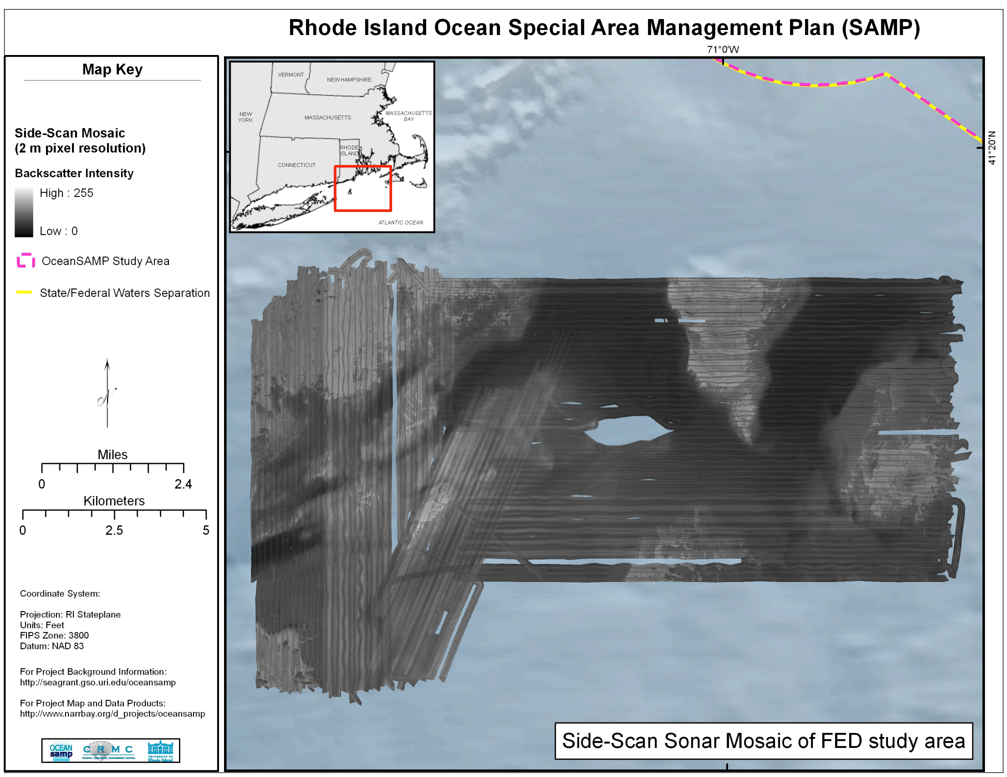

Figure I-7. Side-scan sonar backscatter mosaics of (a.) BI and (b.) FED. The mosaic is displayed on an inverse grey-scale. White (255) represents high backscatter intensity and black (0) represents low backscatter intensity, indicative of reflective (usually harder) surfaces and absorbent (usually softer) surfaces, respectively. The pixel resolution of the backscatter mosaics is 2 m. For the statistical analyses, the pixels were aggregated to 100 m resolution (not shown; see text for more details).

a.

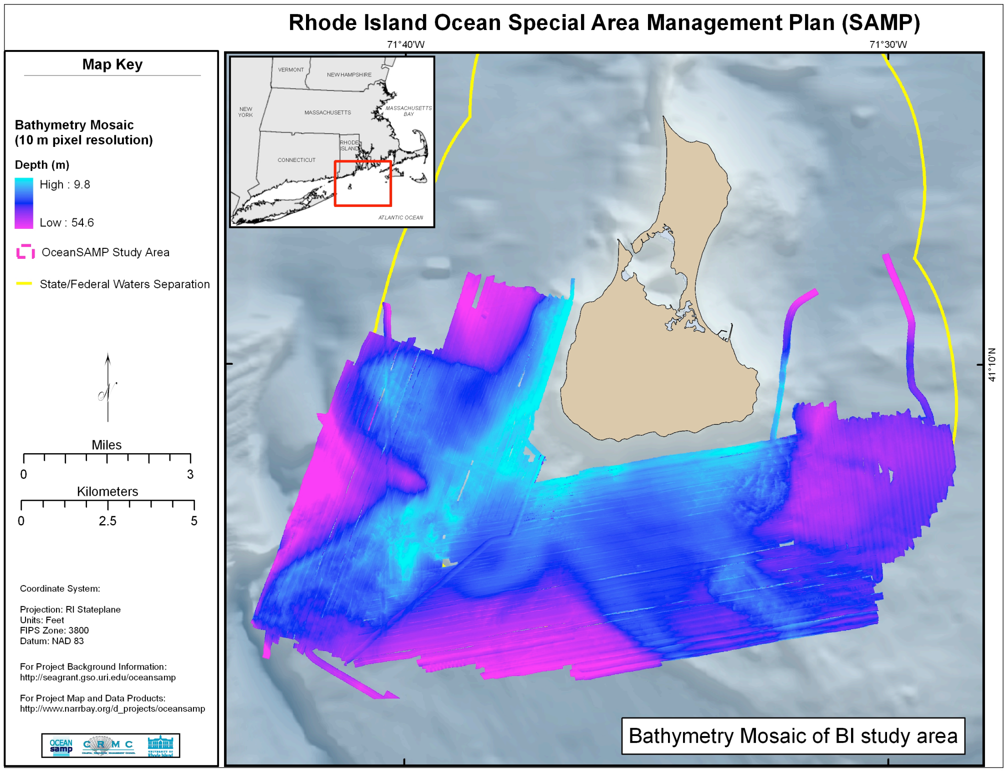

b.

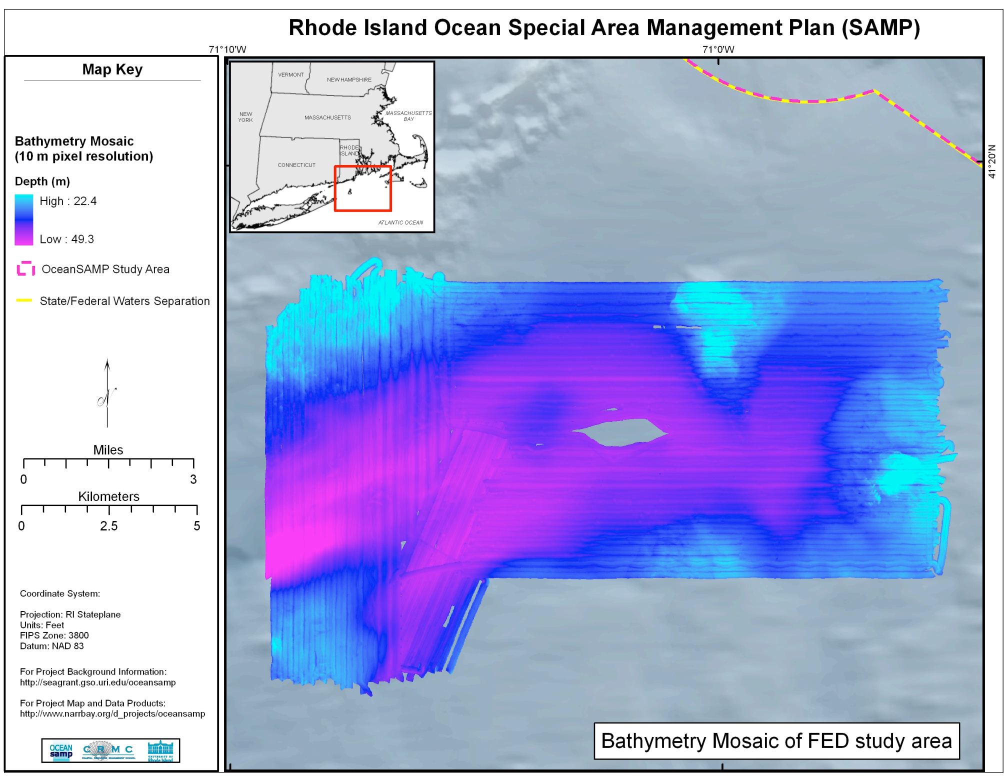

Figure I-8. Bathymetry of (a.) BI and (b.) FED. Water depth within the two study areas ranges from 9.4 m to 54.6 m, with light blue signifying shallower depths and purple signifying deeper depths. Note the scales for BI and FED are different, so as to visually enhance the features within each area. The mosaic pixel resolution is 10 m. For statistical analyses, the pixel resolution was aggregated to 100 m (not shown; see text for further details).

a.

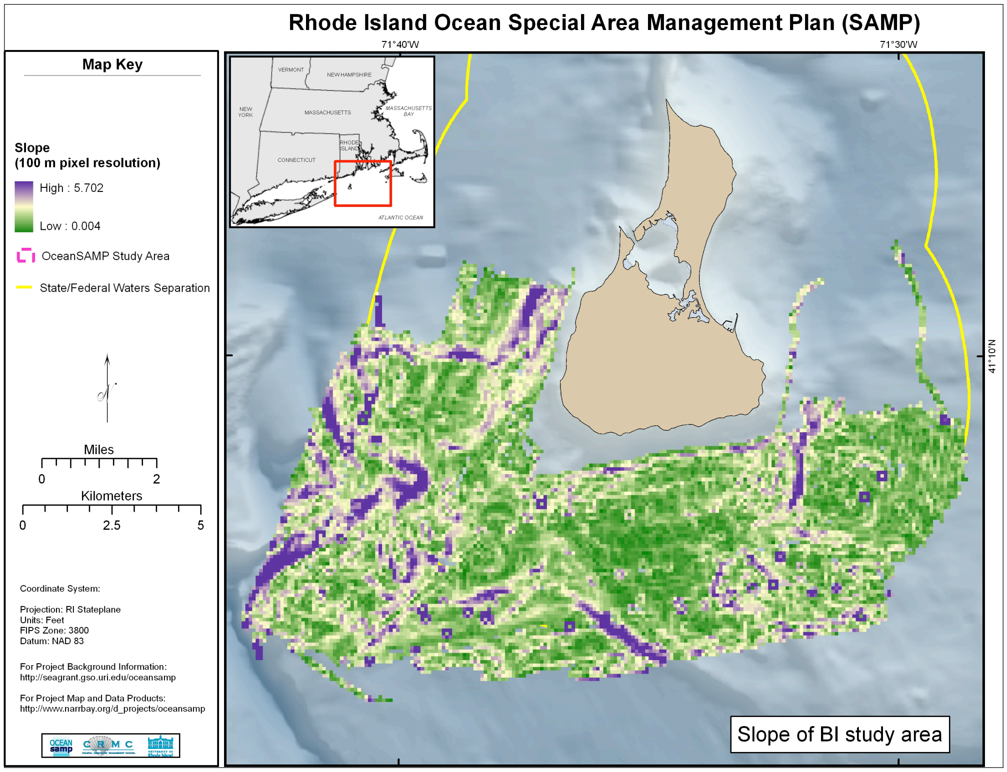

b.

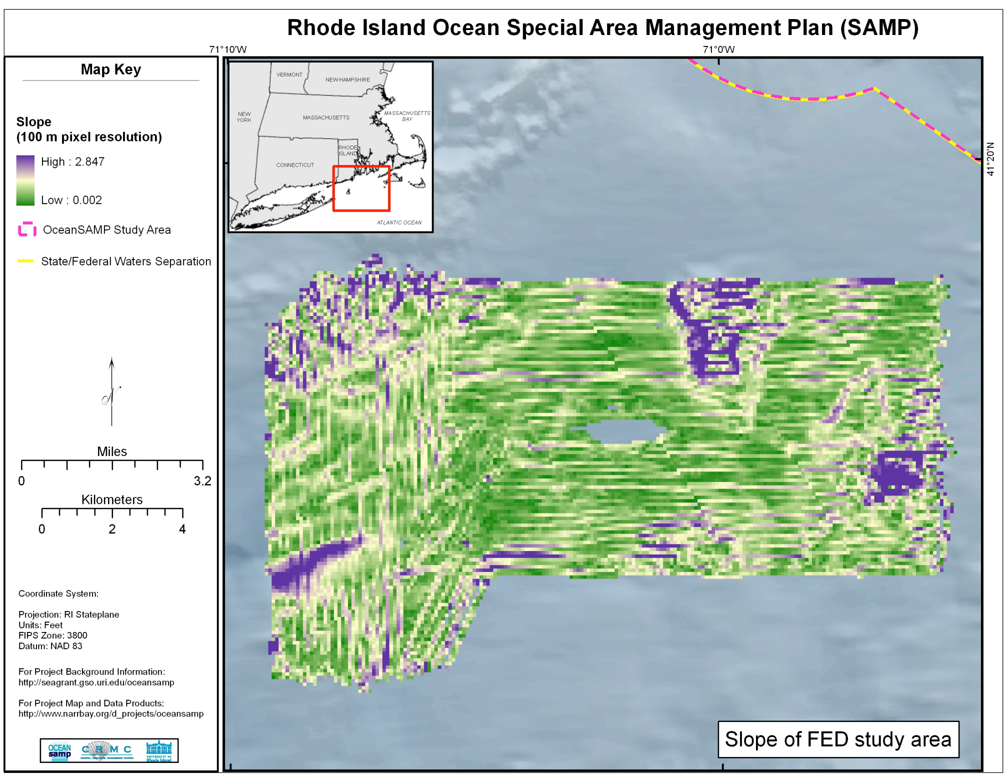

Figure I-9. Slope of (a.) BI and (b.) FED. The slope is measured in degrees, with purple indicating high slope values and green representing low values. Note the scales for BI and FED are different, so as to visually enhance the features within each area. The slope was calculated at 100 m pixel resolution.

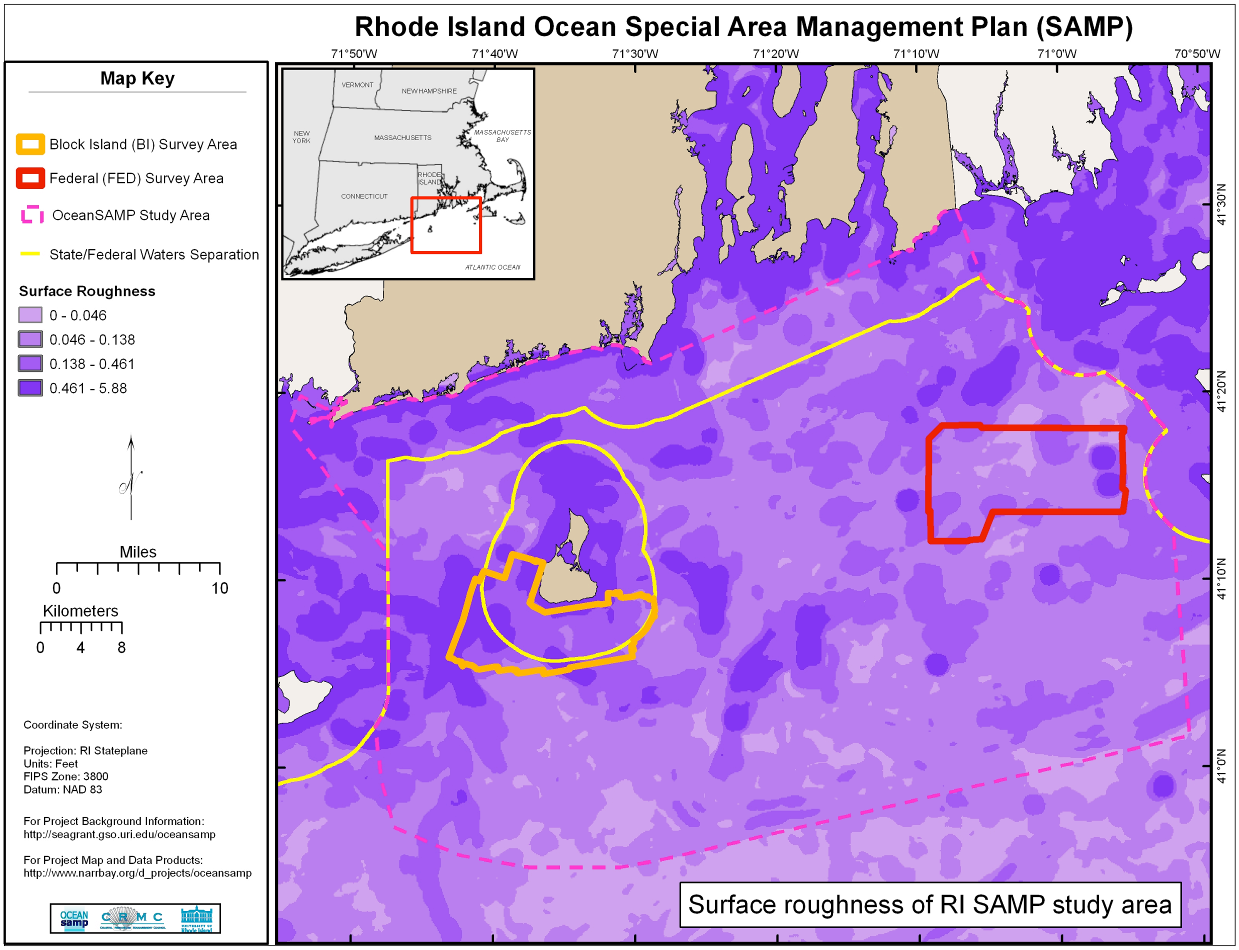

Figure I-10. Surface roughness, a measure of environmental heterogeneity, of the RI Ocean SAMP study area. The dark purple is indicative of high heterogeneity and light purple signifies low heterogeneity. The data layer is 100 m pixel resolution and is calculated as the standard deviation of the slope within a 1000 m radius.

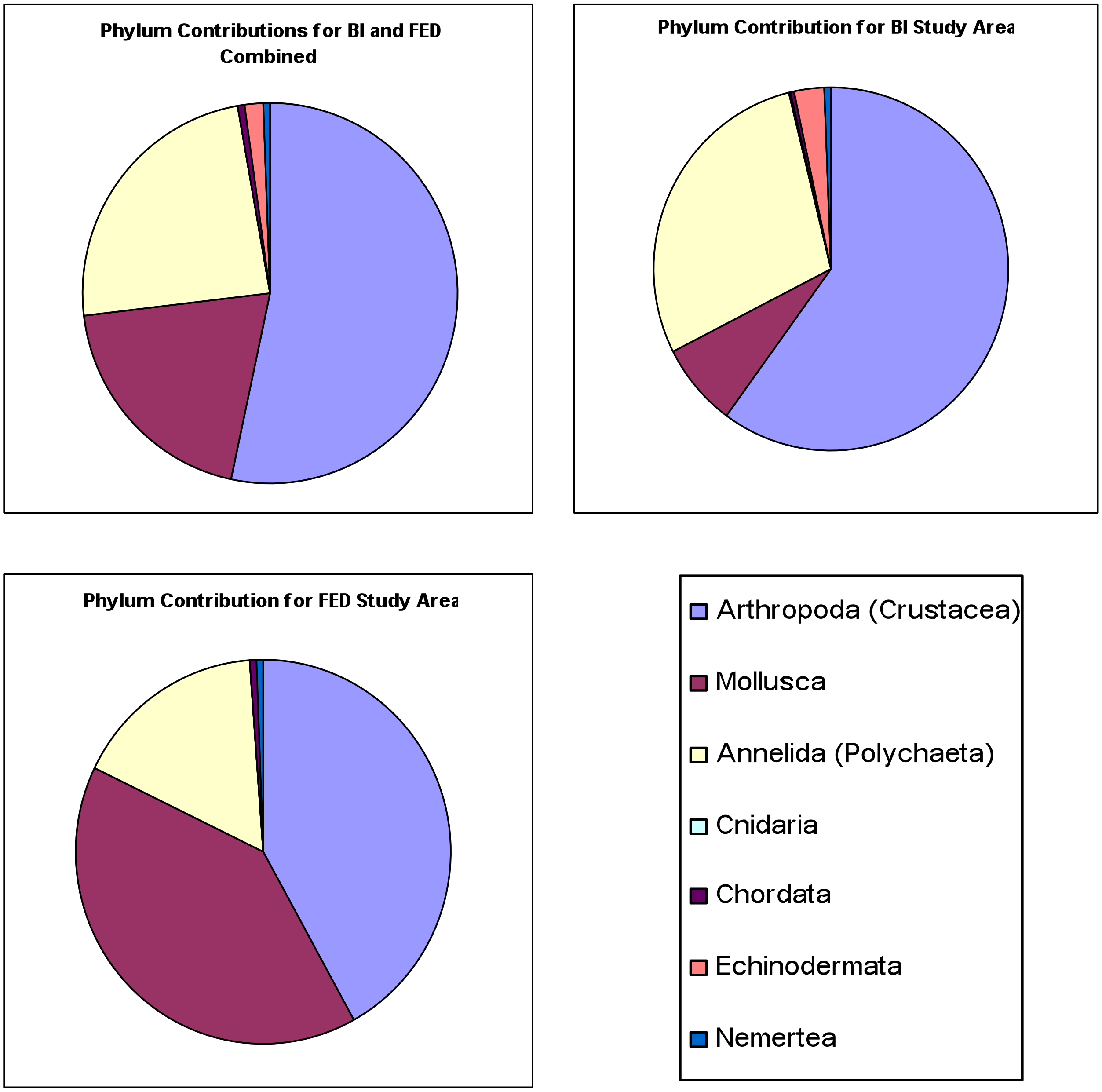

Figure I-11. Pie charts showing the Phyla composition of BI, FED, and BI and FED combined. Crustaceans are the dominant phylum within both study areas. For BI, the second and third most prominent phyla are Polychaetes and Molluscs. This is reversed for FED, with Molluscs being more dominant than Polychaetes. A total of 7 phyla were recovered within BI and FED. All 7 phyla are seen within BI and 6 are present within FED (Cnidaria is absent).

a.

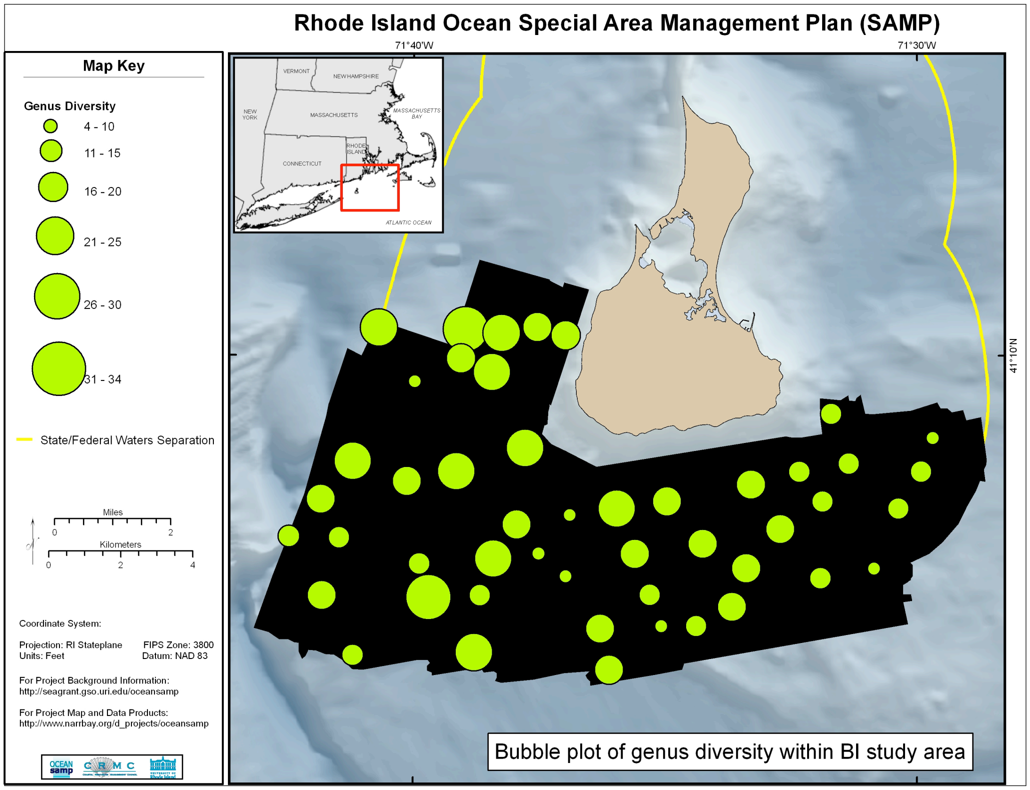

b.

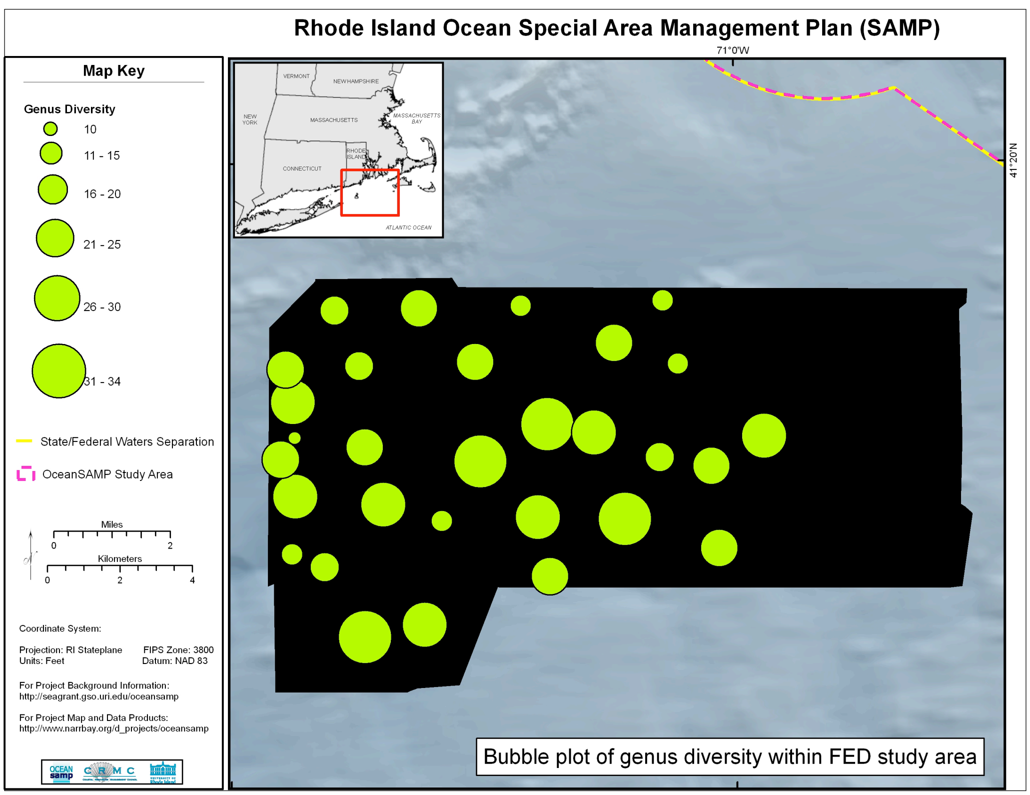

Figure I-12. Bubble plot of diversity within (a.) BI and (b.) FED. The size of the bubble is proportional to the diversity (measured at the genus level) at each station. Note the scales are the same for both BI and FED to allow comparison between study areas.

a.

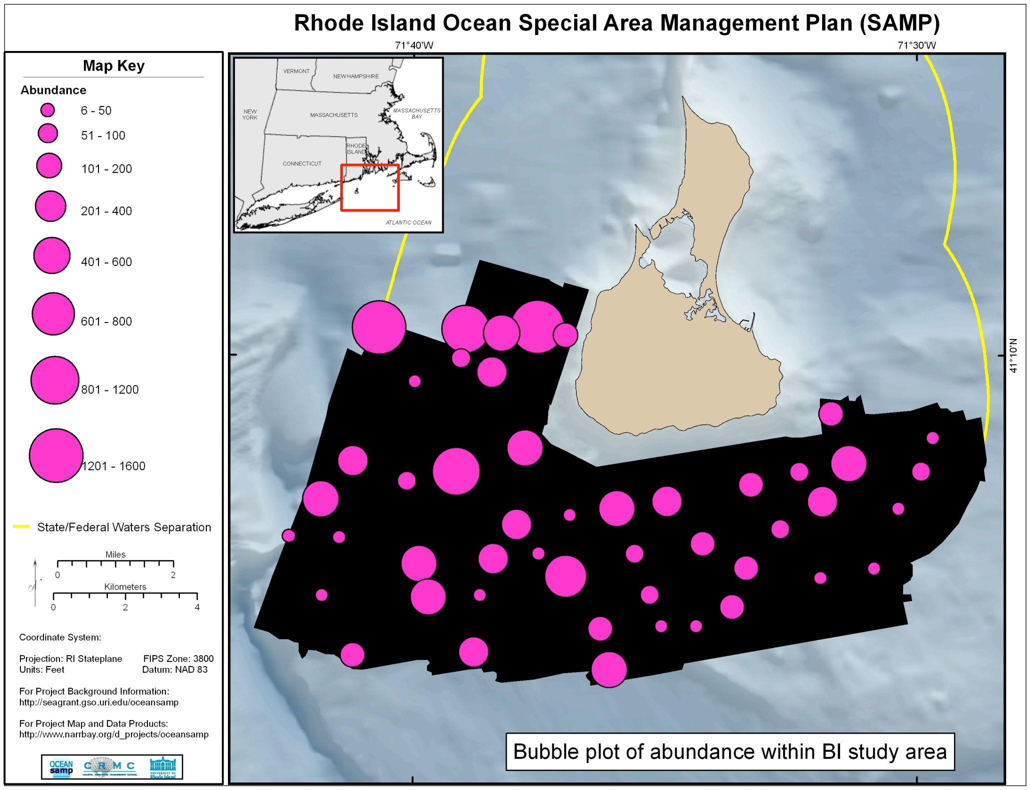

b.

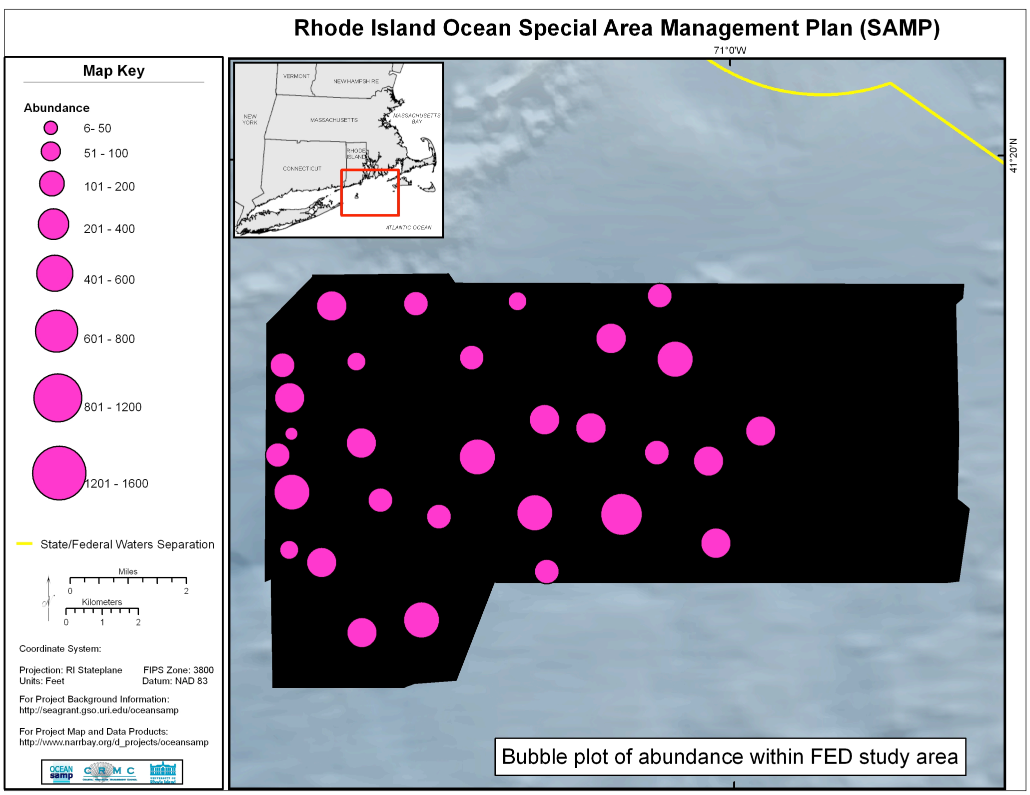

Figure I-13. Bubble plot of abundance within (a.) BI and (b.) FED. The size of the bubble is proportional to the diversity (measured at the genus level) at each station. Note the scales are the same for both BI and FED to allow comparison between study areas.

a.

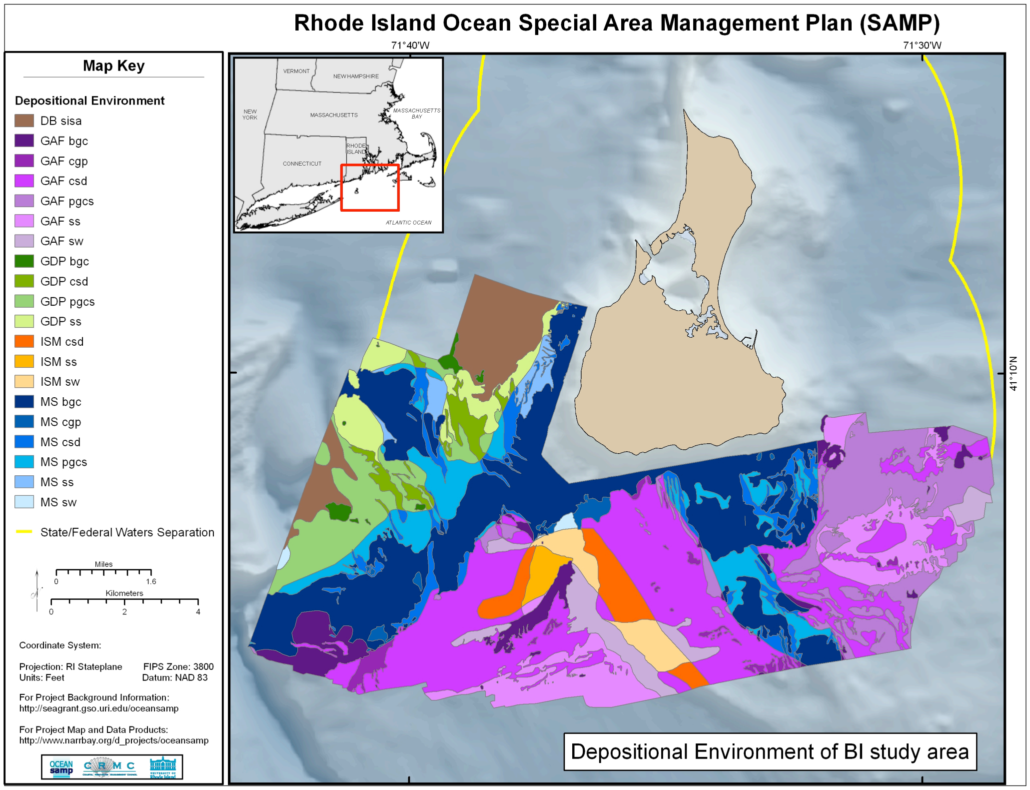

b.

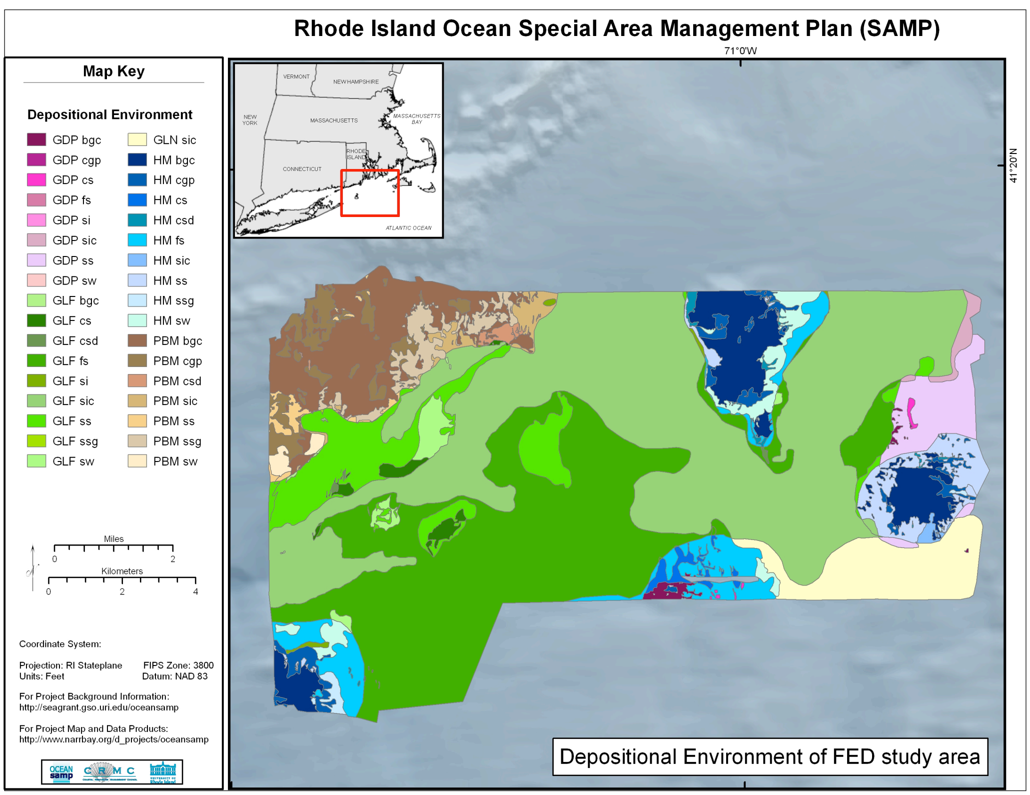

Figure I-14. Benthic geologic environment of (a.) BI and (b.) FED study areas. The environments were derived from side-scan imagery, sub-bottom profile imagery, sediment samples, and underwater video. The polygons are labeled by depositional environment form (capital letters) followed by facies (lower case letters). Shades of the same color are used to place

emphasis on the form type, because this is the unit shown to be most highly correlated to the macrofaunal assemblage (see figure I-15). The unit abbreviations are as follows: Form: DB = Depositional Basin; GAF = Glacial Alluvial Fan; GDP = Glacial Delta Plain; GLF = Glacial Lake floor; GLN = Glacial Lacustrine Fan; HM = Hummocky Moraine; ISM = Inner Shelf Moraine; MS = Moraine Shelf; PBM = PJ-BB Moraine; Facies: bgc = boulder gravel concentrations; cgp = cobble gravel pavement; csd = coarse sand with small dunes; cs = coarse sand; csd = coarse sand with small dunes; fs = fine sand; pgcs = pebble gravel coarse sand; si = silt; sic = coarse silt; sisa = silty sand; ss = sheet sand; ssg = sand sheet with gravel; sw = sand waves.

a.

b.

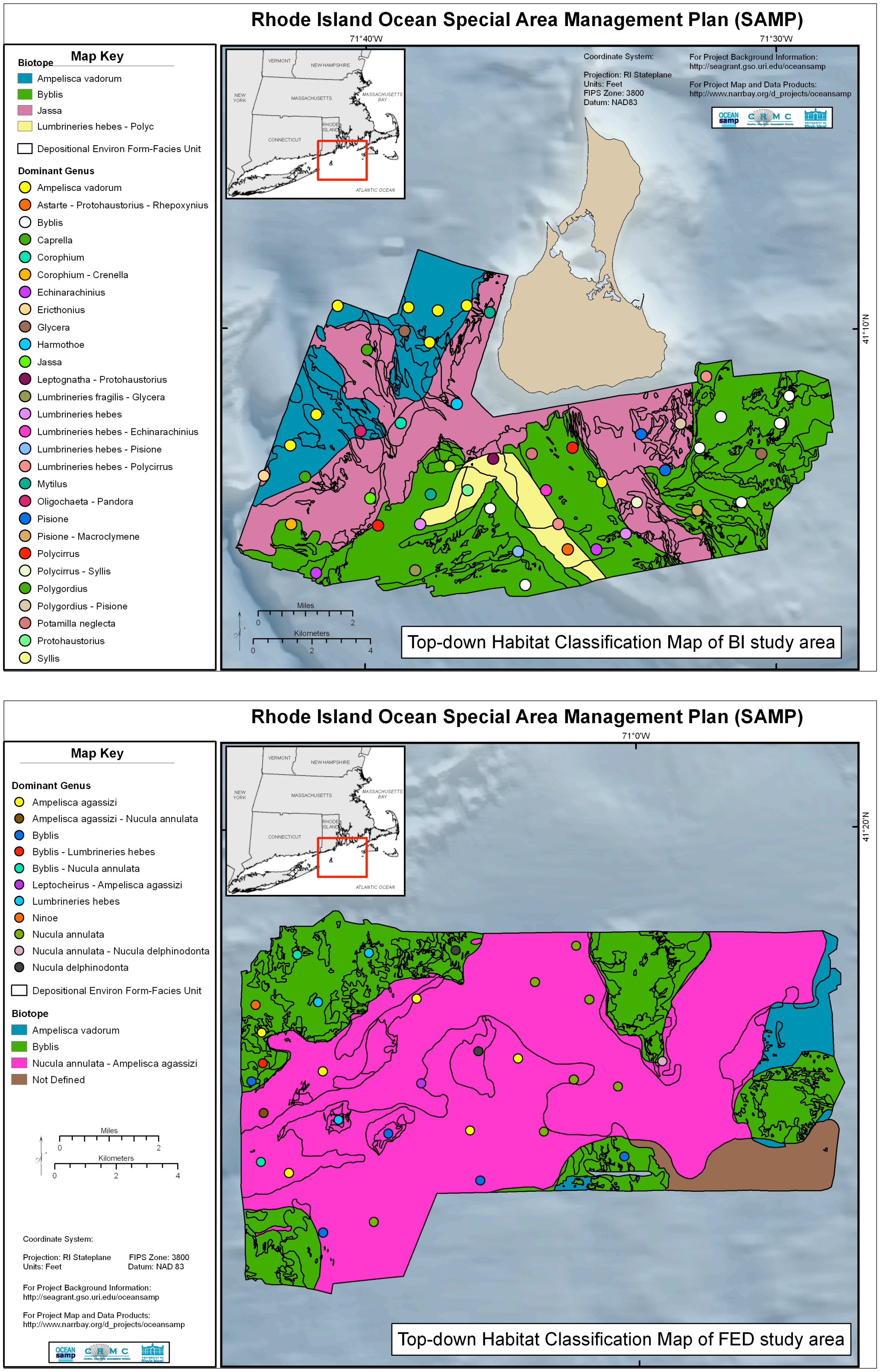

Figure I-15. Top-down habitat classification map of the (a.) BI and (b.) FED study areas. Each map unit, as defined by the form type of the depositional environment, is classified according the most abundant genus. Form type was chosen as the map unit for the BI and FED study areas because an ANOSIM revealed the macrofaunal assemblages within form

type are significantly different (global R = 0.593, p = 0.001). The boundaries of the form-facies unit of depositional environment are outlined in black. The dominant genus found at each sample site is also indicated on the top-down classification maps. This data layer was added to the maps so that the unity and variability among samples with within each map unit could be seen.

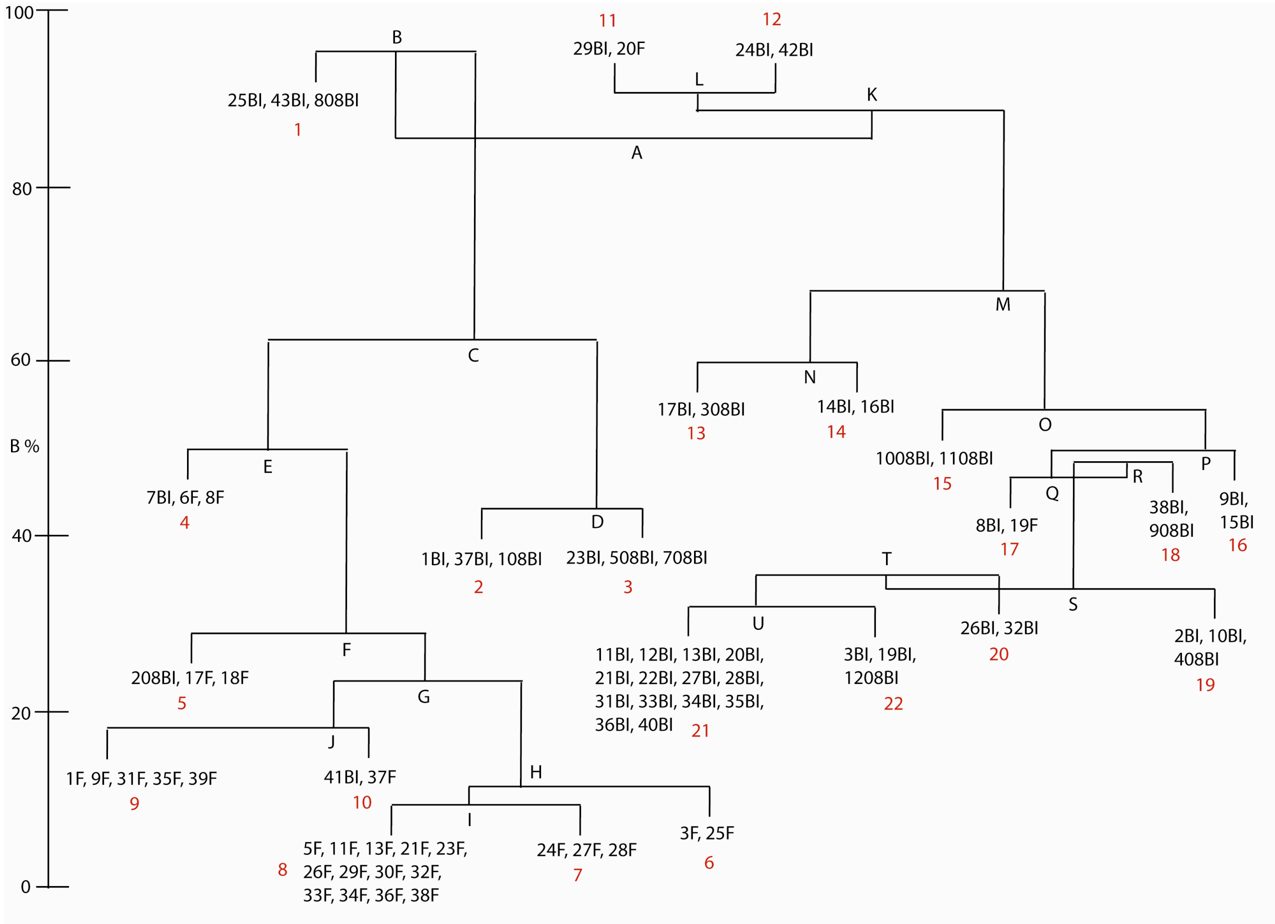

Figure I-16. LINKTREE output for BI and FED. A total of 22 classes were identified within BI and FED (class numbers labeled in red). Each class is defined by a series of quantitative thresholds of the five abiotic variables identified in the BIOENV procedure. Note that BI and FED share five classes, while 13 classes contain only BI samples and four classes contain only FED samples. The threshold for each split (labeled as black letters) is listed in Table I-12.

a.

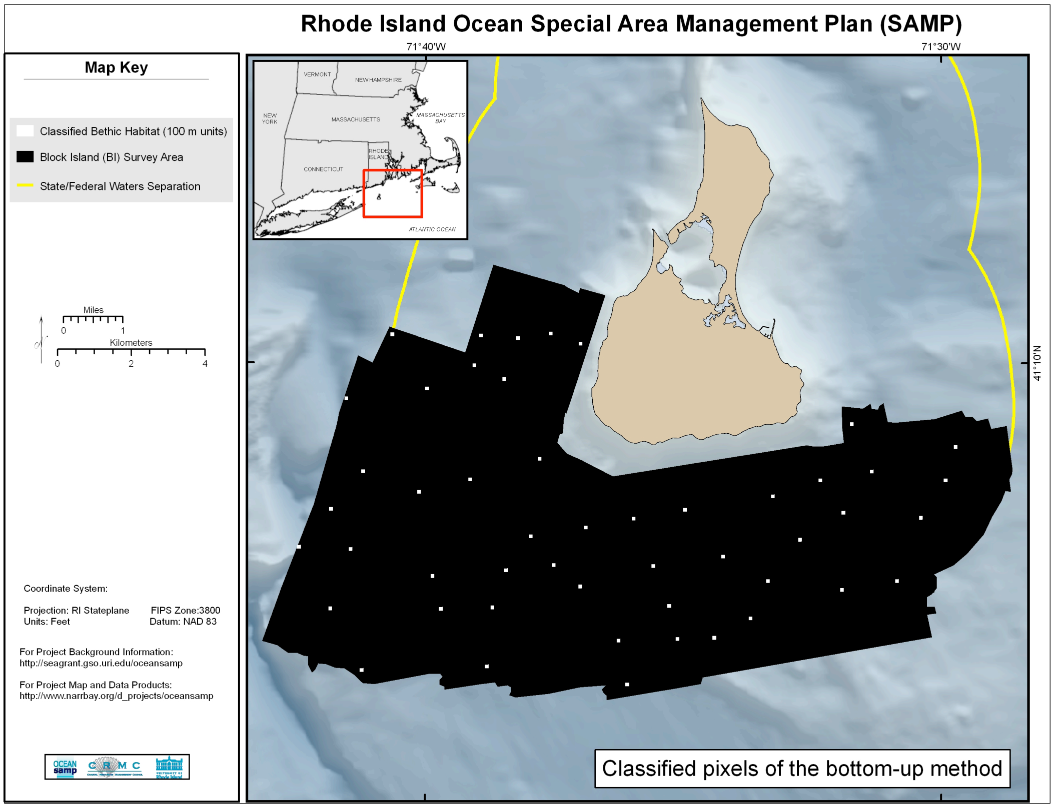

b.

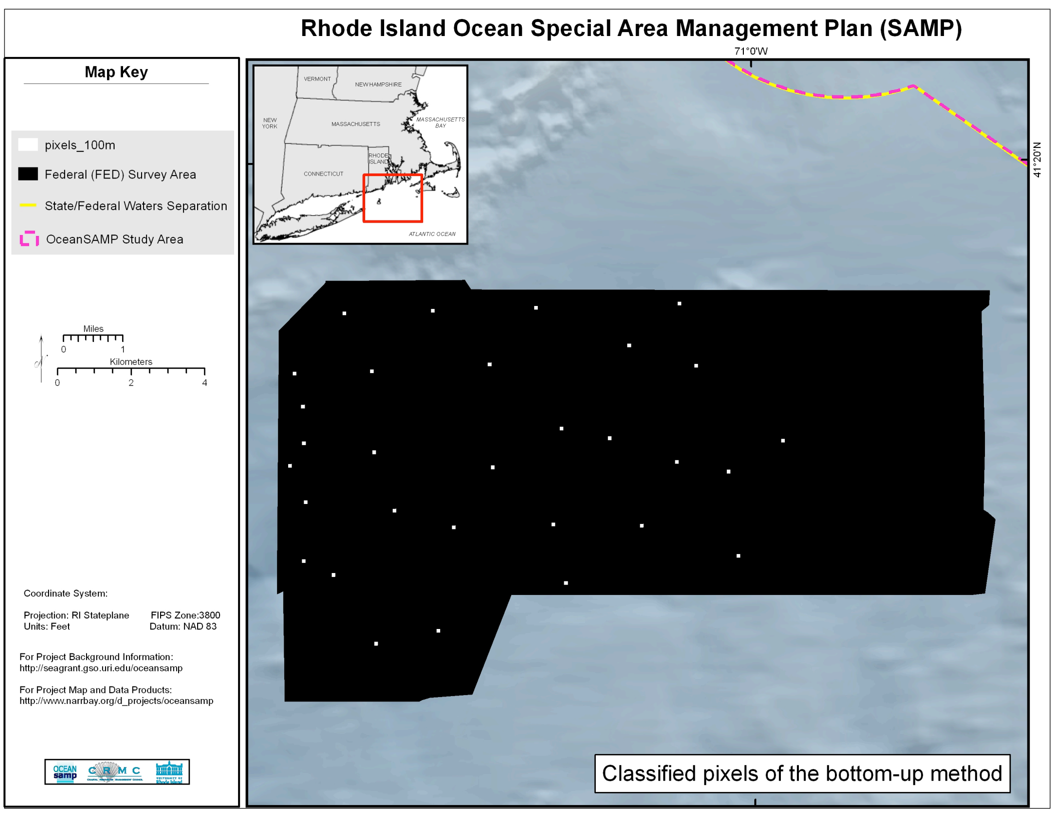

Figure I-17. Spatial extent of habitat classes within (a.) BI and (b.) FED using bottom-up method. The map is comprised of 78, 100 m pixels. Full-coverage maps cannot be made at this time; the lack of auto-correlation between grain size point samples prevents interpolation.

a.

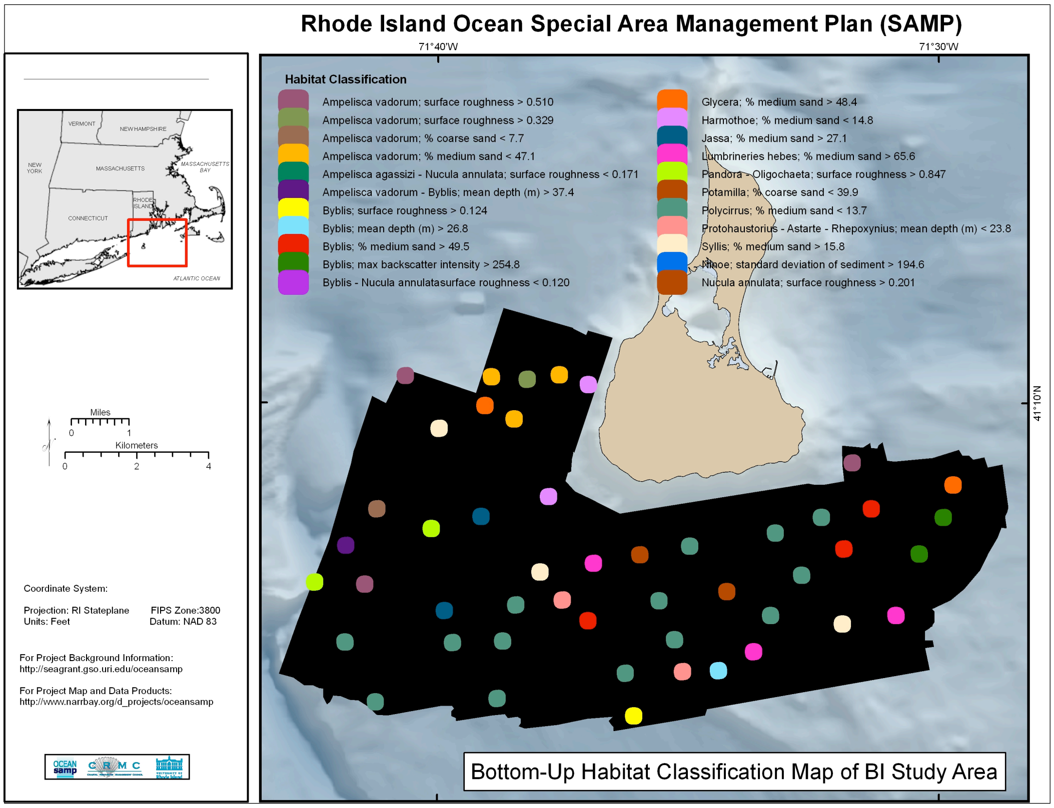

b.

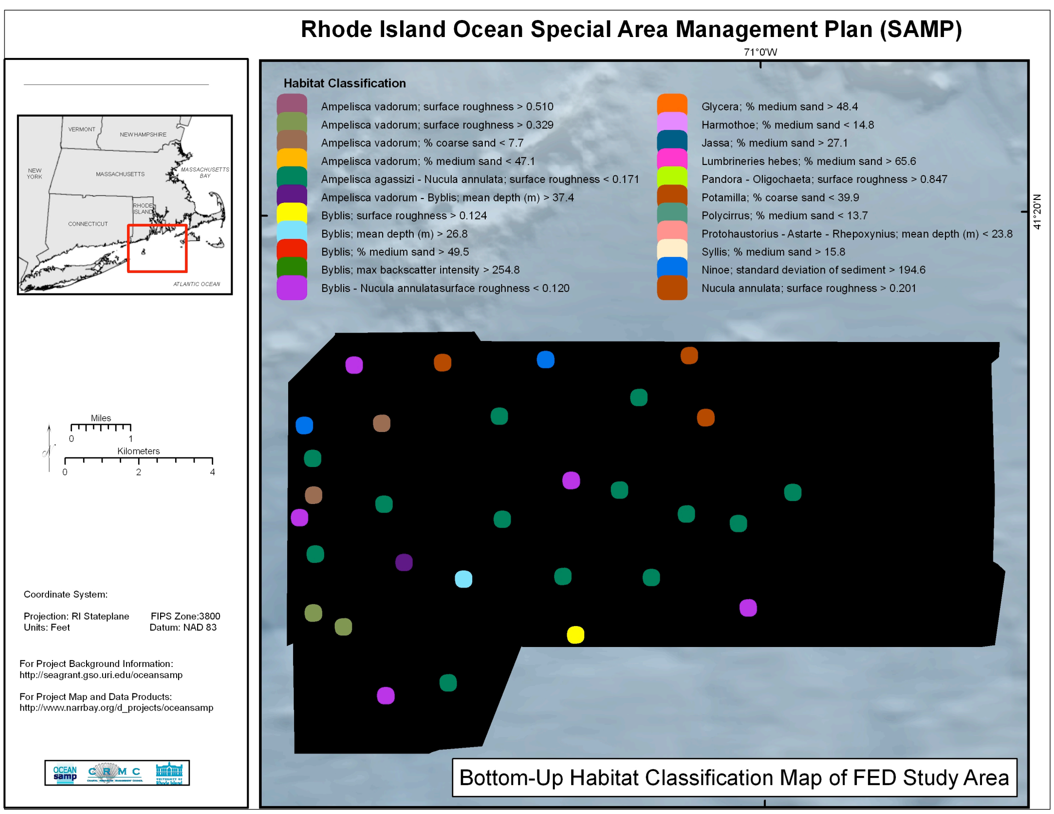

Figure I-18. Bottom-up habitat classification map for (a.) BI and (b.) FED. A total of 22 benthic habitat classes were identified from the analyses. The habitats were classified by the

dominant genus. Between two and three genera were used to classify the habitats if those genera had equal or nearly equal abundances. The final in a series of thresholds defining each habitat class is also provided. Refer to Figure I-16 for the list of all thresholds. BI and FED share five classes and there are 13 habitats present only within BI and 9 only within FED. Note habitat class size is NOT to scale. Classes are mapped at 100 m pixel resolution (see Figure I-17).

Table I-1. Structure of the Geoform, Surface Geology, and Benthic Biotic Components with examples in NOAA's Coastal Marine Ecosystem Classification Standard (CMECS) (Madden, et al., 2010).

System	> Marine
> Subsystem	> Nearshore subtidal

Geoform Component	**> Coastal Region**	> New England seaboard lowland
	> Physiographic Setting	> Coast
	> Geoform (coastal)	> Moraine
	> Subform	> Moraine top
	> Anthropogenic Geoform	> Jetty
Surface Geology Component	**> Class**	> Unconsolidated Substrate
	> Subclass	> Sand
Benthic Biotic Component	**> Class**	> Faunal Bed
	> Subclass	> Epifauna
	> Biotic Group	> Tube-building amphipods
	> Biotope	> *Ampelisca* community

Table I-2. Additional data sets used to interpret the Quaternary depositional environments and benthic geologic habitats.

Sediment samples	Source
National Geophysical Data Center Seafloor sediment grain size database	NOAA NGDC, (1976)
Geophysical data	Source
Geology of Block Island Sound, Rhode Island and New York	Needell and Lewis, (1984)
Digital seismic reflection data from Western Rhode Island Sound	McMullen et al., (2009); Needell et al., 1983
Digital seismic reflection data from Eastern Rhode Island Sound and vicinity	McMullen et al., (2009a); O'Hara and Oldale, (1980)

Table I-3. List of abiotic and biotic variables used in the study. The source, type of coverage attained, and the resolution of each variable is listed. The 15 (+3 video) abiotic variables marked with * were included in the statistical analyses; variables not marked were removed because the draftsman plot revealed it exhibited a high correlation with another variable.

Source	Coverage	Resolution (m)	Variable
Backscatter	Continuous	100	Mean*
			Maximum*
			Minimum*
			Standard Deviation*
Bathymetry (water depth)	Continuous	100	Mean (m)*
			Maximum (m)
			Minimum (m)
			Standard Deviation*
			Aspect (degrees)*
			Slope (degrees)*
			Surface Roughness (Std Dev of Slope within 1000 m Radius)*
Video	Transect	44 stations	Grain Size (%)*
			Bottom Type (%)*
			Number of Patches*
Grain Size	Point	78 stations	% Clay*
			% Fine Silt
			% Course Silt
			% Very Fine Sand*
			% Fine Sand
			% Medium Sand*
			% Coarse Sand*
			% Very Coarse Sand*
			Standard Deviation*
Biology	Point	78 stations	Identification (at least to genus level)
			Counts (individuals)

Table I-4. Ranges of the acoustic variables within BI and FED. Note the wider ranges exhibited by BI for all of the acoustic variables, with the exception of the aspect.

Acoustic Variables	Range		
	BI	Fed	BI and Fed
Mean Backscatter (100m)	40.99 - 239.13	42.97 - 172.40	40.99 - 239.13
Max Backscatter (100m)	88 - 255	60 - 222	60 - 255
Min Backscatter (100m)	1 - 107	1 - 104	1 - 107
Standard Deviation of Backscatter (100m)	10.86 - 98.61	4.35 - 21.79	4.35 - 98.61
Mean Water Depth, m (100m)	13.82 - 38.63	33.75 - 46.08	13.82 - 46.08
Max Water Depth, m (100m)	16.29 - 51.35	34.59 - 46.59	16.29 - 51.35
Min Water Depth, m (100m)	11.77 - 36.71	33.04 - 45.75	11.77 - 45.75
Standard Deviation of Water Depth (100m)	0.17 - 2.61	0.07 - 0.64	0.07 - 2.61
Slope, degrees (100m)	0.06 - 1.38	0.02 - 0.68	0.02 - 1.38
Aspect, degrees (100m)	23.53 - 339.58	4.66 - 329.51	4.66 - 339.58
Standard Deviation of Slope (100m) w/in a 1000m Radius	0.090 - 1.394	0.035 - 0.333	0.035 - 1.394

Table I-5. Percent composition and ranges of the grain size from analysis of the sediment samples within BI and FED. BI is dominated by medium and coarse grained sands while fine and medium sands dominate FED. Within both study areas, the dominant sediment is medium and coarse grained sands. The stations within BI and FED exhibit similar ranges for most of the sediment variables.

Sediment Variables	Percent Composition		
	BI	Fed	BI and Fed
% Clay	1.3	5.3	2.8
% Fine Silt	3.0	10.4	5.8
% Course Silt	0.8	3.3	1.8
% Very Fine Sand	1.5	14.3	6.4
% Fine Sand	10.2	37.8	20.8
% Medium Sand	33.7	23.1	29.7
% Coarse Sand	36.2	5.4	24.3
% Very Coarse Sand	13.3	0.4	8.3
Standard Deviation of Grain Size (um)	--	--	--
Sediment Variables	**Range**		
	BI	**Fed**	**BI and Fed**
% Clay	0 - 10.6	0 - 19.2	0 - 19.2
% Fine Silt	0 - 33.0	0 - 34.1	0 - 34.1
% Course Silt	0 - 7.4	0 - 15.0	0 - 15.0
% Very Fine Sand	0 - 9.9	0 - 34.3	0 - 34.3
% Fine Sand	0 - 57.8	0.5 - 63.1	0 - 63.1
% Medium Sand	0.7 - 76.3	0.4 - 67.8	0.4 - 76.3
% Coarse Sand	0.3 - 69.6	0 - 54.5	0 - 69.6
% Very Coarse Sand	0 - 62.7	0 - 12.8	0 - 62.7
Standard Deviation of Grain Size (um)	90.6 - 459.8	61.4 - 316.2	61.4 - 459.8

Table I-6. Number of phyla, genera, and individuals recovered within BI and FED.

	BI	FED	Combined
Total # of phyla	7	6	7
Total diversity (# of genera)	81	65	87
Total abundance (# of individuals)	13,494	7,705	21,199

Table I-7. a. List of the top ten most spatially abundant genera, as defined by the percentage of the stations the genus is found within. b. List of the top ten most abundant genera in terms of counts of individuals. These top ten are determined based on the degree to which the number of individuals of the genus contributes to the total number of individuals over all samples.

a. 10 Most Spatially Abundant Genera (% of stations found within)

BI and FED Combined			
Phylum	**Genus**	**Description**	**% Contribution**
Annelida	Lumbrineries hebes	Small surface-burrowing polychaete	69.2
Arthropoda	Unciola	Small surface-burrowing crustacean	56.4
Mollusca	Astarte	Clam bed mollusc	52.6
Annelida	Glycera	Large deep-burrowing polychaete	50.0
Mollusca	Crenella	Mussel bed mollusc	48.7
Arthropoda	Byblis	Tube-building amphipod crustacean	42.3
Mollusca	Nucula annulata	Deposit feeding mollusc	42.3
Arthropoda	Leptocheirus	Tube-building amphipod crustacean	41.0
Annelida	Polygordius	Small surface-burrowing polychaete	41.0
Annelida	Scalibregma	Small surface-burrowing polychaete	41.0

BI			
Phylum	**Genus**	**Description**	**% Contribution**
Annelida	Lumbrineries hebes	Small surface-burrowing polychaete	66.7
Nemertea	Nemertean	Small surface-burrowing nemertean	62.5
Annelida	Glycera	Large deep-burrowing polychaete	60.4
Annelida	Polygordius	Small surface-burrowing polychaete	58.3
Annelida	Aricidea	Small surface-burrowing polychaete	52.1
Mollusca	Astarte	Clam bed mollusc	50.0
Annelida	Pisione	Small surface-burrowing polychaete	50.0
Arthropoda	Unciola	Small surface-burrowing crustacean	50.0
Mollusca	Crenella	Mussel bed mollusc	45.8
Echinodermata	Echinarachinius	Sand dollar mollusc	45.8
Annelida	Syllis	Mobile polychaete	45.8

FED			
Phylum	**Genus**	**Description**	**% Contribution**
Mollusca	Nucula delphinodonta	Deposit feeding mollusc	93.3
Arthropoda	Ampelisca agassizi	Tube-building amphipod crustacean	86.7
Arthropoda	Eudorella	Mobile crustacean	86.7

Annelida	Ninoe	Small surface-burrowing polychaete	86.7
Mollusca	Nucula annulata	Deposit feeding mollusc	86.7
Arthropoda	Diastylis	Mobile crustacean	80.0
Arthropoda	Leptocheirus	Tube-building amphipod crustacean	73.3
Annelida	Lumbrineries hebes	Small surface-burrowing polychaete	73.3
Mollusca	Periploma	Clam bed mollusc	73.3
Mollusca	Arctica	Clam bed mollusc	66.7
Annelida	Scalibregma	Small surface-burrowing polychaete	66.7
Arthropoda	Unciola	Small surface-burrowing crustacean	66.7

b. 10 Most Abundant Genera (% of total individuals)

BI and FED Combined			
Phylum	**Genus**	**Description**	**% Contribution**
Arthropoda	Ampelisca vadorum	Tube-building amphipod crustacean	18.6
Arthropoda	Byblis	Tube-building amphipod crustacean	12.6
Mollusca	Nucula annulata	Deposit feeding mollusc	8.3
Arthropoda	Ampelisca agassizi	Tube-building amphipod crustacean	7.0
Arthropoda	Leptocheirus	Tube-building amphipod crustacean	3.4
Annelida	Lumbrineries hebes	Small surface-burrowing polychaete	3.0
Annelida	Polycirrus	Small surface-burrowing polychaete	2.6
Mollusca	Nucula delphinodonta	Deposit feeding mollusc	2.6
Arthropoda	Jassa	Tube-building amphipod crustacean	2.0
Annelida	Ninoe	Small surface-burrowing polychaete	1.8

BI			
Phylum	**Genus**	**Description**	**% Contribution**
Arthropoda	Ampelisca vadorum	Tube-building amphipod crustacean	30.0
Arthropoda	Byblis	Tube-building amphipod crustacean	14.8
Annelida	Polycirrus	Small surface-burrowing polychaete	4.0
Arthropoda	Jassa	Tube-building amphipod crustacean	3.2
Annelida	Lumbrineries hebes	Small surface-burrowing polychaete	3.2
Arthropoda	Leptocheirus	Tube-building amphipod crustacean	3.0
Arthropoda	Corophium	Tube-building amphipod crustacean	2.3
Annelida	Syllis	Mobile polychaete	2.2
Annelida	Metrella	Clam bed mollusc	2.1
Mollusca	Pisione	Small surface-burrowing polychaete	2.1

FED			
Phylum	**Genus**	**Description**	**% Contribution**
Mollusca	Nucula annulata	Deposit feeding mollusc	18.6
Arthropoda	Ampelisca agassizi	Tube-building amphipod crustacean	12.6
Arthropoda	Byblis	Tube-building amphipod crustacean	8.3
Mollusca	Nucula delphinodonta	Deposit feeding mollusc	7.0
Annelida	Ninoe	Small surface-burrowing polychaete	3.4
Arthropoda	Leptocheirus	Tube-building amphipod crustacean	3.0
Mollusca	Periploma	Clam bed mollusc	2.6
Annelida	Lumbrineries hebes	Small surface-burrowing polychaete	2.6
Arthropoda	Eudorella	Mobile crustacean	2.0
Mollusca	Alvania	Mobile gastropod mollusc	1.8

Table I-8. Diversity and Abundance within BI and FED. Diversity is defined as the number of genera per station. Abundance is defined as is the number of individuals per station.

	BI	FED	Combined
Mean diversity per station	16	23	19
Range of diversity per station	4 - 27	10 - 34	4 - 34
Mean abundance per station	281	257	272
Range of abundance per station	6 - 1,541	29 - 611	6 - 1,541

Table I-9. Summary of underwater video collected at BI stations. Video was obtained for BI stations 1-45. The most common bottom type was flat surface, for which the sediment composition ranged from coarse sand to cobble. The most common sediment type was coarse sand. Over half of the stations exhibited one bottom type throughout the 200 m transects. Note: this table is a summary of the video analysis results; the percentage of each parameter found within each station can be found in Appendix II.

Underwater Video Characteristics	# of Stations
Bottom Type	
Dense Tube-mat	4
Flat surface	18
Flat surface w/ small depressions	2
Rippled surface (regular pattern)	9
Rippled surface (irregular pattern)	8
Boulder field	8
Sediment Type	
Fine sediment (silt, clay, fine sand)	6
Fine sand	3
Coarse sand	15
Pebble	11
Gravel and Cobble	15
Boulders	11
# Bottom Types	
1	24
2	3
3	1
4	2
5	2
6	1
7	0
8	1
9	0
10	2
11	1

Table I-10. Depositional environments; a. within BI and FED; b. within BI; c. within FED. The environments described in terms of the unit (form followed by facies) and form categories. Environments in bold font are those with the greatest spatial extent. The unit is labeled by form (capital letters) followed by facies (lower case letters). The abbreviations are as follows: Form: DB = Depositional Basin; GAF = Alluvial Fan; GDP = Glacial Delta Plain; GLF = Glacial Lake floor; GLN = Glacial Lacustrine Fan; HM = Hummocky Moraine; ISM = Inner Shelf Moraine; MS = Moraine Shelf; PBM = PJ-BB Moraine; Facies: sisa = silty sand; bgc = boulder gravel concentrations; cgp = cobble gravel pavement; cs = coarse sand; csd = coarse sand with small dunes; fs = fine sand; pgcs = pebble gravel coarse sand; si = silt; sic = coarse silt; ss = sheet sand; ssg = sand sheet with gravel; sw = sand waves.

a. **BI and FED study areas combined.**

Unit	Area (sq mi) of Unit	Cover (%) of Unit	# of Biology Samples w/in Unit	Area	Form	Area (sq mi) of Form	Cover (%) of Form	# of Biology Samples w/in Form	Area
DB sisa	2.81	2.29	4	BI	Deposit-ional Basin	2.81	2.29	4	BI
GAF bgc	1.93	1.57	2	BI	Glacial Alluvial Fan	24.65	20.05	25	BI
GAF cgp	0.56	0.46	0	BI					
GAF csd	**11.35**	**9.23**	**14**	**BI**					
GAF pgcs	5.08	4.13	5	BI					
GAF ss	4.00	3.25	2	BI					
GAF sw	1.73	1.41	2	BI					
GDP bgc	0.47	0.38	0	BI & FED	Glacial Delta Plain	7.80	6.35	6	BI & FED
GDP cs	0.06	0.05	0*	FED					
GDP csd	0.86	0.70	0	BI					
GDP pgcs	2.67	2.17	4	BI					
GDP sic	0.32	0.26	0*	FED					
GDP ss	3.43	2.79	2	BI & FED					
GLF bgc	0.02	0.02	0	FED	**Glacial Lake floor**	**45.33**	**36.87**	**21**	FED
GLF cs	0.41	0.33	1	FED					
GLF csd	0.04	0.03	0	FED					
GLF fs	**16.61**	**13.51**	**9**	**FED**					
GLF si	0.11	0.09	0	FED					
GLF sic	**23.41**	**19.04**	**7**	**FED**					
GLF ss	4.10	3.33	4	FED					
GLF ssg	0.01	0.00	0	FED					
GLF sw	0.63	0.52	0	FED					
GLN sic	3.17	2.58	0*	FED	Glacial Lacustri	3.17	2.58	0*	FED

					ne Fan				
HM bgc	3.36	2.74	0	FED	Hummo cky Moraine	10.37	8.44	1	FED
HM cgp	0.96	0.78	0	FED					
HM cs	0.31	0.25	0	FED					
HM csd	0.17	0.13	0	FED					
HM fs	2.64	2.15	1	FED					
HM sic	0.10	0.08	0*	FED					
HM ss	1.54	1.26	0	FED					
HM ssg	0.18	0.15	0	FED					
HM sw	1.11	0.90	0	FED					
ISM csd	1.36	1.11	1	BI	Inner Shelf Moraine	2.81	2.29	4	BI
ISM ss	0.4	0.33	1	BI					
ISM sw	1.05	0.85	2	BI					
MS bgc	**11.57**	**9.41**	**5**	**BI**	Moraine Shoal	17.88	14.54	9	BI
MS cgp	0.4	0.33	0	BI					
MS csd	2.19	1.78	1	BI					
MS pgcs	2.98	2.42	2	BI					
MS ss	0.61	0.50	0	BI					
MS sw	0.13	0.11	1	BI					
PBM bgc	4.37	3.56	2	FED	PJ-BB Moraine	8.12	6.61	8	FED
PBM cgp	1.37	1.11	1	FED					
PBM csd	0.18	0.14	0	FED					
PBM sic	0.58	0.47	1	FED					
PBM ss	0.32	0.26	2	FED					
PBM ssg	1.10	0.89	1	FED					
PBM sw	0.21	0.17	1	FED					

b. BI study area.

Unit	Area (sq mi) of Unit	Cover (%) of Unit	# Biology Samples w/in Unit	Form	Area (sq mi) of Form	Cover (%) of Form	# Biology Samples w/in Form
DB sisa	2.81	5.24	4	Depositional Basin	2.81	5.24	4
GAF bgc	1.93	3.60	2	**Glacial Alluvial Fan**	**24.65**	**46.01**	**25**
GAF cgp	0.56	1.05	0				
GAF csd	**11.35**	**21.18**	**14**				
GAF pgcs	**5.08**	**9.48**	**5**				
GAF ss	4.00	7.47	2				
GAF sw	1.73	3.23	2				
GDP bgc	0.26	0.49	0	Glacial Delta Plain	5.43	10.13	6
GDP csd	0.86	1.61	0				
GDP pgcs	2.67	4.98	4				

GDP ss	1.64	3.06	2				
ISM csd	1.36	2.54	1	Inner Shelf Moraine	2.81	5.24	4
ISM ss	0.4	0.75	1				
ISM sw	1.05	1.96	2				
MS bgc	**11.57**	**21.59**	**5**	Moraine Shoal	17.88	33.37	9
MS cgp	0.4	0.75	0				
MS csd	2.19	4.09	1				
MS pgcs	2.98	5.56	2				
MS ss	0.61	1.14	0				
MS sw	0.13	0.24	1				

c. FED study area.

Unit	Area (sq mi) of Unit	Cover (%) of Unit	# Biology Samples w/in Unit	Form	Area (sq mi) of Form	Cover (%) of Form	# Biology Samples w/in Form
GDP bgc	0.21	0.30	0	Glacial Delta Plain	2.37	3.42	0
GDP cs	0.06	0.08	0*				
GDP sic	0.32	0.45	0*				
GDP ss	1.79	2.58	0*				
GLF bgc	0.02	0.03	0	**Glacial Lake floor**	**45.33**	**65.35**	**21**
GLF cs	0.41	0.59	1				
GLF csd	0.04	0.05	0				
GLF fs	**16.61**	**23.94**	**9**				
GLF si	0.11	0.15	0				
GLF sic	**23.41**	**33.76**	**7**				
GLF ss	4.10	5.91	4				
GLF ssg	0.01	0.01	0				
GLF sw	0.63	0.91	0				
GLN sic	3.17	4.57	0*	Glacial Lacustrine Fan	3.17	4.57	0*
HM bgc	3.36	4.85	0	Hummocky Moraine	10.37	14.95	1
HM cgp	0.96	1.39	0				
HM cs	0.31	0.44	0				
HM csd	0.17	0.24	0				
HM fs	2.64	3.80	1				
HM sic	0.10	0.15	0*				
HM ss	1.54	2.23	0				
HM ssg	0.18	0.26	0				
HM sw	1.11	1.59	0				
PBM bgc	**4.37**	**6.30**	**2**	PJ-BB Moraine	8.12	11.71	8
PBM cgp	1.37	1.97	1				

PBM csd	0.18	0.25	0				
PBM sic	0.58	0.84	1				
PBM ss	0.32	0.46	2				
PBM ssg	1.10	1.58	1				
PBM sw	0.21	0.30	1				
			0* = outside sample area				

Table I-11. Biotic description of Depositional Environment form type. For each form type, the stations within the form and the most abundant genus are listed. The overall within-group similarity and the genus most responsible for the within-group similarity, both identified by the SIMPER procedure, are also provided. The forms marked with ** are classes for which the same genus is the most abundant and is the most responsible for the within-group similarity.

Form	Composing Stations	Overall Group Similarity	Most Abundant Genus	Genus Most Responsible for Within-Form Similarity
Depositional Basin (DB)	BI 1, 37, 108, 208	46.46%	Ampelisca vadorum	Ampelisca vadorum (23.25%)
Glacial Delta Plain (GDP)	BI 2, 7, 8, 10, 15, 38	37.22%	Ampelisca vadorum	Astarte (12.43%)
Moraine Shoal (MS)	BI 3, 9, 14, 16, 17, 31, 34, 36, 308	29.11%	Jassa	Polygordius (14.06%)
Glacial Alluvial Fan (GAF)	BI 11 - 13, 19 - 23, 26, 27, 29, 32, 33, 35, 40, 41, 43, 408, 508, 708 - 1208	30.73%	Byblis	Lumbrineries hebes (11.15%)
Inner Shelf Moraine (ISM)	BI 24, 25, 28, 42	33.47%	Lumbrineries hebes - Polycirrus	Protohaustorius (29.30%)
Glacial Lake floor (GLF)	FED 11, 13, 17 - 21, 23, 26- 30, 32 - 39	53.21%	Nucula annulata - Ampelisca agassizi	Nucula annulata (10.15%)
PJ-BB Moraine (PJBBM)	FED 1, 3, 5, 6, 8, 9, 24, 25	43.57%	Byblis	Astarte (10.05%)
Hummocky Moraine (HM)	FED 31	N/a	Byblis	N/a

Table I-12. LINKTREE thresholds. Reported here is the final threshold of each split. The branch to the left side of the LINKTREE is listed first and the branch to the right side of the LINKTREE is listed second in brackets. For example, for split A, the stations on the left side of the split have a threshold of < 24.7 % coarse sand and the stations on the right side of the split have a threshold of > 26.9 % coarse sand. Note that many of the thresholds are defined by narrow ranges of the abiotic variables.

Class	Threshold	Range	R value
A	% coarse sand	< 24.7 (> 26.9)	0.54
B	% medium sand	> 65.6 (< 57.6)	0.79
C	mean depth (m)	> 39.8 (< 32.8)	0.71
D	% medium sand	< 47.1 (> 49.5)	0.67
E	% coarse sand	> 10.8 (< 7.7)	0.81
F	surface roughness	> 0.329 (< 0.269)	0.52
G	% medium sand	< 24.7 (> 28.0)	0.59
H	standard deviation of sediment (um)	< 176.6 (> 194.6)	0.7
I	surface roughness	< 0.171 (> 0.201)	0.67
J	surface roughness	< 0.120 (> 0.124)	0.6
K	standard deviation of sediment (um)	< 196.0 (> 207.6)	0.7
L	mean depth (m)	> 26.8 (< 23.8)	0.5
M	mean depth (m)	< 19.0 (> 19.7)	0.5
N	% medium sand	< 14.8 (> 27.1)	0.5
O	max backscatter intensity	> 254.8 (< 247.9)	0.4
P	surface roughness	< 0.580 (> 0.846)	0.4
Q	mean depth (m)	> 37.4 (< 34.8)	0.42
R	% medium sand	< 46.5 (> 48.4)	0.47
S	surface roughness	< 0.496 (> 0.509)	0.36
T	% coarse sand	> 41.7 (< 39.9)	0.49
U	% medium sand	> 15.8 (< 13.7)	0.56

Table I-13. Biotic description of LINKTREE classes. For each class, the stations comprising the class and the most abundant genus are listed. The overall within-class similarity and the genus most responsible for the within-class similarity, both identified by the SIMPER procedure, are also provided. The classes marked with ** are classes for which the same genus is the most abundant and is the most responsible for the within-class similarity.

LINKTREE Class	Comprising Stations	Overall Within-Class Similarity	Most Abundant Genus	Genus Most Responsible for Within-Class Similarity
1	BI 25, 43, 808	21.11%	*Lumbrineries hebes*	*Nemertean (38.15%)*
2*	BI 1, 37, 108	41.72%	*Ampelisca vadorum*	*Ampelisca vadorum (25.95%)*
3*	BI 23, 508, 708	51.70%	*Byblis*	*Byblis (45.75%)*
4	BI 7, F6, F8	30.54%	*Ampelisca vadorum*	*Lumbrineries hebes (25.86%)*
5	BI 208, F17, 18	36.44%	*Ampelisca vadorum*	*Nucula annulata (18.61%)*
6	F3, 25	24.69%	*Ninoe*	*Eudorella (25.25%)*
7*	F24, 27, 28	52.45%	*Nucula annulata*	*Nucula annulata (16.25%)*
8*	F5, 11, 13, 21, 23, 26, 29, 30, 32, 33, 34, 36, 38	64.76%	*Ampelisca agassizi - Nucula annulata*	*Nucula annulata (9.73%) - Ampelisca agassizi (8.82%)*
9*	F1, 9, 31, 35, 39	60.58%	*Byblis - Nucula annulata*	*Byblis (13.25%)*
10*	BI 41, F37	31.33%	*Byblis*	*Byblis (24.20%)*
11	BI 29, F20	5.80%	*Byblis*	*Lumbrineries fragilis (100%)*
12*	BI 24, 42	58.25%	** Protohaustorius - Astarte - Rhepoxynius*	*Protohaustorius (30.49%)*
13	BI 17, 308	24.66%	*Harmothoe*	*Polygordius (18.95%)*
14*	BI 14, 16	45.41%	*Jassa*	*Jassa (18.31%) - Metrella (17.82%)*
15	BI 1008, 1108	32.32%	*Byblis*	*Glycera - Leptognatha (29.21% each)*
16	BI 9, 15	22.37%	** Pandora - Oligochaeta*	*Lumbrineries hebes - Syllis – Polygordius - Echinarachinius (25.00% each)*
17	BI 8, F19	47.04%	*Ampelisca vadorum - Byblis*	*Unciola (12.42%)*
18	BI 38, 908	6.44%	*Glycera*	*Nemertean (100%)*
19	BI 2, 10, 408	29.72%	*Ampelisca vadorum*	*Marphysa (16.56%) - Lumbrineries hebes (16.29%)*
20	BI 26, 32	34.26%	*Potamilla*	*Lumbrineries hebes (15.74%)*

21	BI 11, 12, 13, 20, 21, 22, 27, 28, 31, 33, 34, 35, 36, 40	48.86%	*Polycirrus*	*Lumbrineries hebes (11.22%) - Pisione (10.30%)*
22	BI 3, 19, 1208	28.28%	*Syllis*	*Polygordius (30.04%)*
			* equal abundances	

Appendix I: Correlation between sediment and acoustic variables

Test Correlation, r^2									
	% clay	% fine silt	% course silt	% very fine sand	% fine sand	% medium sand	% course sand	% very course sand	Std Dev (um)
100m mean backscatter	0.004	0.003	0.013	0.095	0.072	0.005	0.084	0.132	0.202
100m max backscatter	0.083	0.067	0.083	0.345	0.168	0.051	0.210	0.130	0.270
100m min backscatter	0.040	0.041	0.017	0.018	0.010	0.071	0.018	0.010	0.003
100m std dev backscatter	0.099	0.085	0.071	0.228	0.171	0.054	0.220	0.079	0.195
100 m mean depth	0.314	0.309	0.239	0.477	0.338	0.114	0.488	0.270	0.431
100 m max depth	0.144	0.150	0.121	0.237	0.143	0.058	0.237	0.098	0.246
100 m min depth	0.323	0.307	0.241	0.498	0.368	0.120	0.519	0.271	0.465
100 m std depth	0.094	0.071	0.063	0.187	0.176	0.013	0.198	0.201	0.246
Slope 100m	0.073	0.044	0.039	0.116	0.096	0.002	0.140	0.123	0.117
Aspect 100m	0.050	0.049	0.024	0.013	0.000	0.001	0.012	0.032	0.026
Surface Roughness	0.084	0.060	0.049	0.191	0.236	0.002	0.324	0.167	0.190

Appendix II: Detailed results of underwater video transects

Station	Sediment Types Present	Bottom Types Present	# Bottom Patches
1	Fine sediment (silt, clay, fine sand)	Dense Tube-mat	1
2	Fine sediment (silt, clay, fine sand)	Dense Tube-mat	1
3	Very coarse sand, boulders	Flat surface, boulder field	6
7	Fine sediment (silt, clay, fine sand)	Dense Tube-mat	1
8	Fine sand, gravel, cobble, boulders	Flat surface, boulder field	3
9	Coarse sand	Flat surface	1
10	Gravel, cobble	Flat surface	1
11	Very coarse sand, gravel, cobble	Flat surface	4
12	Coarse sand	Flat surface	1
13	Very coarse sand	Flat surface	1
14	Very coarse sand, boulders	Boulder field	1
15	Very coarse sand, gravel, cobble	Flat surface	2
16	Gravel, cobble, boulders	Flat surface	4
17	Gravel, cobble, boulders	Boulder field	10
19	Very coarse sand, gravel	Flat surface	1
20	Very coarse sand	Flat surface	1
21	Coarse sand	Flat surface	1
22	Fine sand, coarse sand	Flat surface w/ depressions throughout, rippled surface	2
23	Very coarse sand	Rippled surface - regular pattern	1
24	Fine sand	Rippled surface - irregular pattern	1
25	Fine sand	Rippled surface - irregular pattern	1
26	Very coarse sand, gravel	Rippled surface - regular pattern	1
27	Very coarse sand	Flat surface	1
28	Coarse sand	Rippled surface - regular pattern	1
29	Coarse sand	Rippled surface - irregular pattern	1
31	Coarse sand, gravel, cobble, boulders	Boulder field, rippled surface - irregular pattern	11

32	Coarse sand, gravel, cobble, boulders	Flat surface, rippled surface - regular pattern	5
33	Very coarse sand, gravel	Rippled surface - regular pattern	1
34	Coarse sand, boulders	Boulder field, rippled surface - regular pattern	8
35	Coarse sand, very coarse sand, boulders	Boulder field, rippled surface - irregular pattern	5
36	Coarse sand, very coarse sand, boulders	Boulder field, rippled surface - irregular pattern	10
37	Fine sediment (silt, clay, fine sand)	Dense Tube-mat	1
38	Coarse sand	Rippled surface - irregular pattern	2
40	Coarse sand	Flat surface	1
41	Fine sediment (silt, clay, fine sand)	Flat surface w/ depressions throughout	1
42	Coarse sand	Rippled surface - regular pattern	1
43	Coarse sand	Rippled surface - irregular pattern	1

References

Brown, C., Cooper, K., Meadows, W., Limpenny, D., Rees, H., 2002. Small scale mapping of sea-bed assemblages in the eastern English Channel using sidescan sonar and remote sampling techniques. Estuarine, Coastal and Shelf Science 54, 263-278.

Brown, C.J., Collier, J.S., 2008. Mapping benthic habitat in regions of gradational substrata: An automated approach utilizing geophysical, geological, and biological relationships. Estuarine, Coastal and Shelf Science 78, 203-214

Clarke, K.R., Gorley, R.N., 2006. PRIMER v6 User Manual/Tutorial. PRIMER-E: Plymouth

Clifton, H.E., 2006. A reexamination of facies models for clastic shorelines, in. Posamentier, H.W., and Walker, R.G., eds, Facies Models Revisited. Society of Economic Paleontologists and Mineralogists, Special publication 84, p. 293-337

CONMAP (Continental Margin Mapping) Sediment Grainsize Distribution for the United States East Coast Continental Margin. U.S. Geological Survey (USGS) Coastal and Marine Geology Program, 2005. Woods Hole Science Center. Open-File Report, 2005-1001. GIS data are available online at: http://woodshole.er.usgs.gov/openfile/of2005-1001/htmldocs/datacatalog.htm

Derous, S., Verfaillie, E., Van Lancker, V., Courtens, W., Stienen, E.W.M., Hostens K., Moulaert I., Hillewaert H., Mees J., Deneudt K., Deckers P., Cuvelier D., Vincx M., Degraer S., 2007. A biological valuation map for the Belgian part of the North Sea: BWZee, Final report, Research in the framework of the BELSPO programme “Global chance, ecosystems and biodiversity” – SPSD II, March 2007, pp. 99

Diaz, R., Solan, M., Valente, R., 2004. A review of approaches for classifying benthic habitats and evaluating habitat quality. Journal of Environmental Management 73, 165-181.

Eastwood, P., Souissi, S., Rogers, S., Coggan, R., Brown, C., 2006. Mapping seabed assemblages using comparative top-down and bottom-up classification approaches. Canadian Journal of Fisheries and Aquatic Sciences 63, 1536-1548.

Ellingsen, K.E., 2002. Soft-sediment benthic biodiversity on the continental shelf in relation to environmental variability. Marine Ecology Progress Series 232, 15-27.

Elliot, M., 1994. The analysis of macrobenthic community data. Marine Pollution Bulletin 28, 62-64.

Environmental Monitoring and Assessment Program (EMAP), National Coastal Assessment Database, Northeast Region, 2000-2002. U.S. Environmental Protection Agency. Dataset names: Benthic Replicate Abundance, Benthic Grab Information by Replicate, Benthic Summary Data by Station. Data catalog authors: J. Kiddon and H. Buffman. Data available online at: http://www.epa.gov/emap/nca/html/data/

Foster-Smith, R., Connor, D., Davies, J. 2007. What is habitat mapping? In: MESH Guide to Habitat Mapping, MESH Project, 2007, JNCC, Peterborough. Available online at: (http://www.searchmesh.net/default.aspx?page=1900, Last accessed 6/1/10.

Goff, J.A., Olson, H.C., Duncan, C.S., 2000. Correlation of side-scan backscatter intensity with grain-size distribution of shelf sediments, New Jersey margin. Geo-Marine Letters 20, 43-49

Gray, J., 1974. Animal-sediment relationships. Oceanography and Marine Biology: An Annual Review 12, 223-262.

Gray, J.S., Clarke, K.R., Warwick, R.M., Hobbs, G., 1990. Detection of initial effects of pollution on marine benthos: an example from the Ekofisk and Eldfish oilfields, North Sea. Marine Ecology Press Series 66, 285-299

Greene, H., Yoklavich, M., Starr, R., O'Connell, V., Wakefield, W., Sullivan, D., McCrea, J., Cailliet, G., 1999. A classification scheme for deepwater habitats. Oceanologica acta 22, 663-678.

Hewitt, J., Thrush, S., Legendre, P., Funnell, G., Ellis, J., Morrison, M., 2004. Mapping of marine soft-sediment communities: Integrated sampling for ecological interpretation. Ecological Applications 14, 1203-1216.

ICES, 2006. Report on the working group on marine habitat mapping (WGMHM). April 4-7, 2006, Galway, Ireland. ICES CM 2006/MHC:05 Ref. FTC, ACE. 132 pp.

ICES, 2007. Acoustic seabed classification of marine physical and biological landscapes. ICES Cooperative Research Report No. 286, 183 pp.

IOPTF (Interagency Ocean Policy Task Force), 2009. Draft interim framework for effective coastal and marine spatial planning. White House Council on Environmental Quality, Washington DC, 35 pp.

Kendall, M.S., Olaf, P.J., Alexander, C., Field, D., McFall, G., Bohne, R., Monaco, M.E., 2005. Benthic mapping using sonar, video transects, and an innovative approach to accuracy assessment: A characterization of bottom features in the Georgia Bight. Journal of Coastal Research 21(6), 1154-1165.

Kenny, A., Cato, I., Desprez, M., Fader, G., Schuttenhelm, R., Side, J., 2003. An overview of seabed-mapping technologies in the context of marine habitat classification. ICES Journal of Marine Science 60, 411-418.

Komar, P. D., 1976, Beach Processes and Sedimentation; Prentice-Hall, Inc., Englewood Cliffs. 429 p.

Kostylev, V., Todd, B., Fader, G., Courtney, R., Cameron, G., Pickrill, R. 2001. Benthic habitat mapping on the Scotian Shelf based on multibeam bathymetry, surficial geology and sea floor photographs. Marine Ecology Progress Series 219, 121-137.

Madden, C., Goodin, K., Allee, R., Cicchetti, G., Moses, C., Finkbeiner, M., Soule, J., King, J., Shumchenia, E., 2010. Coastal and marine ecological classification standard. NOAA and NatureServe, 149 pp.

McArthur, M., Brooke, B., Przeslawski, R., Ryan, D., Lucieer, V., Nichol, S., McCallum, A., Mellin, C., Cresswell, I., Radke, L., 2010. On the use of abiotic surrogates to describe marine benthic biodiversity. Estuarine, Coastal and Shelf Science 88, 21-32.

McBreen, F., Wilson, J., Mackie, A., Aonghusa, C., 2008. Seabed mapping in the southern Irish Sea: predicting benthic biological communities based on sediment characteristics. Hydrobiologia 606, 93-103.

McMaster, R. L., 1960. Sediments of the Narragansett Bay system and Rhode Island Sound, Rhode Island. Journal of Sedimentary Petrology, vol. 30., no 2., pp. 249-274.

McMaster, R. L., and Ashraf, A., 1973. Sub-bottom Basement Drainage System of Inner Continental Shelf off Southern New England. Geological Society of America Bulletin, v. 84, no. 1, p. 187-190.

McMullen, K. Y., L. J. Poppe, E. R. Twomey, W.W. Danforth, T. A. Haupt, and J. A. Crocker, 2007. Sidescan-sonar imagery and surficial geologic interpretations of the sea floor in Rhode Island Sound, off Sakonnet Point, Rhode Island, 2007. U.S. Geological Survey Open-File Report 2007-1150. Report and data available online at: http://woodshole.er.usgs.gov/pubs/of2007-1150/index.html

McMullen, K. Y., L. J. Poppe, T. A. Haupt, and J. M. Crocker, 2008. Sidescan-sonar imagery and surficial geologic interpretations of the sea floor in central Rhode Island Sound. U.S. Geological Survey Open-File Report 2007-1366. Report and data available online at: http://woodshole.er.usgs.gov/pubs/of2007-1366/

McMullen, K. Y., L. J. Poppe, T. A. Haupt, and J. M. Crocker, 2009. Sidescan-sonar imagery and surficial geologic interpretations of the sea floor in western Rhode Island Sound. U.S. Geological Survey Open-File Report 2008-1181. Report and data available online at: http://woodshole.er.usgs.gov/pubs/of2008-1181/index.html

Needell, S. W., O'Hara, C. J., and Knebel, H. J., 1983. Maps showing geology and shallow structure of western Rhode Island Sound, Rhode Island. U.S. Geological Survey Miscellaneous Field Studies Map MF-1537, scale 1:125,000.

Needell, S. W., and Lewis, R. S., 1984. Geology and structure of Block Island Sound, Rhode Island and New York. Miscellaneous Field Studies Map - U. S. Geological Survey, MF-1621 (4 Sheets), scale 1:125,000.

Needell, S.W., O'Hara, C.J., and Knebel, H.J., 1983. Quarternary geology of the Rhode Island inner shelf. Marine Geology, v. 53, p. 41-53.

NOAA CSC (National Oceanic and Atmospheric Administration Coastal Services Center), 2010. Benthic habitat mapping: What is benthic habitat? http://www.csc.noaa.gov/benthic/start/what.htm, Last accessed 6/1/10.

NOAA/NGDC, 1976. NGDC Marine sediment grainsize database, NOAA National Geophysical Data Center.

O'Hara, C. J., and Oldale, R. N., 1980. Maps showing geology and shallow structure of eastern Rhode Island Sound and Vineyard Sound, Massachusetts. Miscellaneous Field Studies Map- U.S. Geological Survey, Report: MF-1186, scale 1:125,000.

Pratt, S.D. 1973. Benthic Fauna. In: Coastal and offshore environmental inventory: Cape Hatteras to Nantucket Shoals. Marine Publication Series No. 2, University of Rhode Island, pp. 5.1-5.70.

Rhoads, D., 1974. Organism-sediment relations on the muddy sea floor. Oceanography and Marine Biology: An Annual Review 12, 200-263.

Rooper, C., Zimmermann, M., 2007. A bottom-up methodology for integrating underwater video and acoustic mapping for seafloor substrate classification. Continental Shelf Research 27, 947-957.

Rosenzweig, M.L., 1995. Species Diversity in Space and Time; Cambridge University Press, Cambridge, M.A.

Schafer, J. P., and Hartshorn, J., 1965. The Quaternary of New England, *in* Frey, J. W. a. D., ed., The quaternary of the United States; Princeton University Press, Princeton, N.J., p. 113-127.

Shumchenia, E., and King, J. 2010. Comparison of methods for integrating biological and physical data for marine habitat mapping and classification. Continental Shelf Research 30, 1717-1729

Sirkin, L. A., 1982. Wisconsinan Glaciation of Long Island, New York to Block Island, Rhode Island, *in* Larson, G. J., and Stone, B. D., eds., Late Wisconsinan glaciation of New England; Dubugue, IA, Kendall/Hunt, p. 35-60.

Snelgrove, P., Butman, C., 1994. Animal-sediment relationships revisited: cause versus effect. Oceanography and Marine Biology: An Annual Review 32, 111-177.

Snelgrove, P.V.R., 1998. The biodiversity of macrofaunal organisms in marine sediments. Biodiversity and Conservation 7, 1123-1132

Solan, M., Germano, J., Rhoads, D., Smith, C., Michaud, E., Parry, D., Wenzhafer, F., Kennedy, R., Henriques, C., Battle, E., Carey, D., Iocco, L., Valente, R., Watson, J., Rosenberg, R., 2003. Towards a greater understanding of pattern, scale and process in marine benthic systems: a picture is worth a thousand worms. Journal of Experimental Marine Biology and Ecology 285/286, 313-338.

Steimle, F.W., 1982. The benthic macroinvertebrates of the Block Island Sound. Estuarine, Coastal and Shelf Science 15, 1-16

Stone, B. D., and Borns jr., H., 1986. Pleistocene glacial and interglacial stratigraphy of New England, Long Island and adjacent Georges Bank and Gluf of Maine, *in* V. Sibrava, D. Q. B. a. G. M. R., ed., Quaternary glaciations in the Northern Hemisphere; New York, Pergamon, p. 39-52.

Stone, B.D., and Sirkin, L.A., 1996. The Geology of Block Island, *in* Johnston, H.E. and Veeger, A., eds. The water resources of Block Island, Rhode Island. U.S. Geological Survey Water Resources Bulletin 94-4096

Valesini, F.J., Hourston, M., Wildsmith, M.D., Coen, N.J., Potter, I.C., 2010. New quantitative approaches for classifying and predicting local-scale habitats in estuaries. Estuarine, Coastal and Shelf Science 86, 645-664.

Van Lancker, V. and Foster-Smith, R. 2007. How do I make a map? In: MESH Guide to Habitat Mapping, MESH Project, 2007, JNCC, Peterborough. Available online at: (http://www.searchmesh.net/default.aspx?page=1900), Last accessed 6/1/10.

Verfaillie, E., Degraer, S., Schelfault, K., Willems, W., Van Lancker, V., 2009. A protocol for classifying ecologically relevant marine zones, a statistical approach. Estuarine, Coastal and Shelf Science 83, 175-185.

Warwick, R.M., Clarke, K.R., 1991. A comparison of some methods for analyzing changes in benthic community structure. Journal of the Marine Biological Association of the United Kingdom 71, 225-244

U.S. Geological Survey, (Poppe, L. J., S.J. Williams, V. F. Paskevich) , 2005. East Coast Sediment Texture Database: Procedures, Database, and GIS. . USGS Open-File report 2005-1001. U.S.G.S. Coastal and Marine Geology Program, Woods Hole Science Center, Woods Hole, MA. Data available online at: http://pubs.usgs.gov/of/2005/1001/htmldocs/datacatalog.htm

usSEABED (U.S. Geological Survey, University of Colorado), 2005. Data available online at: http://coastalmap.marine.usgs.gov/regional/contusa/eastcoast/atlanticcoast/data.html.

Warwick, R.M., Clarke, K.R., 1993. Comparing the severity of disturbance: a meta-analysis of marine macrobenthic community data. Marine Ecology Press Series 92, 221-231

Wille, P.C., 2005. Sound Images of the Ocean in Research and Monitoring; Springer, Stürtz GmbH, Würzburg, Germany. 471 pg.

SECTION II: SUBSURFACE GEOLOGY

II.1 Introduction

The goal of the subsurface geology studies as to determine if the sub-bottom sediments were unconsolidated and thick enough to readily install structures by pile-driving. We used a high resolution sonar to characterize the subsurface geology of the study area. We interpreted the depth to a hard subsurface lithology only, and did not examine the details of the overlying soft sediments.

II.2 Background

Prior studies by McMaster, *et al*., 1968, and a series of U.S. Geological Survey surveys (McMullen, *et al*., Needell and Lewis, 1984, Poppe, *et al*., 2002) provide good coarse-resolution coverage of the northern part of the SAMP area, and very limited coverage of the southern part of the SAMP area. The trackline coverage of the these surveys is shown in Figure II-1. Additional information and interpretation from the USGS surveys, as well as a significant number of GIS data layers, are available online through a series of digital data releases and Open File reports. Online addresses are included with the references. The McMaster, *et. al.* (1968) data is not available in digital format

II.3 Methods

Sub-bottom seismic data were obtained with a 400-Hz bubble pulser towed profiling system along GPS-navigated survey lines. The target vessel speed was 4 kts with a shotpoint interval of 0.25 s, which resulted in an along-track shotpoint interval of 0.5 m with a maximum seismic penetration of 200 m (assuming 1600 m/s seismic velocity of sediments). A digital sampling interval of 100 ms along individual traces results in a 2 mm vertical sampling interval.

Seismic data were collected in two primary survey areas (Fig. 2): 1) Block Island, along the southern half of the island extending from the shoreline out to 5-10 km offshore, and 2) Federal Area, southwest of Martha's Vineyard in an 8 km x 18 km rectangular region surrounding the WHOI buoy field. The Block Island seismic data were collected on several cruises aboard the 28' R/V McMaster during July (14^{th}, 15^{th} and 29^{th}) and August (6^{th}) of 2009. Typical spacing between adjacent lines was about 0.5-1 km with more widely spaced crossing tie lines. The seismic data from the Federal Area were collected aboard the R/V Endeavor during cruise EN468 from September 17 to September 25, 2009. Seismic operations were limited by daylight and weather conditions during the latter cruise; so seismic trackline spacing is more variable (0.5-3 km) in this region.

Post-processing of the sub-bottom seismic data involved two steps: band-pass filtering and time-dependant normalization. A band-pass filter was applied to each seismic line with a low-cut frequency of 300-400 Hz and a high-cut frequency of 1000-2000 Hz. The band-pass frequency ranges were chosen qualitatively from a matrix of seismic panels with incremental variations in frequencies. The time-dependant normalization was achieved with automatic gain control with a window length of 50-100 ms and a gain of 1-1.5 dB. As with the band-pass filtering, the automatic gain control parameters were chosen based on a matrix of varying window length and gain.

II.4 Results

Representative examples of interpreted processed seismic data from each region are shown in Figure 3 and 4. A sediment thickness map of the Federal Area was generated by digitizing the sediment-water interface and the deepest visible reflection in the processed seismic data (Figure 5). The along-track location of each reflector was digitized at least every 200 m and wherever significant changes in reflector depth occurred. Linearly interpolated and geo-referenced seismic horizons were then generated with SonarWeb software from which sediment thickness estimates at each shot-point were calculated. These geo-referenced sediment thickness estimates were used as input in contouring and two-dimensional surface-fitting algorithms from Generic Mapping Tool to create sediment isopach maps. It should be noted that these sediment thickness estimates and associated isopach maps represent minimum sediment thicknesses; there likely exists deeper sediment/sediment or sediment/basement interfaces.

II.5 Discussion

The comparison of sediment isopach maps from previous USGS surveys and our recent survey in the Federal Area provides several useful observations. First, in the eastern half of the survey area, the sediment thickness estimates from both surveys are very similar and indicate sediment thicknesses in excess of 100 m. These thicker sediments correlate to darker regions in the side-scan data and appear to represent two southward-merging buried valleys. The brighter regions in the side-scan data are associated with thinner sediments (< 20 m). Second, in the central portion of the survey area, both sets of seismic data identify a NW-SE trending ridge buried by a thinner sediment layer (< 20 m). Finally, in the westernmost portion of the survey area, both surveys indicate increased sediment thickness; however, the sediment is significantly thicker in the USGS survey data. The most likely reason for the difference is the inability of our recent data to resolve the deeper seismic reflections; the closely spaced seismic lines in the recent data do not have crossing tie-lines and the sea state was significantly degraded during the collection of these survey lines. Therefore, the interpretation from the USGS study is likely to be more representative of the region. It is also interesting to note that a correlation between sediment thickness and side-scan reflectivity does not exist in the western half of the survey area, so side-scan reflectivity alone may not be appropriate to infer relative sediment thickness.

The subsurface geology can be interpreted in terms of effort required to install wind turbines. Ease of construction is based on the technology needed to install wind turbines in areas with specific sub-bottom types. Sub-bottom sediment types that are unconsolidated and thick enough to allow pile-driving as the installation technology are rated between 1 and 3, with 1 being the easiest. Any lithology that would require drilling for installation of piles would be rated greater than 3. For example, Figure II-6 shows interpreted construction efforts within the BI study area.

II.6 Conclusions

The subsurface geology studies allow us to identify areas that would be suitable for the installation of foundation structures by pile-driving. It is apparent from Figure II-6 that most areas located to the south of Block Island are suitable for installation of piles by pile-driving including the site proposed by Deep Water Wind shown by the yellow dots (representing borehole locations).

Our studies of the FED indicate that there are also suitable locations in the central to western part of the survey area for installation of piles by pile-driving.

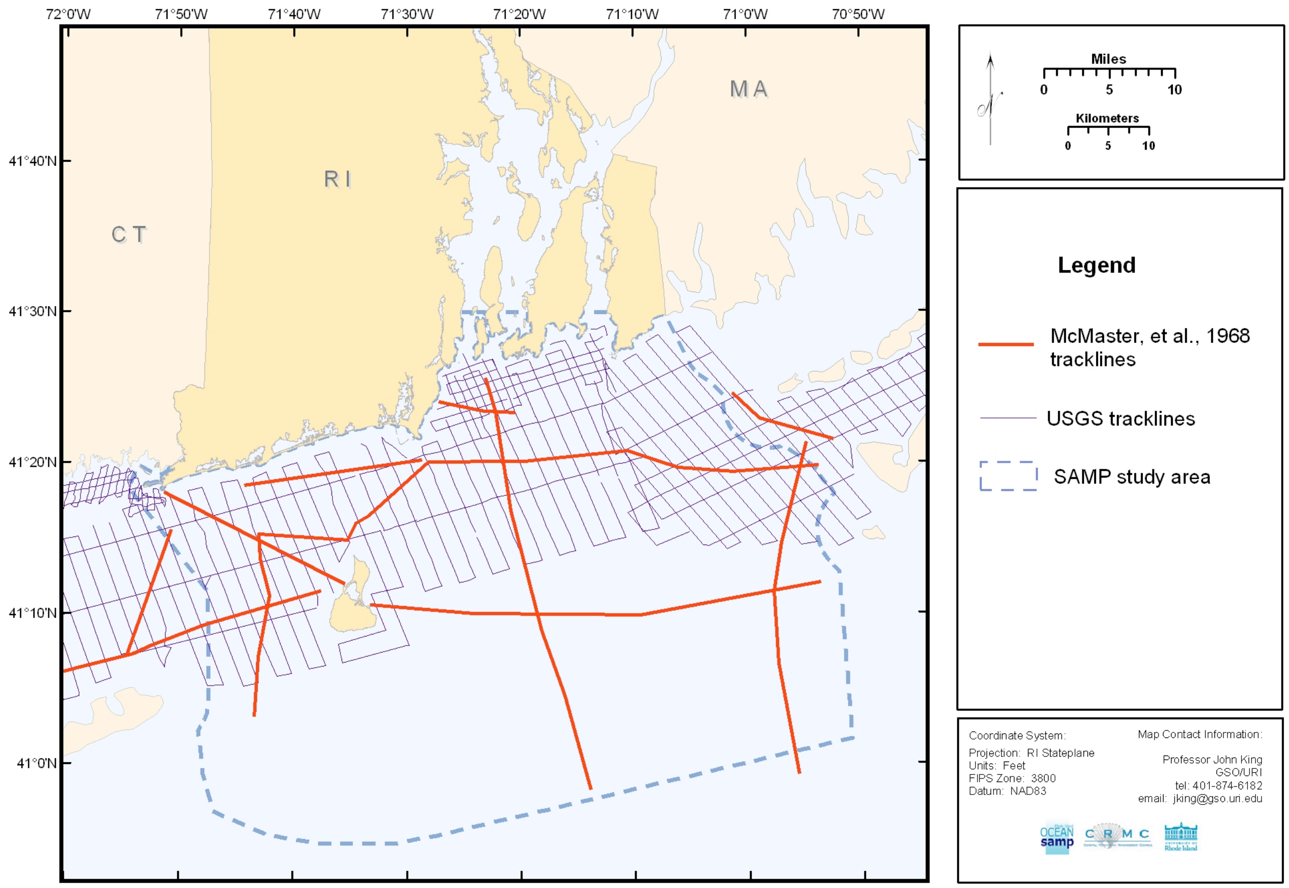

Figure II-1. Map showing locations of previous sub-bottom surveys within the SAMP area.

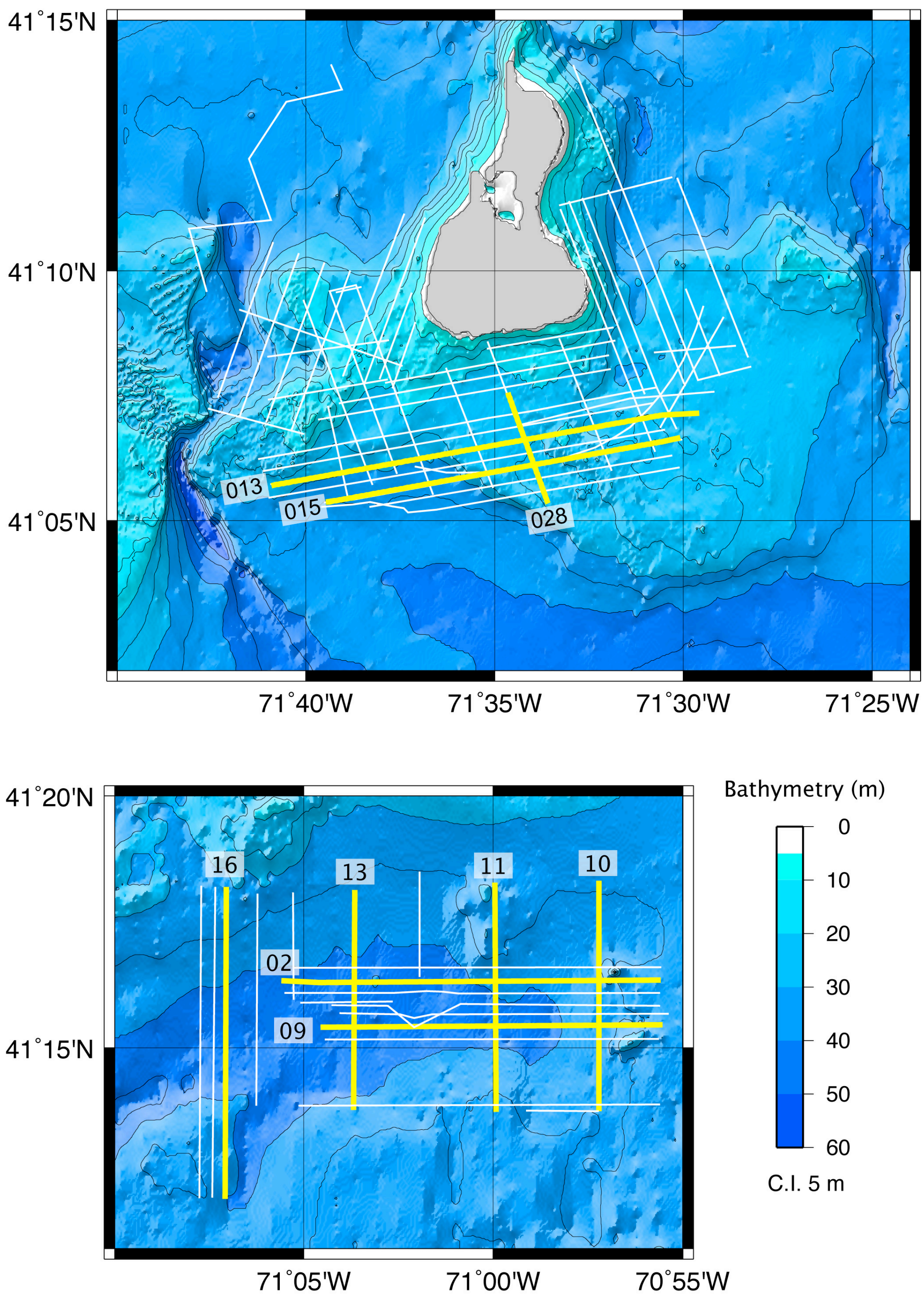

Figure II-2. Sub-bottom seismic tracklines (white lines) superimposed on bathymetry (http://www.ngdc.noaa.gov/mgg/coastal/crm.html) for the Block Island (top) and the Federal (bottom) survey areas. The yellow lines identify the location of seismic sections shown Figures 3 and 4.

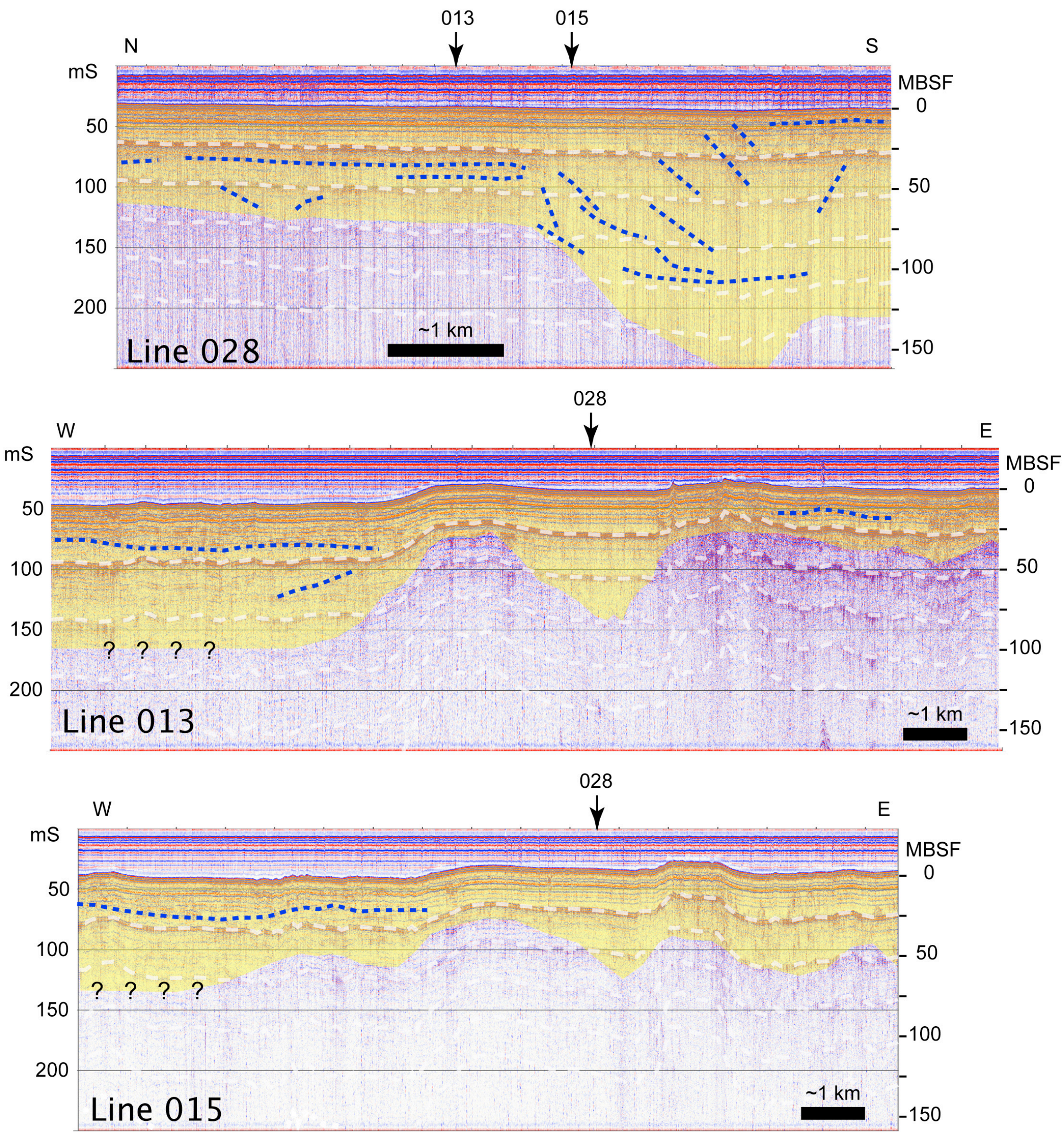

Figure II-3. Processed seismic cross-sections of selected lines from Block Island survey area (see Fig 2, top) with sub-bottom interpretations. The yellow regions correspond to the sediment-water interface at the top and the deepest visible reflection at the bottom. The questions marks indicate sections of the seismic record where our identified deepest reflector extends below the resolvable depth limit. Multiple reflections of the sediment-water interface (white dashed lines) and internal reflectors (blue dashed lines) within the identified sediment package are indicated. The locations of crossing lines are indicated with arrows and appropriate line number. The vertical axis of the section is plotted as two-way travel time (milliseconds) and thickness of the sediment section (MBSF, meters below seafloor), assuming a seismic velocity of 1500 m/s.

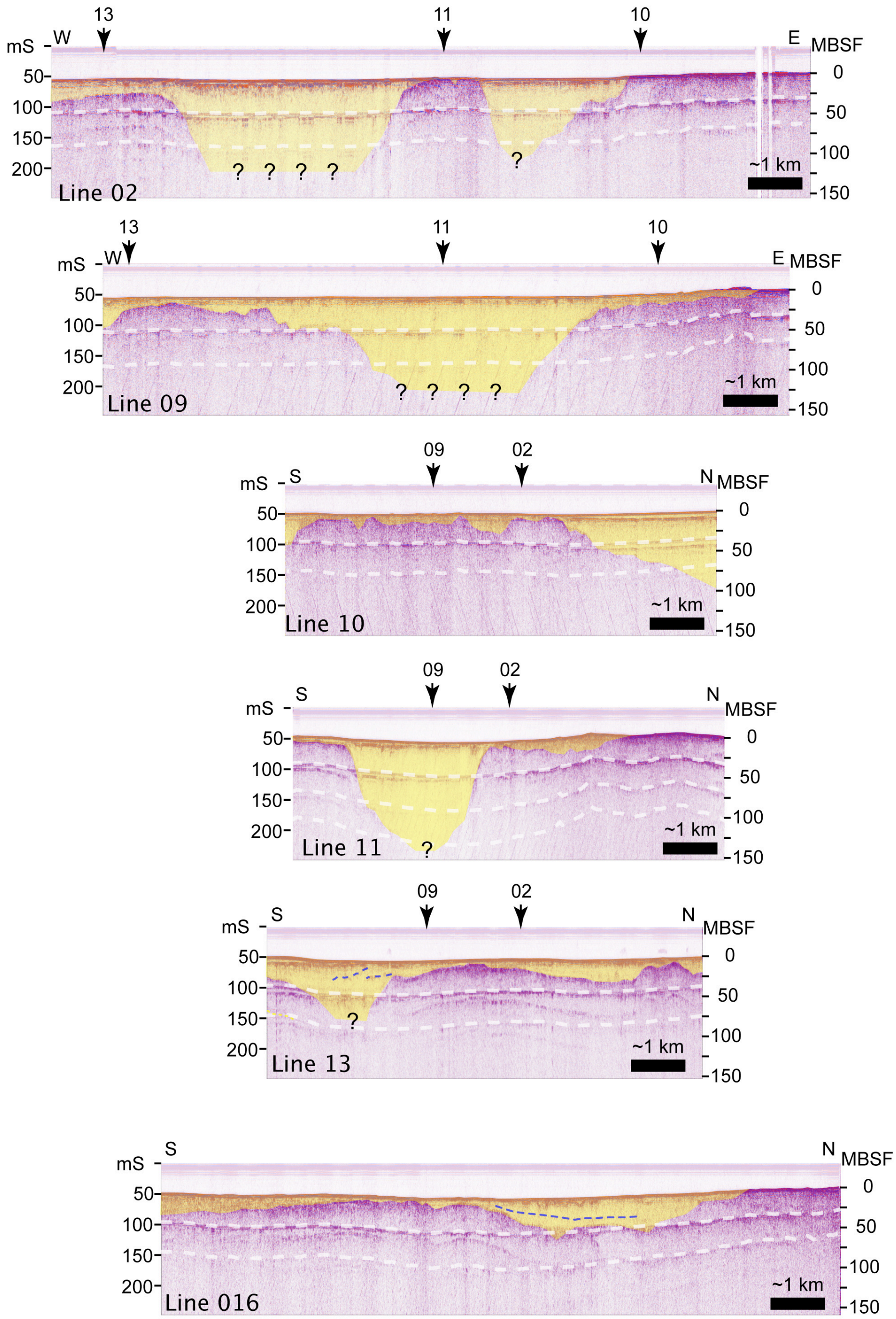

Figure II-4. Processed seismic cross-sections of selected lines from Federal survey area (see Fig 2, bottom) with sub-bottom interpretations. Axes labels and highlighted attributes are the same as in Figure 3.

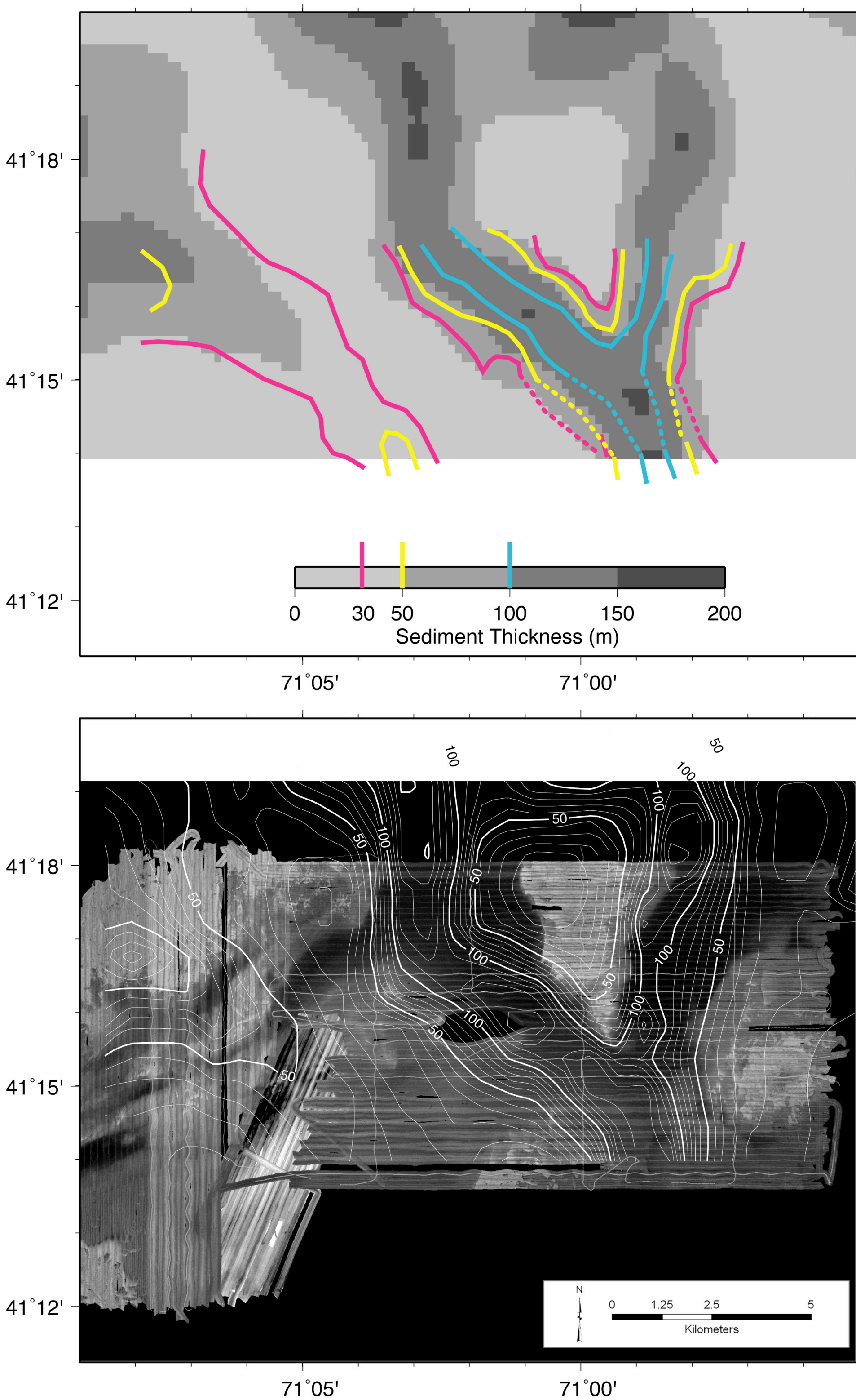

Figure II-5. (top) Sediment isopach of the Federal survey area comparing our sediment thickness estimates (colored contours) with a previous study (gray shading) by O'Hara, [1980]. (bottom) Sediment thickness contours from the O'Hara study are overlain on side-scan reflectivity.

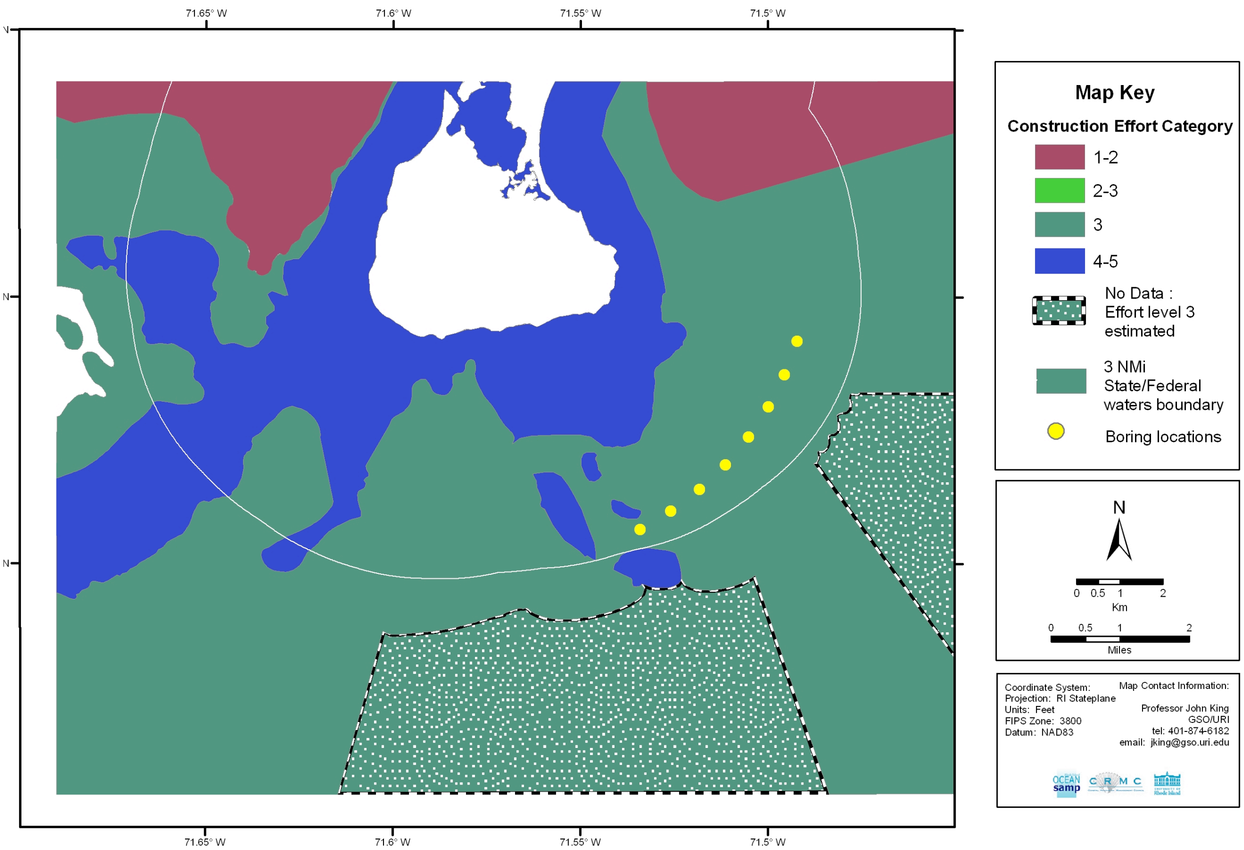

Figure II-6. Map showing ease of construction for wind turbines in the BI study area.

II.7 References

McMaster, R., L., R. P. Lachance, and L. E. Garrison, 1968. Seismic-reflection studies in Block Island and Rhode Island Sounds. *The American Association of Petroleum Geologists Bulletin*, 52:3, 465-474.

McMullen, K. Y., L. J. Poppe, and N. K. Soderberg, 2009. Digital seismic-reflection data from western Rhode Island Sound, 1980. *U.S. Geological Survey Open-File Report 2009-1002.* Report and data available online at: http://pubs.usgs.gov/of/2009/1002/index.html

Needell, S. W., and Lewis, R. S., 1984. Geology of Block Island sound, Rhode Island and New York. Geological framework data from Long Island Sound, 1981-1990 - A digital data release. *U.S. Geological Survey Open-File Report 02-002*

O'Hara, C.J., 1980, High-resolution seismic-reflection profiling data from the Inner Continental Shelf of southeastern Massachusetts: *U.S. Geological Survey Open-File Report 80-178.*

Poppe, L. J., V. F. Paskevich, R. S. Lewis, and M. L. DiGiacomo-Cohen, 2002. Geological Framework Data from Long Island Sound, 1981-1990: A Digital Data Release. *U.S. Geological Survey Open-File Report 02-002*. Report and data available online at: http://woodshole.er.usgs.gov/openfile/of02-002/index.htm